



THE HONG KONG
POLYTECHNIC UNIVERSITY

香港理工大學

Pao Yue-kong Library
包玉剛圖書館

Copyright Undertaking

This thesis is protected by copyright, with all rights reserved.

By reading and using the thesis, the reader understands and agrees to the following terms:

1. The reader will abide by the rules and legal ordinances governing copyright regarding the use of the thesis.
2. The reader will use the thesis for the purpose of research or private study only and not for distribution or further reproduction or any other purpose.
3. The reader agrees to indemnify and hold the University harmless from and against any loss, damage, cost, liability or expenses arising from copyright infringement or unauthorized usage.

If you have reasons to believe that any materials in this thesis are deemed not suitable to be distributed in this form, or a copyright owner having difficulty with the material being included in our database, please contact lbsys@polyu.edu.hk providing details. The Library will look into your claim and consider taking remedial action upon receipt of the written requests.

The Hong Kong Polytechnic University
Department of Mechanical Engineering

Improvement of the Mechanical Properties of Polymer-based
Materials using Layered
Silicates for Product Development

Lam Chun Ki

A thesis submitted in partial fulfilment of the requirements
for the Degree of Doctor of Philosophy

May 2007



Certificate of Originality

I hereby declare that this thesis is my own work and that, to the best of my knowledge and belief, it reproduces no material previously published or written, nor material that has been accepted for the award of any other degree or diploma, except where due acknowledgement has been made in the text.

Mr. Lam Chun Ki



ABSTRACT

Recently, nanoclay/epoxy composites (NCs) have attracted much attention by researchers from different fields. Many studies have reported that the mechanical properties of epoxy can be improved with only mixing a small amount of nanoclays (3-5 wt.%). Polymer and advance composite industries can highly benefit from such achievements both economically and practically. From recent researches, it was reported that the degree of exfoliations of nanoclay platelets in epoxy is extremely important for altering the mechanical properties of the NCs. Due to an increase of interfacial bonding surface area of exfoliated nanoclay platelets, the bonding strength as well as stress transferability between nanoclays and epoxy therefore increase, which result in improving the overall mechanical properties of the NCs.

Nevertheless, purely exfoliated nanoclay platelet structures can only be found in carefully controlled laboratory environments. It is difficult to achieve through traditional manufacturing processes, such as, extrusion and injection moldings. Non-uniform pressure distribution in mixtures is always the major cause of agglomerations of nanoclays during the manufacturing process.



Many studies have reported that agglomerations of particles decrease the total kinetic energy in a two-phase mixture. Therefore, the movements of particles decrease and they adhere to each other to form larger molecules that consist of many single particles, which are called clusters. The agglomerating phenomenon in particles explains the cause of formation of nanoclay clusters with intercalated structures in the NCs. Hence, there is a need to have an indepth study on the effects of the inclusion of intercalated nanoclay clusters in the NCs in order to suit the real engineering applications.

In this project, the mechanical properties of the NCs with intercalated nanoclay clusters (hereafter called “nanoclay clusters”) are studied in detail. With the X-ray diffraction (XRD), Scanning Electron Microscopy (SEM) and Energy Dispersive X-ray (EDX) materials characterizations, the co-relation of the size and shape of the nanoclay clusters formed in the NCs with different manufacturing parameters are investigated. Vickers micro-hardness, wear resistance and creep tests are conducted on NC samples for the visualization of the mechanical properties by the reinforcements of nanoclay clusters. Nucleation of nanoclay clusters in the NCs is explained by the nucleation theory while the distribution of nanoclay clusters in the NCs is examined by nanoindentation.



Mathematical models are proposed to facilitate the estimation of the mechanical properties of the NCs with different amount of nanoclay clusters. The importance of the thermo-mixing process during production of the NCs is analyzed from the Flory's principle. Creep mechanism of the NCs with intercalated nanoclay clusters is also studied by nanoindentation and a modified model with the aid of the Kelvin-Voigt model.

From the various mechanical property tests and mathematical models, maximal mechanical properties were found at 4 wt.% of nanoclays in the NCs. With the analyses in this project, the principles of the formation of nanoclay clusters and the mechanical properties of NCs with nanoclay clusters are interpreted in detail that have not been studied elsewhere previously.



PUBLICATIONS

Journal articles (submitted)

1. **LAM CK** and Lau KT. Mechanical Performance by Intercalated Nanoclay Clusters inside Nanoclay/epoxy Composites. *Composites Science and Technology*, 2007; Submitted.
2. **LAM CK**, Lau KT and Zhou LM. Creep Mechanism of Nanoclay/Epoxy Composites. *Composites Part A: Applied Science and Manufacturing*, 2007; Submitted.

Journal articles (accepted and published)

3. **LAM CK** and Lau KT. The effect of thermo-mixing energy to the mechanical performance of a nanoclay/polymer composite. *Composites Part A: Applied Science and Manufacturing*, 2007; Accepted.
4. **LAM CK** and Lau KT. Tribological behavior of nanoclay/epoxy



composites. *Materials Letters*, 2007; In press.

5. **LAM CK** and Lau KT. Optimization Effect of Micro Hardness by Nanoclay Clusters in Nanoclay/Epoxy Composites. *Journal of Thermoplastic Composite Materials*, 2007; In press.
6. **LAM CK** and Lau KT. Enhancement of Hardness and Wear Resistance of Epoxy-based Materials using Clay Nanoparticles. *HKIE Transactions*, 2007; **14**(1): In press.
7. **LAM CK**, Lau KT and Zhou LM. Nano-mechanical creep properties of nanoclay/epoxy composite by nano-indentation. *Key Engineering Materials*, 2007; **334-335**: 685-688.
8. **LAM CK** and Lau KT. Localized elastic modulus distribution of nanoclay/epoxy composites by using nanoindentation. *Composite Structures*, 2006; **75**(1-4): 553-558.
9. Ho MW, **LAM CK**, Lau KT, Ng HL and Hui D. Mechanical properties of



- epoxy-based composites using nanoclays. *Composite Structures*, 2006; **75**(1-4): 415-421.
10. Lau KT, Lu M, Qi JQ, Zhao DD, Cheung HY, **LAM CK**, Xiao LN and Li HL. Cobalt Hydroxide Colloidal Particles Precipitation on Nanoclay Layers for the Formation of Novel Nanocomposites of Carbon Nanotubes/Nanoclay. *Composites Science and Technology*, 2006; **66**(3-4), 450 – 458.
11. **LAM CK**, Lau KT, Cheung HY and Ling HY. Effect of ultrasound sonication in nanoclay clusters of nanoclay/epoxy composites. *Materials Letters*, 2005; **59**(11), 1369 – 1372.
12. **LAM CK**, Cheung HY, Lau KT, Zhou LM, Ho MW and Hui D. Cluster size effect in hardness of nanoclay/epoxy composites. *Composites Part B: Engineering*, 2005; **36**(3), 263 – 269.
13. Lau KT, Lu M, **LAM CK**, Cheung HY, Sheng FL and Li HL. Thermal and mechanical properties of single-walled carbon nanotube bundle-reinforced



epoxy nanocomposites: the role of solvent for nanotube dispersion.

Composites Science and Technology, 2005; **65**(5), 719 – 725.

14. Ling HY, Lau KT and **LAM CK**. Effects of embedded optical fibre on mode II fracture behaviours of woven composite laminates. *Composites Part B: Engineering*, 2005; **36**(6-7), 534 – 543.

(II) International Refereed Conference Papers

15. **LAM CK** and Lau KT. Modeling of tribological behavior of nanoclay/epoxy composite. The Proceeding of the 16th International Conference on Composite Materials (ICCM16), 2007, Kyoto, Japan; Accepted.
16. **LAM CK**, Lau KT and Zhou LM. Micro-mechanical properties of clay-cluster/polymer composite. The Proceeding of the 5th Asian-Australasian Conference on Composite Materials (ACCM-5), 27-30 November, 2006, Hong Kong; Nanocomposite Special Symposium; Page 20.



17. Li XF, Lau KT and **LAM CK**. Nano-mechanical properties of coiled carbon nanotube reinforced epoxy composites. The Proceeding of the 5th Asian-Australasian Conference on Composite Materials (ACCM-5), 27-30 November, 2006, Hong Kong. Nanocomposite Special Symposium; Page 21.

18. **LAM CK** and Lau KT. Localized mechanical properties of nanoclay/epoxy composites by nanoindentation. The Thirteenth International Conference on Composite Structures (ICCS/13), Melbourne 14 - 16 November 2005; Nanocomposites; Paper No. 109.

19. **LAM CK** and Lau KT. Effect of nanoclay clusters in mechanical properties of nanoclay/epoxy composites. The Proceeding of the 15th International Conference on Composite Materials (ICCM15), 27 June 2005- 1 July 2005, Durban, South Africa; Nano Materials and Composites; Page 31-32.



AWARD

An award was received during the postgraduate study:

Li Po Chun Charitable Trust Fund Scholarship for Postgraduate Students

2006/07

Selection criteria are based on the academic excellence and the research quality during postgraduate studies. Only two postgraduate students in Hong Kong, among all universities are granted for this merit every year.



ACKNOWLEDGEMENTS

I would like to take this opportunity to address the most sincere and gratitude to my chief supervisor Dr. K. T. Lau. His valuable comments and supervision during the ongoing of my research progress do give me definite positive impact. His expertise in nanocomposites always gives me a clue when conducting complicated situations during my research progress. I would also like to thank for his continuous support and encouragement, especially the valuable friendship with him and his family.

I would also like to thank my co-supervisor Prof. L. M. Zhou for his support and recommendations for the research. A special acknowledgement goes to Mr. M. N. Yeung of the Materials Research Center in the Hong Kong Polytechnic University for his kind helpfulness in the advice for the materials characterization tests. I also wish to thank my research teammates for their support.

Last but not least, I would like express my gratitude to my parents for their continuous support of my education in my early age. Their encouragements and understanding give me power to overcome the hurdles in my researches. Finally, I would dedicate the thesis to Karen for her continuous support and encouragement for my research.



TABLE OF CONTENTS

TITLE PAGE	
CERTIFICATE OF ORIGINALITY	i
ABSTRACT	ii
PUBLICATIONS	v
AWARD	x
ACKNOWLEDGEMENTS	xi
TABLE OF CONTENTS	1
LIST OF FIGURES	3
1. INTRODUCTION	7
2. LITERATURE REVIEW	16
3. MATERIALS CHARACTERIZATIONS	26
3.1 X-RAY DIFFRACTION (XRD)	26
3.2 SCANNING ELECTRON MICROSCOPY (SEM)	29
3.3 ENERGY DISPERSIVE X-RAY (EDX)	31
4. MECHANICAL PROPERTIES OF NANOCLAY/EPOXY COMPOSITES	33
4.1 MATERIALS	33
4.2 EXPERIMENT PRINCIPLES AND APPARATUS FOR MECHANICAL PROPERTY TESTS	34
4.2.1 VICKERS MICRO-HARDNESS TEST	34
4.2.2 ULTRASOUND SONICATION TEST	37
4.2.3 ABRASIVE TEST	38
4.2.4 NANOINDENTATION TEST	39
4.3 SAMPLE PREPARATION FOR MECHANICAL PROPERTY TESTS	44
4.3.1 VICKERS MICRO-HARDNESS	44
4.3.2 ULTRASOUND SONICATION	45
4.3.3 WEAR RESISTANCE	45
4.3.4 NANOINDENTATION	46
4.4 EXPERIMENTAL RESULTS	48



4.4.1	X-RAY DIFFRACTION (XRD)	48
4.4.2	SCANNING ELECTRON MICROSCOPY (SEM)	49
4.4.3	VICKERS MICRO-HARDNESS	59
4.4.4	WEAR RESISTANCE	64
4.4.5	NANOINDENTATION	66
5.	THEORETICAL ANALYSIS	71
5.1	MICRO-HARDNESS AND WEAR RESISTANCE	71
5.2	CREEP MECHANISM	77
5.2.1	KELVIN-VOIGT CREEP MODEL	80
5.2.2	NANOINDENTATION CREEP MODEL	83
5.3	THERMO-MECHANICAL MIXING ENERGY	91
5.3.1	ENTROPY OF THE MIXTURE	92
5.3.2	INTERACTION ENERGY OF THE MIXTURE	95
5.3.3	MATHEMATICAL OPTIMIZATION	99
5.4	FORMATION OF NANOCCLAY CLUSTERS	102
6.	CONCLUSION	107
	REFERENCES	113
	APPENDIX	128

LIST OF FIGURES

- Figure 1.1 Three typical forms of montmorillonite (MMT) inside polymer matrix. (a) intercalated, (b) flocculated, and (c) exfoliated*
- Figure 2.1 Schematic diagram of the atomic structure of nanoclays*
- Figure 2.2 Three possible structures of nanoclays in epoxy resins*
- Figure 2.3 Illustration of the “matrix” and “particle” domain in (a) conventional composite and (b) nanocomposite*
- Figure 2.4 Micromechanical modeling techniques of nanocomposites with nanoclays*
- Figure 3.1 Schematic diagram of XRD*
- Figure 3.2 Schematic diagram of SEM*
- Figure 3.3 Schematic diagram of EDX*
- Figure 3.4 EDX image (a) away from nanoclay cluster (b) at the nanoclay cluster*
- Figure 4.1 Vickers micro-hardness tester*
- Figure 4.2 Parameters of Vickers micro-hardness test*
- Figure 4.3 Ultrasound frequency spectrum*
- Figure 4.4 Abrasive test machine*

- Figure 4.5 Abrasive testing mechanism*
- Figure 4.6 Nanoindenter sample*
- Figure 4.7 Berkovich indenter specifications*
- Figure 4.8 Hysitron triboindenter*
- Figure 4.9 Nanoindentation profile*
- Figure 4.10 XRD spectrum of NCs with different wt.% of nanoclays*
- Figure 4.11 SEM photograph of pure epoxy*
- Figure 4.12 SEM photograph of 4 wt.% of NCs*
- Figure 4.13 SEM photograph of 15 wt.% of NCs*
- Figure 4.14 Variation of nanoclay cluster sizes in NCs with different wt.% of nanoclays*
- Figure 4.15 SEM of NCs with sonicating time of 5 minutes at 4 wt. % of nanoclay content*
- Figure 4.16 SEM of NCs with sonicating time of 10 minutes at 4 wt. % of nanoclay content*
- Figure 4.17 SEM of NCs with sonicating time of 15 minutes at 4 wt. % of nanoclay content*
- Figure 4.18 Surface morphologies of the fractured surface of NCs with different sonication temperatures, (a) 40 °C (b) 80 °C (c) 100 °C*

Figure 4.19 EDX examinations on the fractured surfaces of NCs. (a) non-circled regions and (b) circled regions

Figure 4.20 Schematic diagram of intercalated nanoclay clusters in NCs

Figure 4.21 Vickers micro-hardness of NCs with different wt.% of nanoclays

Figure 4.22 Vickers micro-hardness of the NCs at different sonicating times at 4 wt. % of nanoclay content

Figure 4.23 Wear index of NCs with different wt.% of nanoclays

Figure 4.24 Comparisons between the top and bottom layers of the fractured surface of NCs subject to 40 °C sonication temperature

Figure 4.25 Comparisons between the top and bottom layers of the fractured surface of NCs subject to 80 °C sonication temperature

Figure 4.26 Comparisons between the top and bottom layers of the fractured surface of NCs subject to 100 °C sonication temperature

Figure 4.27 Relative elastic modulus of NCs subject to different sonication temperature treatments

Figure 5.1 Micro-hardness of NCs with different wt. % of nanoclays

Figure 5.2 Wear Index of NCs with different wt.% of nanoclays

Figure 5.3 Nanoindentation profile

Figure 5.4 Kelvin-Voigt model



Figure 5.5 Three different stages of nanoindentation of NCs. (a) before nanoindentation; (b) during nanoindentation and (c) after nanoindentation due to creep effect

Figure 5.6 Creeping strain of different wt.% of NCs

Figure 5.7(a) Result of fitted ε vs t curve of 2 wt.% NCs

Figure 5.7(b) Result of fitted ε vs t curve of 4 wt.% NCs

Figure 5.7(c) Result of fitted ε vs t curve of 6 wt.% NCs

Figure 5.7(d) Result of fitted ε vs t curve of 8 wt.% NCs

Figure 5.8 Creeping strain variation of NCs at different nanoclay content

Figure 5.9 Entropy variation of NCs with different wt.% of nanoclays

Fig. 5.10 Reaction efficiency factor of NCs with different wt.% of nanoclays



1. INTRODUCTION

In the past decade, a great deal of research was conducted to investigate the use of nanofillers to enhance the mechanical properties of polymers. The form of nanocomposites was found to have better mechanical properties than the enhancement by microcomposites. The resulting composite properties can be improved because the nanoparticles have a very high specific surface area. This area can generate a new material behavior, which is widely determined by interfacial interactions, offering unique properties and a completely new class of materials. Therefore, it is obvious to expect a basic change in the mechanical properties. For instance, if a small crack starts to propagate in the nanocomposites, then it is required to break through many nanoparticles or shear off the bonding between the nanoparticles and their surrounding matrix as compared with just a few microparticles. As a result, the energy consumption for the small crack to go through the nanocomposites is higher and thus the fracture toughness is improved.

In the recent development of nanocomposites, layered silicate (hereafter called “nanoclays”)/polymer nanocomposites have attracted much attention in the composites community. In a low dosage of nanoparticles (3 – 5 wt.%), the



mechanical properties of polymer matrix have already been significantly improved. For examples, increased elastic modulus, decreased the coefficient of thermal expansion, reduced gas permeability, increased solvent resistance and enhanced ionic conductivity when compared to pristine polymers. In previous research, different nanofillers and polymers including epoxy thermosets, polyamide, polyimide, polystyrene, polyurethane and polypropylene were mixed to investigate the efficiency of enhancement on their mechanical properties.

Nanoclay/epoxy composites (NCs) demonstrate a significant improvement in their mechanical properties in comparison to pristine epoxy with no weight penalty. Hardness, fracture toughness, stiffness and heat resistance are greatly upgraded by the introduction of a small amount (3-5 wt.%) of nanoclays into epoxy. Exfoliation of nanoclay platelets is significant for the improvement of mechanical and thermal abilities in the NCs. Fig. 1.1 shows three possible forms of nanoclay platelets inside the NCs.



(a)



(b)



(c)

Figure 1.1 Three typical forms of montmorillonite (MMT) inside polymer matrix. (a) intercalated, (b) flocculated, and (c) exfoliated

Fully exfoliated nanoclay platelets provide a tortured path for heat and mechanical force penetration inside NCs. Thus, heat and mechanical energies can



be dissipated and reduced by the exfoliation of the nanoclay platelets. Another reason for supporting fully exfoliated NCs is the increase in the number of interacting surface areas between the nanoclays and epoxy. This can increase the efficiencies in mechanical adhesion and interfacial bonding between nanoclays and epoxy, and thus improve the mechanical properties of the NCs. However, fully exfoliated nanoclay structures can only be formed under strictly controlled laboratory conditions. Uneven internal pressure is induced in general industrial production process of the NCs, especially during extrusion and injection molding processes. From the nucleation theory, the particles inside a liquid tend to form tiny clusters due to the increase of surface energy or interfacial tension when the size of clusters increases. For a cluster containing n atoms, its surface energy $\sigma A(n)$ is given by:

$$4\pi\sigma\left(\frac{3V}{4\pi}n\right)^{\frac{2}{3}} \quad (1.1)$$

where σ is the interfacial tension per unit area, $A(n)$ is the surface area of the cluster, and v is the volume per molecule in the bulk liquid.



Thus, when uneven pressure is introduced into precured NC mixtures, the probability for the nanoclays to collide and nucleate with each other naturally increases. Intercalated nanoclay clusters are overwhelmingly formed during extrusion and injection molding processes. The significance of investigations on the improvements of mechanical properties by intercalated nanoclay clusters in the NCs is growing dramatically in order to suit the form of the NCs during the manufacturing processes. Several papers have reported that intercalated nanoclay clusters exist in the NCs. Nevertheless, a systematic analysis of the effects on the mechanical properties of the NCs by intercalated nanoclay clusters has not previously been conducted elsewhere.

In the project, the mechanical properties of the NCs with intercalated nanoclay clusters were studied through Vickers micro-hardness, wear resistance, creep mechanism. The optimized wt. % of nanoclays in the NCs was proved through rigorous experimental interpretations and mathematical analysis. It is important to visualize the factors that may affect the size of nanoclay clusters of the NCs during manufacturing processes before in-depth study in their mechanical properties. The environmental factors that control the size of nanoclay clusters in the NCs were



experimentally studied. During the preparation of the NCs, the following factors affected the ease of formation of nanoclay clusters:

1. Weight percentage of nanoclays in the NCs
2. Sonicating time of NC mixtures before curing
3. Reaction temperature of the NC mixtures
4. Vacuuming time of the NC mixtures before curing

Firstly, the weight percentage of the nanoclays in the NCs plays an important role in the dispersion effect of the nanoclay platelets. The dispersion effect is limited by adding more nanoclays in the epoxy when the volume is unchanged.

Secondly, the sonicating times of the NC mixtures are also very important to the exfoliation of the nanoclay platelets. Extra energy is given to the nanoclay platelets to move around when sonicating the NC mixtures. If less energy is given to the mixture, the nanoclay platelets do not have enough energy to exfoliate within the nanoclay clusters, thus, the aid for dispersion is limited. However, if the nanoclay platelets have too much energy to move around, then the frequency of collision between each single nanoclay platelet increases. The chance of



nanoclay platelets to tangle up and react to form a larger nanoclay cluster increases. Hence, the dispersion mechanism may be adversely affected when too much energy is given to the nanoclay platelets. Therefore, an optimum sonicating time must be achieved in order to have the maximum dispersion ability.

Thirdly, just like the sonicating mechanism, the reacting temperature affects the dispersion effects of the NC mixtures by providing energy to the nanoclays. When the reacting temperature is increased, so does the energy for each nanoclay platelets to break apart from others. Thus, increasing the reacting temperature of the NC mixtures increases the tendency for the nanoclay platelets to break the bonding and enhances the dispersion effects.

Finally, gas bubbles inside the NC mixtures also deteriorate the mechanical properties as the bonding between the nanoclay clusters and epoxy is altered. Hence, vacuuming the NC samples is significant to ensure that the mechanical properties of the NCs have not been adversely affected. As a result, it is important to control the vacuuming time of the NCs.



Therefore, the mechanical property tests conducted in this project were based on studying these four factors that would affect the mechanical properties of resultant composites.

Chapter 2 presents the literature review on recent works on nanocomposites and illustrates the structure and building blocks of nanoclays. The method of exfoliation of nanoclay platelets in epoxy is observed, such as, by adding organic solvents. Moreover, the study of mechanical properties of the NCs from previous researches is shown.

Chapter 3 describes the methods used to characterize the materials properties of the NCs, they are (i) x-ray diffraction (XRD), (ii) scanning electron microscopy (SEM) and (iii) energy dispersive x-ray analysis (EDX). They are important to characterize the internal structure of the NCs before carrying out mechanical property tests.

In Chapter 4, the mechanical properties of the NCs are studied. Mechanical property tests that were employed in this project are introduced and explained in detail. The principles and the apparatus of Vickers micro-hardness test, ultrasound



sonication, wear resistance test and nanoindentation are presented. Experimental results of the mechanical properties of the NCs with nanoclay clusters are demonstrated. The mechanical properties of the NCs by introducing nanoclay clusters are then explained from the results obtained. The chapter concludes with an explanation of the optimization effects by the nanoclay clusters in the NCs.

After measuring the mechanical properties of intercalated nanoclay clusters in the NCs, several mathematical models use to predict the mechanical properties of the NCs with intercalated nanoclay clusters are established in Chapter 5. Mathematical models of Vickers micro-hardness, wear resistance and creep mechanism of the NCs with intercalated nanoclay clusters are proposed. In addition, the effect of thermo-mechanical mixing energy in the preparation of the NCs is modeled. Finally, the formation of intercalated nanoclay clusters is also explained mathematically. From the mathematical model constructed in this chapter, the behavior of intercalated nanoclay clusters in the NCs can be understood and predicted.

Chapter 6 concludes the project and proposes future possible research areas.



2. LITERATURE REVIEW

The development on mechanical, bio-medical engineering and aeronautical components has recently been miniaturized into different scale levels. Because of the increasing need of micro/nano-sized devices and structural members in nano-tech and space industries, the development of new advanced materials which are able to sustain their strength despite extreme temperatures and in all chemical environments without being mechanically, chemically or thermally degraded and to be manufactured to high degree of defect-free properties, particularly for space and automotive applications will become a challenge in this decade.

In the past few years, National Aeronautics and Space Administration (NASA) and John Space Centre (JSC) have driven breakthrough technologies to expand human exploration of space. The goal is to develop new materials with strength-to-weight ratio that far exceeds any of today's materials. Nanocomposites have emerged as a very efficient strategy to upgrade properties of synthetic polymers to the level where performance of these nanocomposites exceed those of conventional composites. Veprek et al. have found that



nanocomposites exhibit superior hardness and elasticity, and a high level of thermal stability. Carbon nanotubes and nanoclays have been recognized as the best nano-fillers for the polymer-based composites to fulfill these requirements by Lau et al.. Bradley et al. have stated that successful use of nanotube/polymer and nanotube/metal composites in space applications is dependent on the structural integrity and mechanical performances of the composites at extreme low temperatures, under heat and radiation, and in vacuum environments, particularly for reusable launch vehicles. However, Lau et al., Schadler et al., Sandler et al. and Qian et al. have reported that the nanotubes do not bond well to aerospace-used polymer matrices because of their perfect hexagonal atomic architecture on the nanotubes' surface. Zhou et al. and Lau et al. have proven that a good bonding strength between internal reinforcements and matrix is a dominant factor in the outstanding mechanical properties of advanced composite structures. By using chemical catalysts to improve the bonding strength of composite systems, may damage the carbon-carbon bond that accounts for the extraordinary mechanical and electrical properties of nanotubes.

LeBaron et al. and Alexandre et al.. have found that commercial organoclays (layered silicates such as montmorillonite which has a fairly large aspect ratio,

hereafter called “nanoclays”) could be used to make aerospace epoxy nanocomposites with excellent mechanical strength and low coefficient of thermal expansion at relatively low cost and ease of fabrication. Companies such as Nanocor, Southern Clay Products and Zhejiang Fenghong Clay Chemicals Co. in the United States, Japan and China have patented technologies for the production of nanoclays. Fig. 2.1 shows the schematic atomic structure of nanoclays by Ray et al..

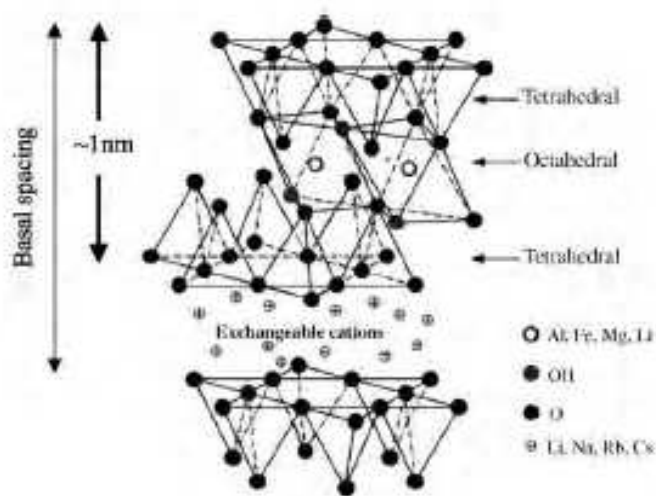


Figure 2.1 Schematic diagram of the atomic structure of nanoclays (Captured from Sinha Ray S. et. al., *Prog Polym Sci*, 28, 1539–1641; 2003)

Several polymer companies in the United States and Japan are producing nylon nanocomposites for automotive and packaging applications. Giannelis and Vaia et al. have reported that a few weight percentages of nanoclays with a thickness



of about 1 nm in polymer boots the heat distortion temperature by 80°C, making structural applications possible under conditions that pristine polymer would normally fail. The existence of silicate platelets inhibits the polymer chain rotation that influences the mechanical and thermal properties of the nanocomposites. Dietsche et al. found that in some cases, these platelets could inhibit the crack propagation due to the formation of micro-voids when the nanocomposites are under stress, thus increasing the fracture toughness. Alexandre et al. and Lau et al. have proven that the mechanical and thermal properties of composites could be modulated by nano-fabrication process of intermetallic compounds. A latest literature has revealed that intercalated and exfoliated morphologies of nanoclay/polymer composites are highly affected by the manufacturing time and temperature, which in turn influenced the cross-linking interaction of polymer. The amount of nanoclays inside the polymer also appeared to show different mechanical, thermal and electrical properties of nanocomposites. The permeability of water, oxygen and other gases of the nanoclay composites also decreased, making these composites ideal for building advanced composite fuel tanks for tomorrow's reusable launch vehicles. Timmerman et al. clearly demonstrated that the number of transverse cracking of carbon fibre/epoxy laminates as a response to cryogenic cycling was significantly



reduced when nano-fillers were used. The development of these polymer-based nanocomposite materials allows the manufacture of advanced structures with high strength and thermal stability. It thus minimizes the risk of geometrical and thermal distortions caused by changes in the ambient temperature and therefore maintains the aerodynamic profiles of the structures. Because the layered silicate nanocomposites achieve composite properties at much lower volume fraction of reinforcements, they avoid many of the costly and cumbersome fabrication techniques common to conventional fibre-reinforced polymer materials.

Ke et al. and Song et al. claimed that the appropriate addition of a small amount of nanoclays, typically in the range of 3 - 5 wt.%, could provide an efficient upgrade on the mechanical and thermal performances of conventional polymer-based composites. From an industrial point of view, the lightest particles could be used to produce greater stiffness and thermal stability in structural components at low cost and no weight penalty. Recently, many product manufacturing organizations and commercial companies have started to investigate the possibility of producing this type of nanocomposites in order to fabricate plastic products with high strength and low thermal distortion. However, these properties depend on the dispersion property and inter-planar arrangements

of nanoclays inside the composites, as reported by Sinha Ray et al..

Wetzel et al. and Ng et al. have reported that the impact and wear resistance, as well as fracture toughness of advanced composites could be improved by mixing an optimal amount of nanoclays. The optimal amount of the nanoclays in the composites depends on particle size and shape, homogeneity, dispersion property and interfacial bonding properties between the particles and matrix. Figure 2.2 shows Sinha Ray et al.'s three possible structures of nanoclays in epoxy resin.

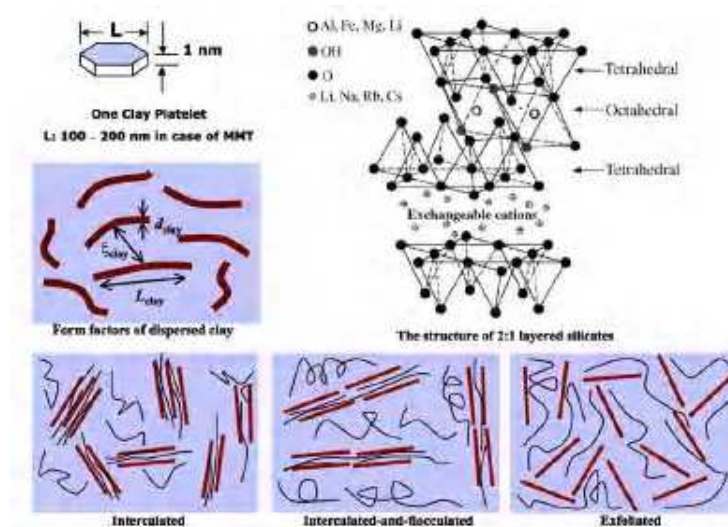


Figure 2.2 Three possible structures of nanoclays in epoxy resins (Captured from Sinha Ray S. et. al., *Prog Polym Sci*, 28, 1539–1641; 2003)

Many researchers have investigated the fully exfoliated nanoclay platelets in nanoclay/polymer mixture. They propose that fully exfoliated nanoclay platelets



can maximize the interfacial area for mechanical bonding between nanoclays and the polymer matrix. Hence, the study of intercalated nanoclay clusters in nanoclay/polymer structure has never been conducted to date. Both exfoliated and intercalated planar structures can only be found in laboratory studies, since this is difficult to achieve during the extrusion and injection moulding processes. During the processes, uneven pressure is always introduced into a nanoclay/epoxy mixture and so nanoclays tend to agglomerate into tiny nanoclay clusters in everyday manufacturing procedures.

Sheng et al. have proposed a mathematical model to estimate the mechanical properties of nanocomposites with an estimation of “effective clay particles” by multi-scale modeling techniques. Figures 2.3 and 2.4 shows the schematic diagram of an effective particle in nanocomposites and the micromechanical modeling techniques of nanocomposites reproduced from Sheng et al. respectively.



Figure 2.3 Illustration of the “matrix” and “particle” domain in (a) conventional composite and (b) nanocomposite (Captured from Sheng N. et. al., *Polymer*, 45, 487-506; 2004)

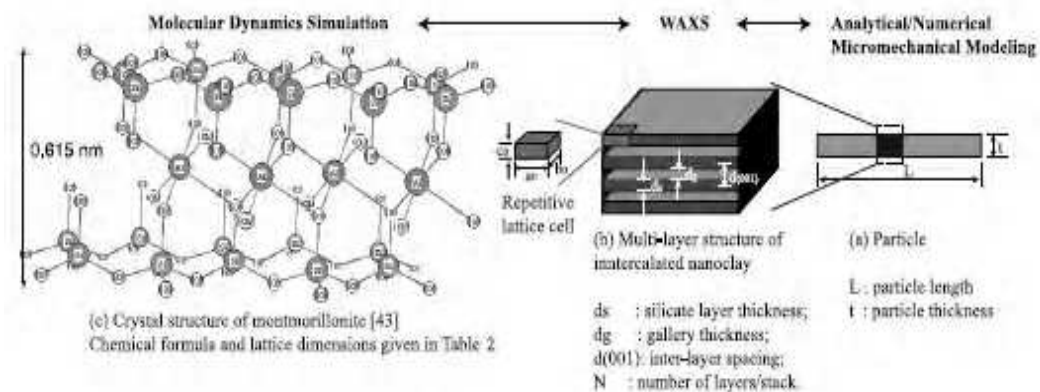


Figure 2.4 Micromechanical modeling techniques of nanocomposites with nanoclays (Captured from Sheng N. et. al., *Polymer*, 45, 487-506; 2004)

Nevertheless, the mathematical modeling is only an approximation and estimation of nanoclay clusters in polymer matrix. In real situations, the shape of intercalation and agglomeration of nanoclay clusters in polymer matrix has not been studied carefully and explained through rigorous experimental techniques.

This project is aimed at studying the mechanical performance of nanoclay/epoxy



composites (NCs) with intercalated nanoclay clusters in detail. With the XRD, SEM and EDX material characterization techniques, the formation, size and shape of nanoclay clusters in the NCs will be explained by changing the manufacturing parameters. Vickers micro-hardness, wear resistance and creep mechanism will be conducted on NC samples for the visualization of the mechanical performance by the inclusion of nanoclay clusters in the NCs. The nucleation of nanoclay clusters in the NCs will be explained by the nucleation theory. Distribution of nanoclay clusters in the NCs will be examined by the use of nanoindentation.

Mathematical models will be proposed for the estimation of the mechanical properties of the NCs with intercalated nanoclay clusters. The importance of the thermo-mixing process during the production of the NCs will be analyzed by using Flory's principle. The creep mechanism of the NCs with intercalated nanoclay clusters will be studied by nanoindentation and modeled extensively with the aid of the Kelvin-Voigt model.

Through the studies of the agglomerated nanoclay structures in epoxy resins, the significance of intercalated nanoclay clusters in the NCs can be understood and



thus help industrialists to decide every engineering procedure of NC products according to the models and findings in this project.



3. MATERIALS CHARACTERIZATIONS

It is important to illustrate the materials characterizations used in the project since they are the major analyzing tools for the determination of the degree of exfoliation of the nanoclays inside NCs. Besides, surface imaging of NC samples is significant to visualize the morphology of nanoclays inside and thus aid the establishment of mathematical analysis and theoretical interpretation of the optimization of mechanical properties of the NCs.

3.1 X-RAY DIFFRACTION (XRD)

X-ray diffraction is a material characterization that employed the diffraction of x-ray from the reflected x-ray beams. Fig. 3.1 shows the schematic diagram of x-ray diffraction in a testing sample.

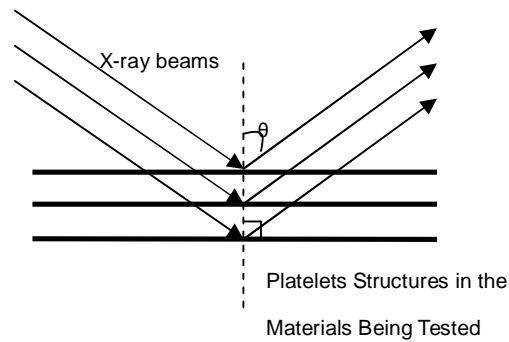


Figure 3.1 Schematic diagram of XRD

The diffraction of the x-ray beams is different in different materials depending on their interplanar structures. By collecting diffracted x-ray beams, the interplanar distances inside testing samples can be obtained by the Bragg's formula as shown in Eq. 3.1.

$$2d \sin \theta = n\lambda \quad (3.1)$$

where d = interplanar distance in the material structures

θ = angle between the diffracted x-ray beams and the interplanar structure (Bragg's angle)

λ = wavelength of x-ray beams



For different materials, their angle of diffraction is different for different interplanar structure arrangements. Hence, XRD is commonly employed for the identification of components in materials.

In this project, XRD was used to determine the degree of exfoliation of nanoclay platelets in the NCs. According to the Bragg's formula, as λ was fixed in experiments, the degree of exfoliation of nanoclay platelets was directly proportional to the interplanar distance and inversely proportional to the Bragg's angle in Eq. (3.1). Therefore, for fully exfoliated NCs, the Bragg's angle detected should tend to zero and vice versa.

3.2 SCANNING ELECTRON MICROSCOPY (SEM)

Scanning electron microscopy (SEM) was used in this project to visualize the surface morphology of NC samples. It helped to identify to size and location of nanoclay clusters in NCs. In a SEM experiment, the reflected electron beams are collected from the testing sample as shown in Fig. 3.2.

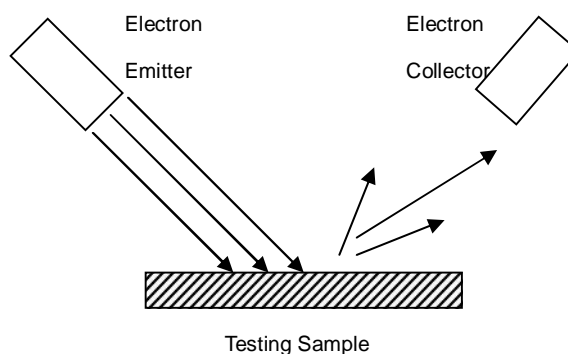


Figure 3.2 Schematic diagram of SEM

The electron emitter produced parallel electron beams and emitted them on the testing samples. As the surface of the testing sample has certain imperfections and roughness, the reflected electron beams must have certain degree of diffractions when arriving the electron collector as shown in Fig. 3.2. As a result, by scanning over the surface of the testing samples, a diffracted pattern of



electron beams according to the surface roughness of the testing sample is collected. The pattern is interpreted by the computer and the surface image of the testing sample is then generated.

However, the surface of the testing sample must be conductible for the effective reflection of electrons. Thus, for SEM imaging of the surface of NCs, a thin layer of gold coating must be placed on the surface before testing. Since the thickness of the gold coating was only several nanometers, therefore, it did not affect the outcome of the resulting SEM imaging.

3.3 ENERGY DISPERSIVE X-RAY (EDX)

Energy dispersive x-ray (EDX) is a method to identify the element composition of the point being tested. EDX is commonly built in a SEM machine. Fig 3.3 shows the schematic diagram of EDX.

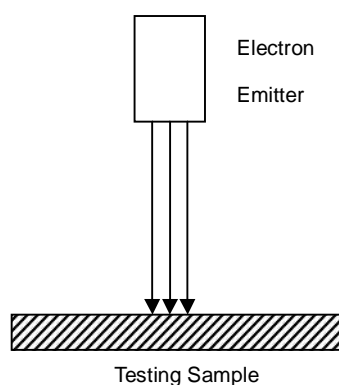
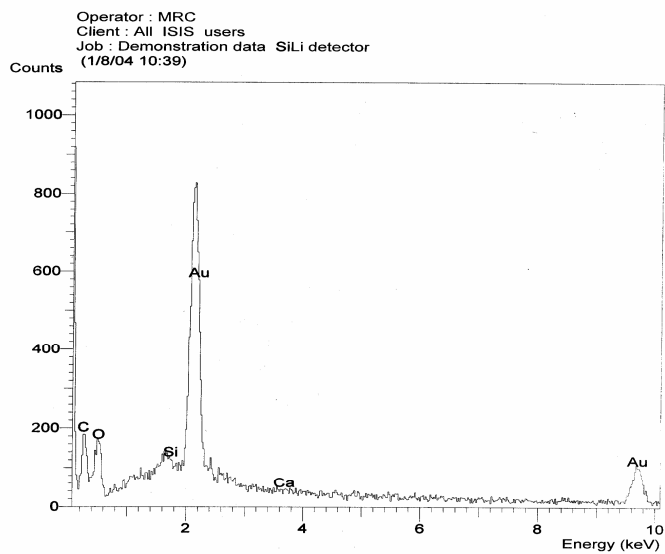
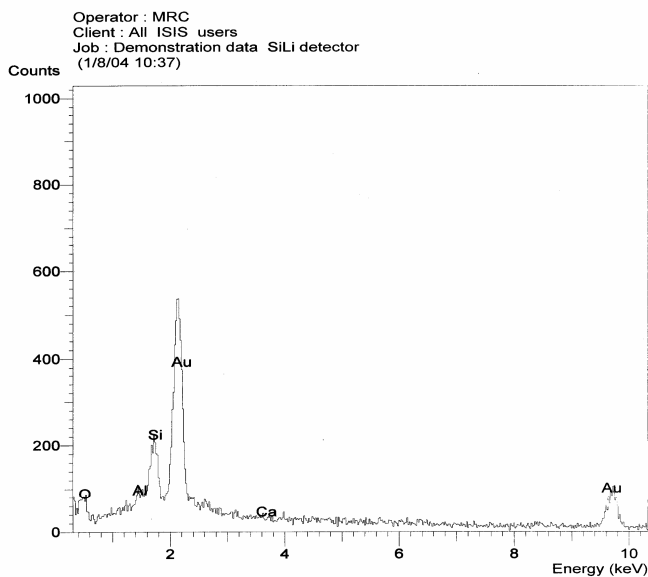


Figure 3.3 Schematic diagram of EDX

From Fig. 3.3, only one point of the testing sample can be tested on the element composition at each time. Therefore, it can help to identify the location of nanoclay clusters inside NCs. Fig. 3.4 shows the typical graph of EDX if a nanoclay cluster was hit. The Si content was higher at the nanoclay clusters as silicate was the major component of nanoclays.



(a)



(b)

Figure 3.4 EDX image (a) away from nanoclay cluster (b) at the nanoclay cluster



4. MECHANICAL PROPERTIES OF NANOCLAY/EPOXY COMPOSITES

In this chapter, the results from different mechanical property tests of NCs with nanoclay clusters are presented. Before moving on discussing the details of the results, it is absolutely important to understand the basic principles of the mechanical property tests as they are the backbones of interpretation of the testing results.

4.1 MATERIALS

Nanoclay particles (SiO₂ Nanolin DK1 series from the Zhejiang Fenghong Nanoclay Chemical Technology Company) were used as nano-reinforcements for polymer in this study. The mean diameter, density and moisture content of the nanoclays were 25 nm, 0.45 g/cm³ and more than 95% of SiO₂, respectively. Epoxy was chosen as the resin due to its high applicability in modern engineering structures, such as the aircrafts, when mixing with nanoclays. The epoxy resin and hardener selected for this project were Araldite[®] GY 251 and Hardener HY 956 respectively. As recommended by the manufacturer, they were

mixed in a ratio of 5 to 1 parts by weight.

4.2 EXPERIMENT PRINCIPLES AND APPARATUS FOR MECHANICAL PROPERTY TESTS

4.2.1 VICKERS MICRO-HARDNESS TEST

Vickers micro-hardness test was used to examine the micro-hardness of NCs with different preparation treatments. The Vickers micro-hardness test in this project was examined on a micro-hardness tester (FM-7E) of the Future-Test Corporation from Tokyo, Japan as shown in Fig. 4.1.

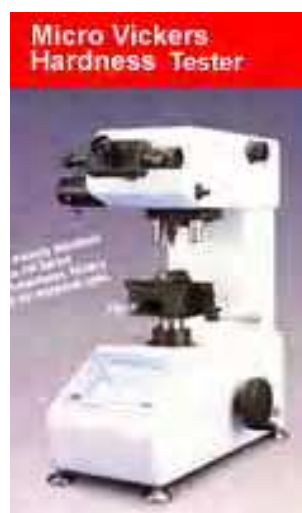


Figure 4.1 Vickers micro-hardness tester

The Vickers micro-hardness test makes use of creating an indent on the surface of the testing sample with a diamond indenter with 136° separations between the indenter faces. Each indentation loading is between 1 to 100 kgf. The holding time for full load on the sample surface is normally 10 to 15 seconds. A rhombus-like indent is left on the sample surface with 2 apparent diagonals. The area of the indent is then obtained. Fig. 4.2 is a schematic diagram illustrates the parameters of Vickers micro-hardness indenter.

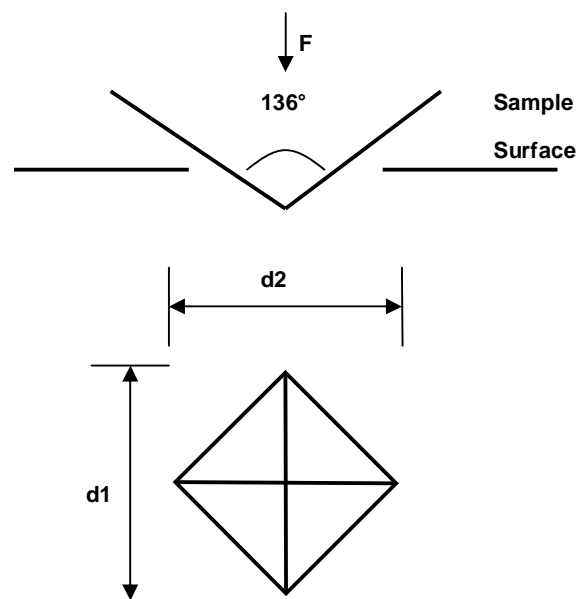


Figure 4.2 Parameters of Vickers micro-hardness test

The Vickers micro-hardness is the quotient between the indentation force and indentation area according to Eq. (4.1).



$$HV = \frac{2F \sin\left(\frac{136^\circ}{2}\right)}{d^2} \quad (4.1)$$
$$HV \approx 1.854 \frac{F}{d^2}$$

F = Load in kgf

d = Arithmetic mean of the two diagonals, $d1$ and $d2$ in mm

HV = Vickers hardness

For the conversion from HV into SI unit (MPa), the force needs to change from kgf into N and the area change from mm^2 to m^2 . Eq. (4.2) shows the conversion factor from HV to MPa.

$$1\text{MPa} = 9.807\text{HV} \quad (4.2)$$

There are other micro-hardness testing units, for example, Knoop micro-hardness, while Vickers micro-hardness was employed for the micro-hardness test in this project.

4.2.2 ULTRASOUND SONICATION TEST

Dispersion by ultrasound is a consequence of microturbulences caused by fluctuation of pressure and cavitation. Ultrasound sonication was used in this project to disperse the nanoclays inside NCs evenly. It is a technique makes use of the energy of ultrasonic waves to cause the nanoclays to move around in the untrasonic frequency as shown in Fig. 4.3.

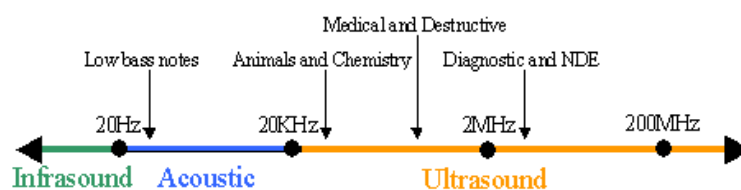


Figure 4.3 Ultrasound frequency spectrum

The reason for employing ultrasound to disperse nanoclays instead of mechanical stirring is due to the fact that the dispersion of nanomaterials can be hardly achieve by only traditional mechanical stirring. As the highest mechanical stirring frequency must be much lower then the ultrasonic frequency as shown in Fig. 4.3 and the size of nanoclays are nanometric, therefore, ultrasound can provide a more even dispersion for the nanoclays in the NCs.

4.2.3 ABRASIVE TEST

Wear resistance of the NC samples was obtained from abrasive test performed on the circular NC samples with 4-inches in diameter in a 5131 Abraser of Taber Industries, North Tonawanda, N. Y., USA as shown in Fig. 4.4.

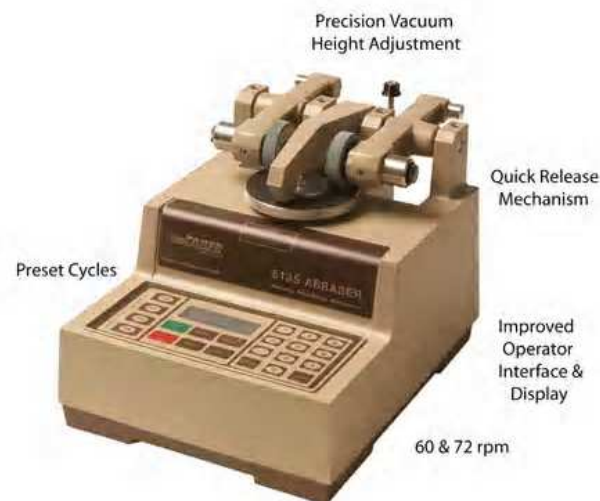


Figure 4.4 Abrasive test machine

Up to 0.5 inch thick specimens, were mounted to a rotating turntable and subjected to the wearing action of two abrasive wheels, which were applied at a specific pressure.

Characteristic rub-wear action is produced by contact of the test sample, turning on a vertical axis, against the sliding rotation of two abrading wheels. The wheels are driven by the sample in opposite directions about a horizontal axis displaced tangentially from the axis of the sample. One abrading wheel rubs the specimen outwardly towards the periphery and the other, inwardly towards the center. The resulting abrasion marks form a pattern of crossed arcs over an area approximately 30 square centimeters. Fig. 4.5 illustrates the abrasive testing mechanism.

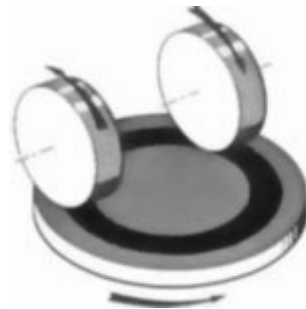


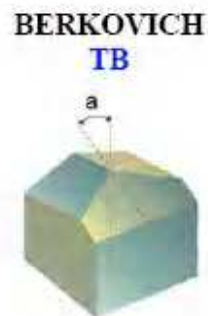
Figure 4.5 Abrasive testing mechanism

4.2.4 NANOINDENTATION TEST

The nanoindentation experiment in this project was carried out in a Hysitron Triboindenter with a Berkovich indenter. Fig. 4.6 and 4.7 show an example of nanoindenter and the specification of a Berkovich indenter respectively.



Figure 4.6 Nanoindenter sample



Berkovich: $a = 65.03^\circ$
Mod. Berkovich: $a = 65.27^\circ$
Available as
Traceable Standard

Figure 4.7 Berkovich indenter specifications

Fig. 4.8 shows the diagram of Hysiton Triboindenter that was used in the project.

It has an anti-noise platform for the testing samples that avoids any environmental vibrations which may cause inaccuracies in the data obtained.

Thermal drift is automatically rectified in the nanoindentation system. A thermal

enclosure also provides a thermal stable environment to ensure the testing quality.



Figure 4.8 Hysitron triboindenter

Nanoindentation is a newly invented technique for the determination of localized material properties that was introduced by Oliver and Pharr in 1992. Elastic modulus, nano-hardness and contact stiffness of a material can be determined by nanoindentation nanoscopically. Fig. 4.9 shows a typical nanoindentation profile for determination of localized mechanical properties in polymer composites.

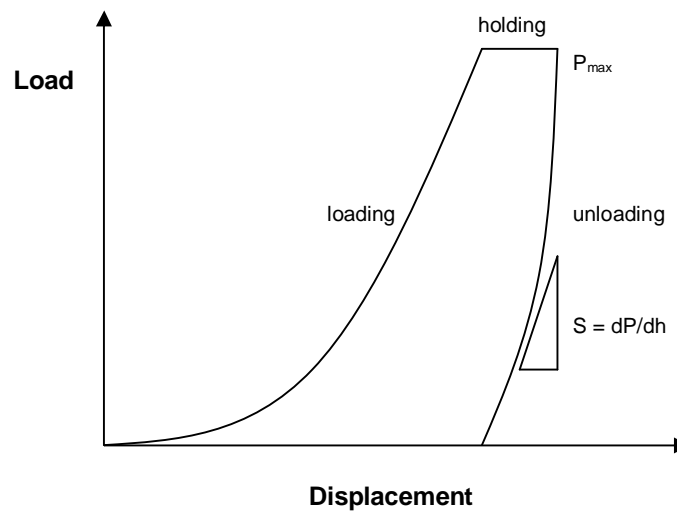


Figure 4.9 Nanoindentation profile

This technique makes use of creating a permanently plastically deformed surface on a material being tested. Based on the force applied on the surface and the indentation depth of the indent, relative elastic modulus can be obtained by the equations given as,

$$A_c = f(h_c) \quad (4.3)$$



$$E_r = \frac{\left(\frac{\sqrt{\pi}}{2}\right)}{\left(\frac{S}{\sqrt{A_c}}\right)} \quad (4.4)$$

where h_c is the contact height, A_c is the contact surface area between the nanoindenter and the material surface and S is the contact stiffness that is the slope of the unloading portion in the nanoindentation profile as shown in Fig.

4.9.



4.3 SAMPLE PREPARATION FOR MECHANICAL PROPERTY TESTS

In this section, NC sample preparation procedures for different mechanical property tests are described in detail.

4.3.1 VICKERS MICRO-HARDNESS

The NC samples were fabricated by using mechanical mixing process with different amount of nanoclays, 0 wt.% (NC-0), 2 wt.% (NC-2), 4 wt.% (NC-4), 6 wt.% (NC-6), 10 wt.% (NC-10) and 15 wt.% (NC-15). The predetermined amount of nanoclays were dispersed into epoxy resin. The mixtures were hand stirred for 10 minutes until the epoxy resin and the nanoclays were well mixed at room temperature. Ultrasound sonication was employed to further disperse the nanoclays into the resin. The sonication time was fixed at 20 minutes for all samples in order to ensure their maximized mechanical properties as reported from literatures. Hardener was added into sonicated mixtures by hand stirring and followed by vacuuming for 24 hours at room temperature for curing. To increase the accuracy of measurement, all sample's surfaces were well polished using high-grade sandpapers prior to the test.



4.3.2 ULTRASOUND SONICATION

At the beginning of manufacturing process of the NC samples, 4% of nanoclays were added into the resin by hand stirring and followed by different sonicating time, namely, 5 minutes, 10 minutes, 15 minutes, 30 minutes and 60 minutes at room temperature. The hardener was then added into the mixtures by mechanical stirring and followed by vacuuming for 24 hours for curing. To increase the accuracy of measurement, all sample's surfaces were well polished using high-grade sandpapers prior to the test.

4.3.3 WEAR RESISTANCE

The NC samples were fabricated by using mechanical mixing process with different amount of nanoclays, 0 wt.% (NC-0), 1 wt.% (NC-1), 2 wt.% (NC-2) and 4 wt.% (NC-4). The dispersing and vacuuming procedures were the same as mentioned in section 4.3.1. After hardener was added, the abrasive testing NC samples were prepared by curing them in same grade of surface-treated circular polypropylene discs with 4-inches in diameter.



4.3.4 NANOINDENTATION

4.3.4.1 Nanoclay Clusters Distribution

The NC samples were fabricated by mechanical mixing process with specified nanoclay content. The mixture was hand stirred by a glass rod for 10 minutes until the epoxy resin and the nanoclays were well mixed in room temperature. Ultrasound sonication was employed to further disperse the nanoclays in the epoxy resin. Before sonicating the NC samples, each of them was subjected to a different level of preheating in order to study the dispersion effect of the localized elastic modulus at different temperature. Three types of NC samples were fabricated in this study; they were NCs with 40°C, 80°C and 100°C preheating for 5 minutes before ultrasound sonication. The preheating was done on an electronically controlled thermo heater. After the preheating, the dispersing and vacuuming procedures were the same as mentioned in section 4.3.1. All of the NC samples were subjected to fine polishing by SiC paper and followed by diamond paste polishing to 6 μm accuracy before nanoindentation in order to ensure the reliability of the results obtained.



4.3.4.2 Creep Mechanism

The NC samples were fabricated by using mechanical mixing process with different amount of nanoclays, 2 wt.% (NC-2), 4 wt.% (NC-4), 6 wt.% (NC-6) and 8 wt.% (NC-8). The dispersing and vacuuming procedures were the same as mentioned in section 4.3.1. The nanoindentation specimens were made by cutting the samples to 18mm x 3mm x 3mm by size before polishing. All of the NC samples were subjected to fine polishing by SiC papers and followed by diamond paste polishing to 6 μm accuracy before nanoindentation in order to ensure the reliability of the results obtained.

4.4 EXPERIMENTAL RESULTS

Before conducting the mechanical property tests on NC samples, material characterization examinations were carried out to ensure the internal structures of the NC samples were in the form of intercalated nanoclay clusters. As the dispersion and curing procedures were the same in all of the NC samples, therefore, XRD and SEM results were applicable to all of the NC samples in this project.

4.4.1 X-RAY DIFFRACTION (XRD)

XRD was conducted on NCs and pure nanoclays and the results are shown in Fig. 4.10. In the figure, one peak in the XRD at $\theta = 18.8^\circ$ is shown. By using the Bragg's formula, $2d\sin\theta = n\lambda$, the interplanar distance between nanoclay platelets was 0.239 nm approximately. For a fully exfoliated NC sample, the angle 2θ in the XRD spectrum should be as small as possible in order to achieve the largest interplanar separation between the nanoclay platelets. Hence, there should be no obvious peaks in the XRD spectrums of totally exfoliated NC samples. Therefore, all of the nanoclay platelets of the NC samples in the experiments were

intercalated.

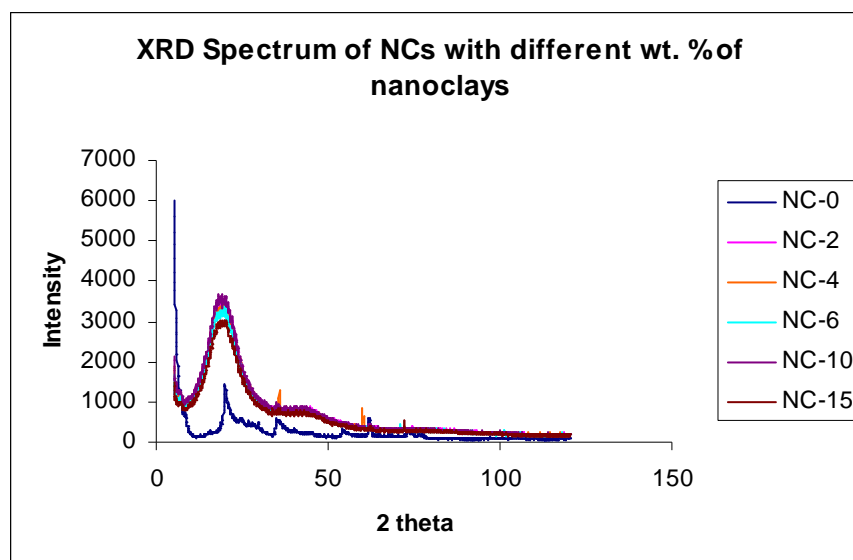


Figure 4.10 XRD spectrum of NCs with different wt.% of nanoclays

4.4.2 SCANNING ELECTRON MICROSCOPY (SEM)

In Figs. 4.11 to 4.13, morphological observations on the fractured surfaces of the NC samples with different nanoclay contents are shown. It is obvious that clusters were formed in the sample with 4 wt.% nanoclays. The average diameter of the clusters measured throughout the whole sample at different EDX verified locations was about 125 nm. The clusters were evenly distributed throughout the sample, which reflected that those small nanoclays intended to agglomerate with

each other to form clusters.

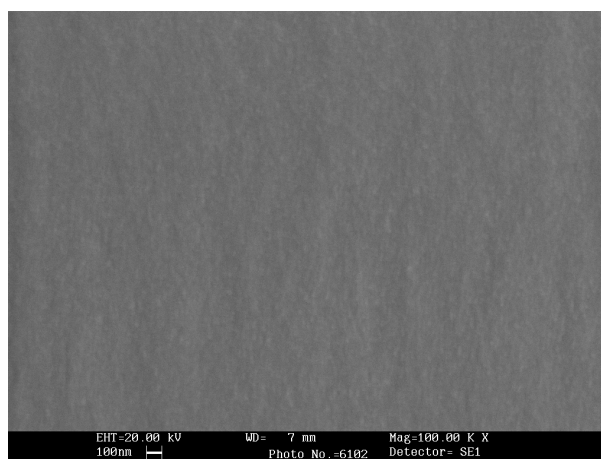


Figure 4.11 SEM photograph of pure epoxy

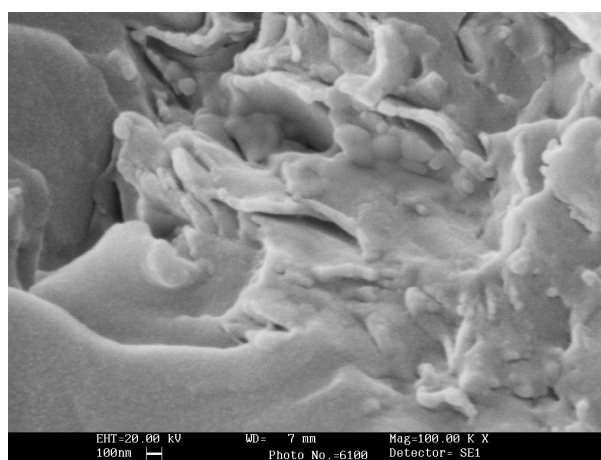


Figure 4.12 SEM photograph of 4 wt.% of NCs

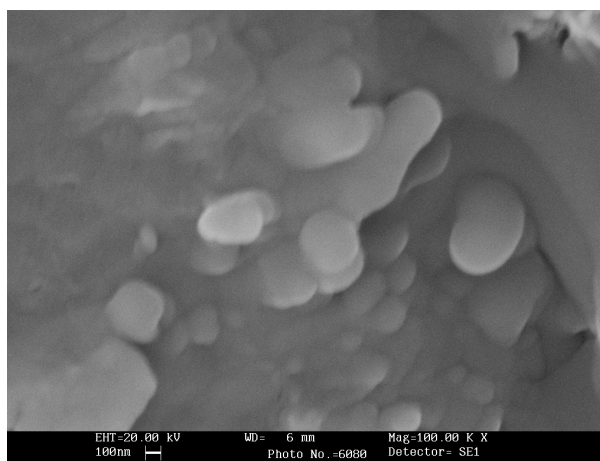


Figure 4.13 SEM photograph of 15 wt.% of NCs

This phenomenal observation denotes that those nanoclays could not be easily dispersed although it was subjected to sonication. This was due to the fact that the viscosity of the room temperature cured epoxy was too high to allow the diffusion of monomers into planar structures of the nanoclays. Thus, the agglomeration of nanoclays was resulted during the curing process. The nanoclays moved toward each others and partly bond with epoxy matrix to form clusters. The size of the clusters is dependent on the amount of nanoclays inside the uncured matrix. In Fig. 4.13, a micrograph of the sample with 15 wt.% of nanoclay particles is shown. Comparing with Fig. 4.12, the size of the clusters was apparently bigger than that of the one with only 4 wt.% nanoclays. The diameter of the clusters in the NC sample with 15 wt.% of nanoclays measured



from the SEM was about 400 nm. In fact, this phenomenon is explainable. As the wt.% of the nanoclays increases, the free volume allows nanoclays to move around would be decreased. Therefore, the mechanical stirring and ultrasound sonication cannot be effectively used to separate the agglomerations of the nanoclays, as higher the wt.% of nanoclays in the epoxy, the less the free volume for each nanoclays to live in. At the same time, the cross-link density of the NCs is then increased and it therefore results in increasing the tendency for the nanoclays to form pairs or clusters. As the amount of nanoclays increases in the composites, the inertia for the nanoclays to form clusters is also increased. Therefore, larger clusters of nanoclays would be easily formed. The average cluster sizes of NCs with different amounts of nanoclays are plotted in Fig. 4.14. The cluster size increases with increasing the wt.% of the nanoclays.

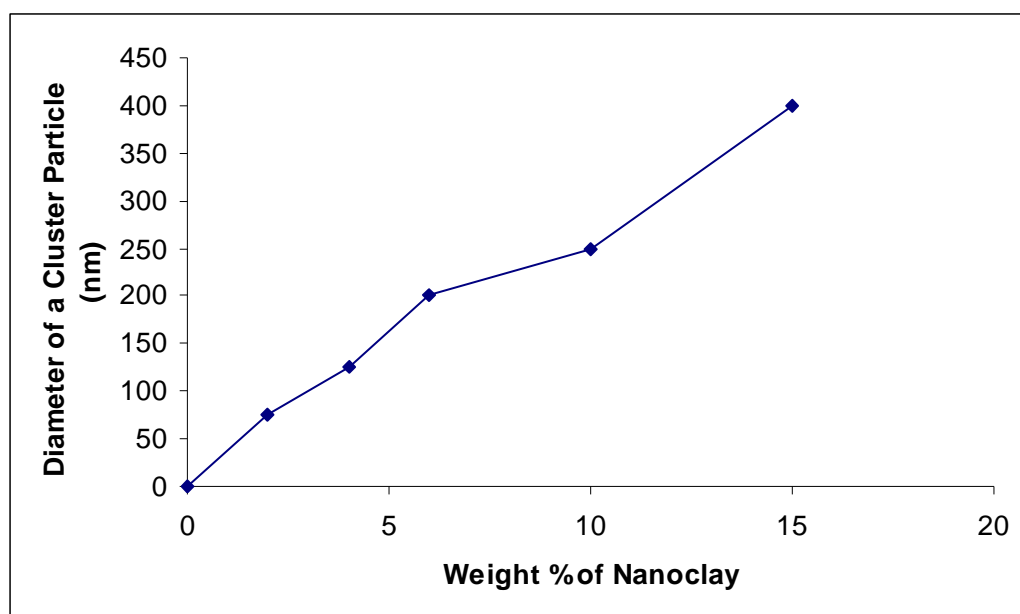


Figure 4.14 Variation of nanoclay cluster sizes in NCs with different wt.% of nanoclays

In the test for the mechanical properties of different ultrasound sonication time in the NCs, the nanoclay content was fixed at 4 wt.% of nanoclays while the sonication time was varied in this test. In Figs. 4.15 – 4.17, SEM photographs of fractured NC samples with 5 minutes, 10 minutes and 15 minutes sonicating time are shown respectively. It is obvious that nanoclay clusters were formed in all of the samples.

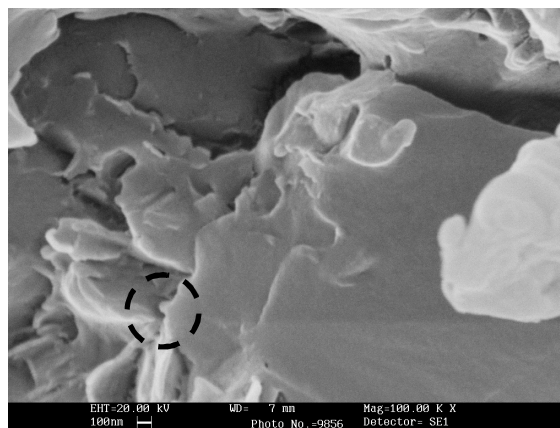


Figure 4.15 SEM of the NCs with sonicating time of 5 minutes at 4 wt. % of nanoclay content

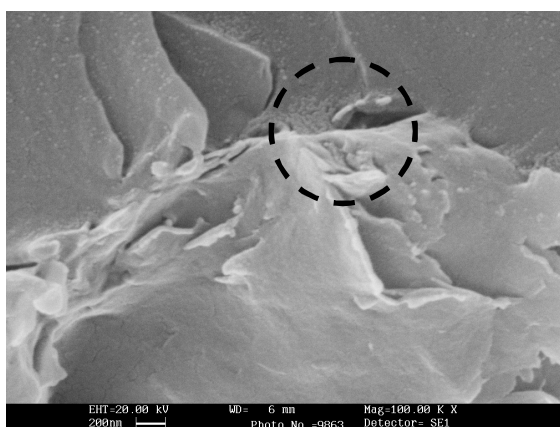


Figure 4.16 SEM of the NCs with sonicating time of 10 minutes at 4 wt. % of nanoclay content

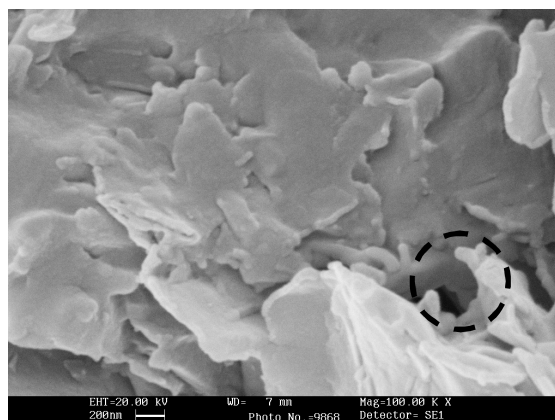


Figure 4.17 SEM of the NCs with sonicating time of 15 minutes at 4 wt. % of nanoclay content

In Fig. 4.15, SEM of the NC sample with sonicating time of 5 minutes is shown.

The size of the nanoclay clusters was about 100 nm in diameter and they were separated from each other with a longer distance as compared with other

compositions. SEM of the NC sample with sonicating time of 10 minutes is shown in Fig. 4.16. Comparing with the cluster size in Fig. 4.15, the size of the

nanoclay clusters reduced drastically to 10 nm in diameter. The distance between each cluster was shorter. Hence, the surface area for the interaction between the

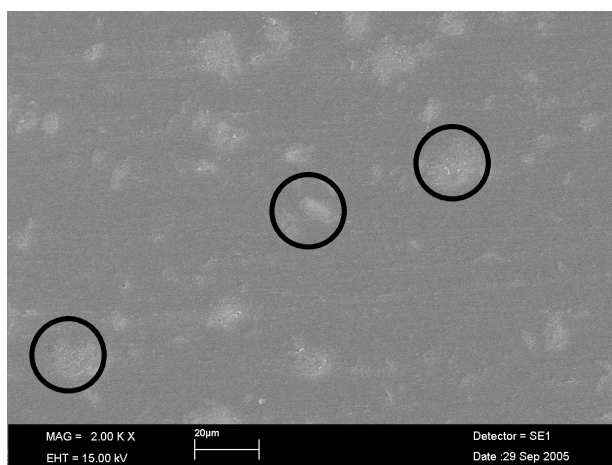
nanoclay clusters and the epoxy were increased and provided better

reinforcement in mechanical properties of the NC sample. Fig. 4.17 shows that

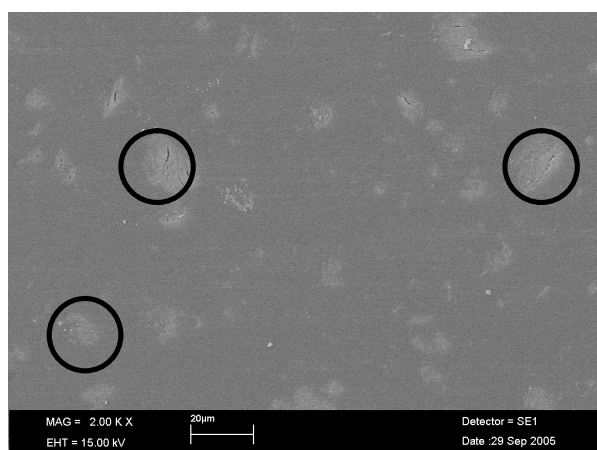
the size of the nanoclay clusters increased again at sonication time of 15 minutes

and the distance between the nanoclay clusters was also increased.

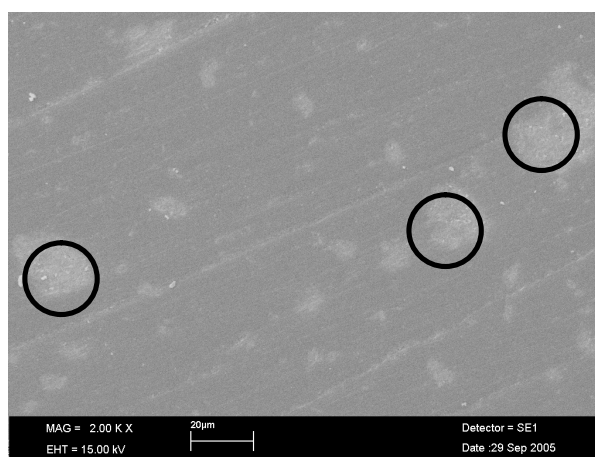
Fig. 4.18 shows the surface morphologies of the fractured surfaces of NCs treated at different sonication temperatures. Fig. 4.19 shows the EDX examinations on both circled and non-circled regions in Fig. 4.18.



(a)

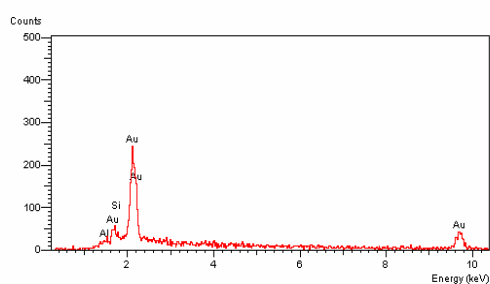


(b)

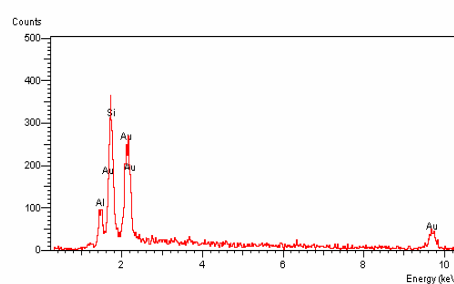


(c)

Figure 4.18 Surface morphologies of the fractured surface of NCs with different sonication temperatures, (a) 40 °C (b) 80 °C (c) 100 °C



(a)



(b)

Figure 4.19 EDX examinations on the fractured surfaces of NCs. (a) non-circled regions and (b) circled regions

It shows an obvious increase of Si content in the circled regions and thus nanoclays agglomerated in the circled regions. The size of nanoclay clusters increased while the number of nanoclay clusters decreased when the sonication



temperatures increased. This result proves that when the viscosity of the epoxy decreases with the increase of sonication temperature, nanoclays tend to form larger clusters due to less restraining force by the surrounding epoxy. They can be flowed around easily with the aid of sonication that provides extra kinetic energy for the nanoclays. The significance of increasing the kinetic energy of the nanoclays is to overcome interfacial tension between the nanoclay clusters and the epoxy.

Hence, the nanoclays inside the NCs were in the form of intercalated nanoclay clusters based on the results from XRD and SEM characterizations. Fig. 4.20 illustrates the schematic diagram of intercalated nanoclay clusters in NCs.

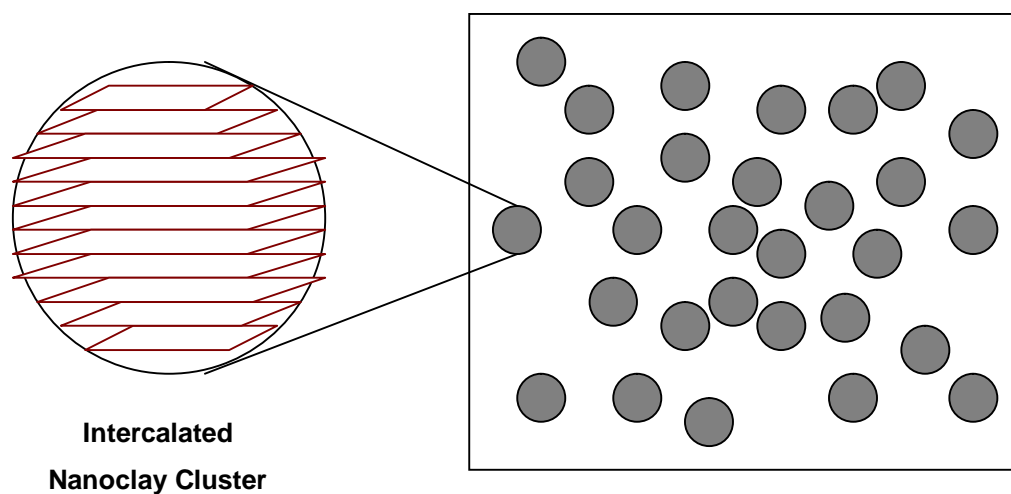


Figure 4.20 Schematic diagram of intercalated nanoclay clusters in NCs

4.4.3 VICKERS MICRO-HARDNESS

As introduced in Chapter 1, there are four parameters that control the mechanical properties of NCs during their manufacturing process. In the project, the variation of wt.% of nanoclays and sonication time of the NCs were tested on the Vickers micro-hardness.

Fig. 4.21 shows the Vickers micro-hardness for the variation of nanoclay contents in NCs. It is obvious that the hardness increased with increasing the nanoclay content. The maximum hardness was measured where the nanoclay



content at 4 wt%. A decline of the hardness also appeared if further increasing the amount of nanoclays; the hardness decreased in a drastic manner from 12.75 Hv (4 wt% of nanoclays) to 2.68 Hv (15 wt% of nanoclays). Alexandre et. al., Dasari et. al., Duquensne et. al., Kojima et. al., LeBaron et. al. and Wetzel et. al. have indicated that adding a small amount of nanoclays into polymer-based materials could potentially enhance their strength, like hardness of the current samples with the nanoclay content below 4 wt%. However, it was also reasonable to believe that it should have an optimal limit since the physical properties between these nano-structural materials and matrix were different. In the current study, it was demonstrated that the hardness was dropped if the amount of the nanoclays was beyond 4 wt%. Besides, for the sample with more nanoclay contents, the time required for solidification was also longer as well as the surface of the sample was relatively soft compared with other samples. The surface condition of the NC samples with the nanoclay content beyond 4 wt.% after curing, were sticky and remained adhering on the mold surface. It was suspected that the nanoclays might retard the chemical reaction between the hardener and resin, and cause incomplete curing process of the composites. As a consequence, for all samples beyond 4 wt.% of nanoclays, the epoxy might not be fully cured and cause the inefficiency in mechanical properties

reinforcements.

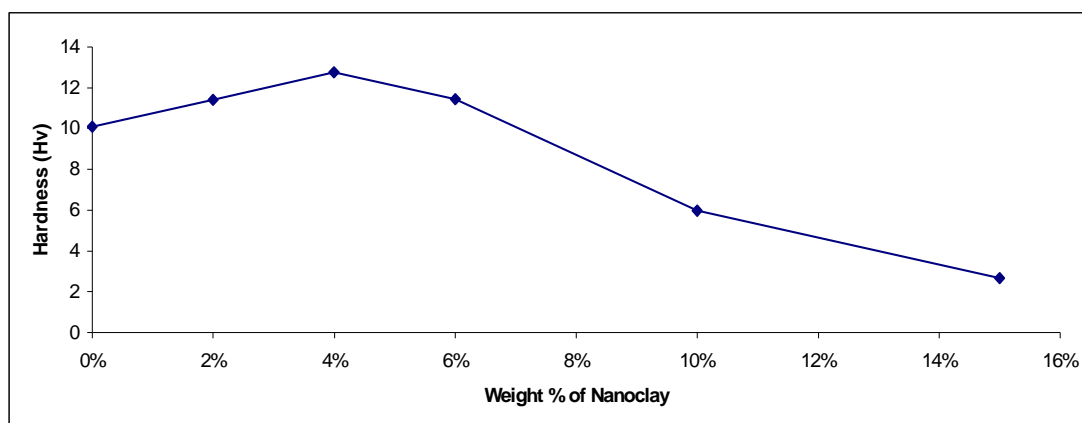


Figure 4.21 Vickers micro-hardness of NCs with different wt.% of nanoclays

Fig. 4.22 shows the micro-hardness measured experimentally of the NCs at different sonicating times. An average hardness was calculated by ten indentation measurements. As observed in the figure, there was a maximum hardness at the NCs with sonicating time of 10 minutes. The micro-hardness of the nanoclay sample was decreasing from 10.6 Hv (pure epoxy) to 9.03 Hv (5 minutes sonicating time). Further increasing the sonication time beyond the optimum time, the micro-hardness decreased gradually from 12.05 Hv (10 minutes sonicating time) to 7.09 Hv (60 minutes sonicating time). From the trend of the micro-hardness value in NC samples at different sonicating times, the time for the ultrasound sonication must be adequately controlled in order to achieve the

maximum mechanical properties of the NCs. At any sonicating time lower or higher than the optimum time, the micro-hardness is adversely affected and may be even worse than the original pure epoxy sample.

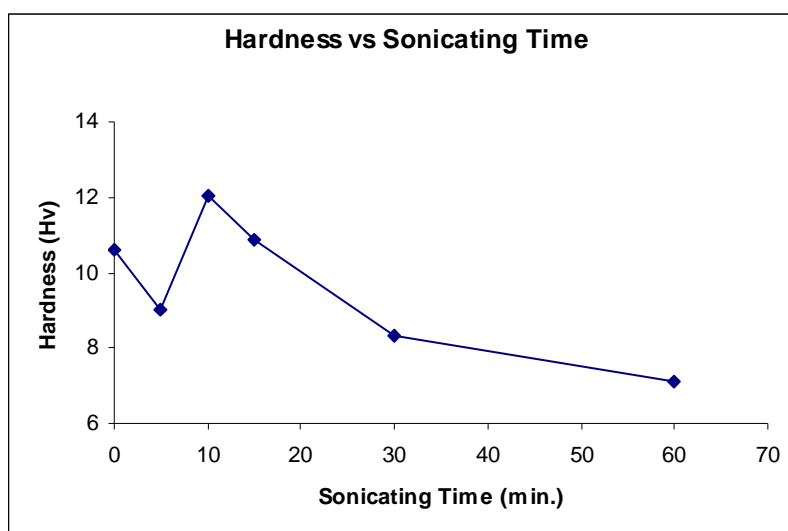


Figure 4.22 Vickers micro-hardness of NCs at different sonicating times at 4 wt. % of nanoclay content

According to the results obtained, ultrasound sonication could aid the enhancement of the mechanical properties in the NCs with properly controlling the sonicating time. Ultrasound sonication is a form of vibration that provides energy for the nanoclay platelets to escape from the surrounding restraining force. Extra energy is given to the nanoclay platelets to move around when sonicating the nanoclay/epoxy mixture. If there is not enough energy given to the mixture,



the nanoclay platelets cannot escape the restraining force within the nanoclay clusters, thus, the aid for dispersion is limited. On the other hand, if too much energy is given to the nanoclay platelets to move around, then the frequency of collision between each single nanoclay platelets is increased. The chance for each single platelet to tangle up and react to form a larger nanoclay cluster is increased. Hence, the dispersion mechanism may be adversely affected with too much energy give to the nanoclay platelets. Therefore, an optimum sonicating time must be achieved in order to have the maximum dispersion ability. Nevertheless, if there are nanoclay clusters formed, the interplanar distance of the nanoclay platelets would not be affected by the ultrasound sonication. Instead, the size of the nanoclay clusters are reduced in accompany with the increase of the number of nanoclay clusters when the optimum sonicating time is reached. Therefore, the surface area for the interaction between the nanoclay clusters and the epoxy is increased and provides the maximum reinforcement. If further increasing the sonicating time beyond the optimum value, the size of the nanoclay clusters will start growing and therefore the number of the nanoclay clusters will then decrease. Thus, the surface area for the interaction between the nanoclay clusters and the epoxy is reduced and the mechanical properties of the composites are adversely affected.



4.4.4 WEAR RESISTANCE

In the abrasive test, NC samples with different wt.% of nanoclays were tested on the wear resistance. A theoretical model of the results from the abrasive test will be demonstrated in Chapter 5.

Wear resistance of the NC samples was obtained from the abrasive tests performed on the circular NC samples with 4-inches in diameter in a 5131 Abraser of Taber Industries, North Tonawanda, N. Y., USA. The sliders were two circular-disked like silicon carbide abrasive wheels manufactured by Taber Industries. They were secured on two separate clamps with 1000 grams loading on each of the clamp and they slid on a rotating steel plate with the testing NC samples secured on it before testing. Each NC sample was subjected to 1000 grams loading with 2000 abrasive testing cycles at the same rotating velocity. The wear resistances of the NC samples were compared by the wear index calculated by Eq (4.5),

$$WI = \frac{1000(W_s - W_f)}{R} \quad (4.5)$$

where WI is the wear index, W_s (measured in grams) is the initial weight of the NC sample before testing, W_f (measured in grams) is the final weight of the NC sample after testing and R is the number of testing cycles.

Fig. 4.23 shows the test results of wear resistance of the NC samples. The higher the wear index, the lower the wear resistance and vice versa.

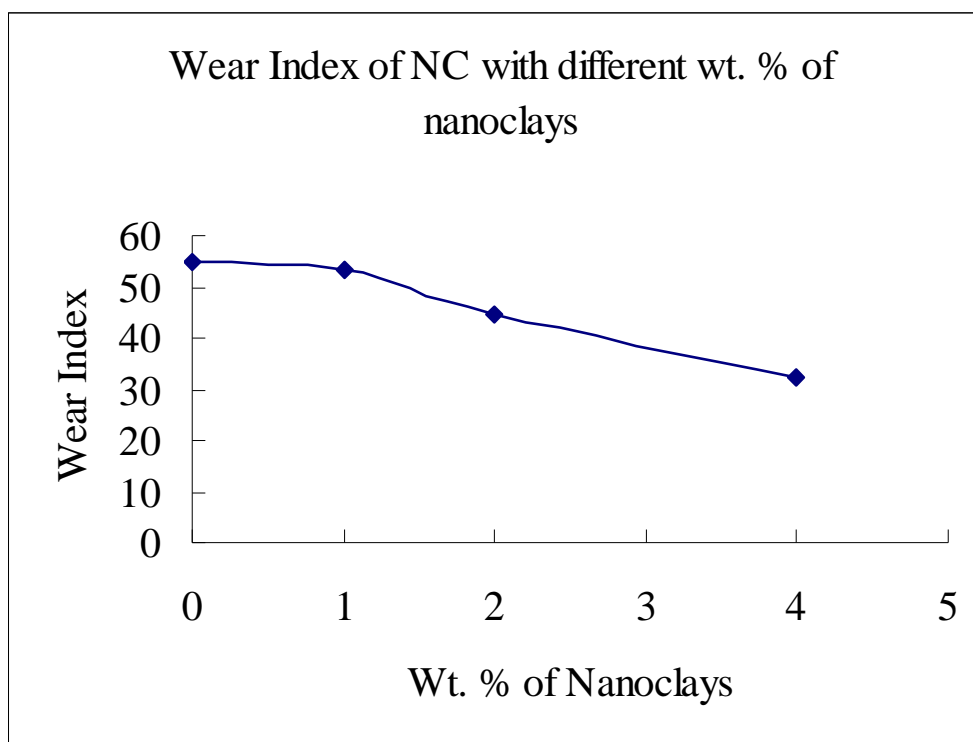


Figure 4.23 Wear index of NCs with different wt.% of nanoclays

4.4.5 NANOINDENTATION

Figs. 4.24 to 4.26 show the comparisons of the nanoindentation profiles between the bottom layer and the top layer of the cured NCs with different sonication temperatures. The preheating was controlled by an electronically controlled thermo heater as mentioned in Section 4.3.4. The comparisons of the behavior of the difference in the nanoindentation depth of the loading portion are significant as the deeper the nanoindentation depth in the loading portion, the softer the material is.

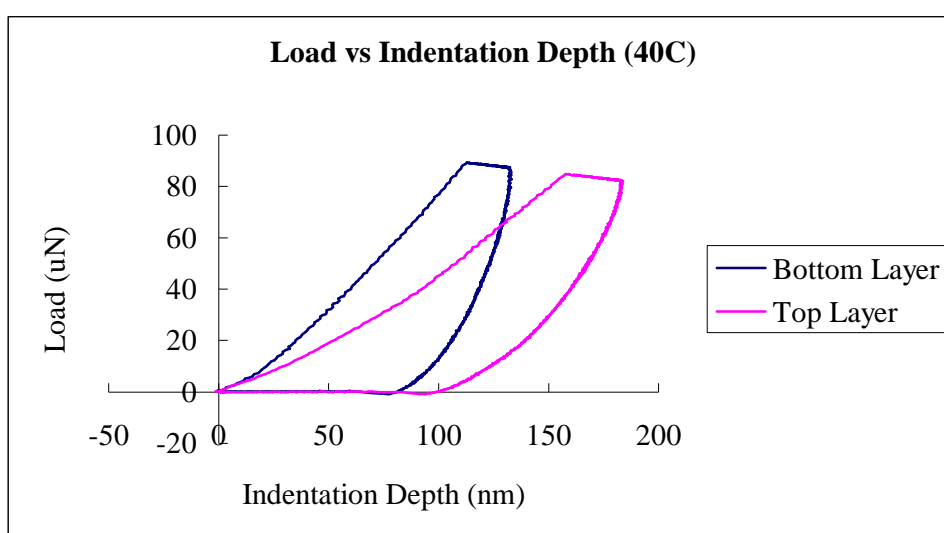


Figure 4.24 Comparisons between the top and bottom layers of the fractured surface of NCs subject to 40 °C sonication temperature

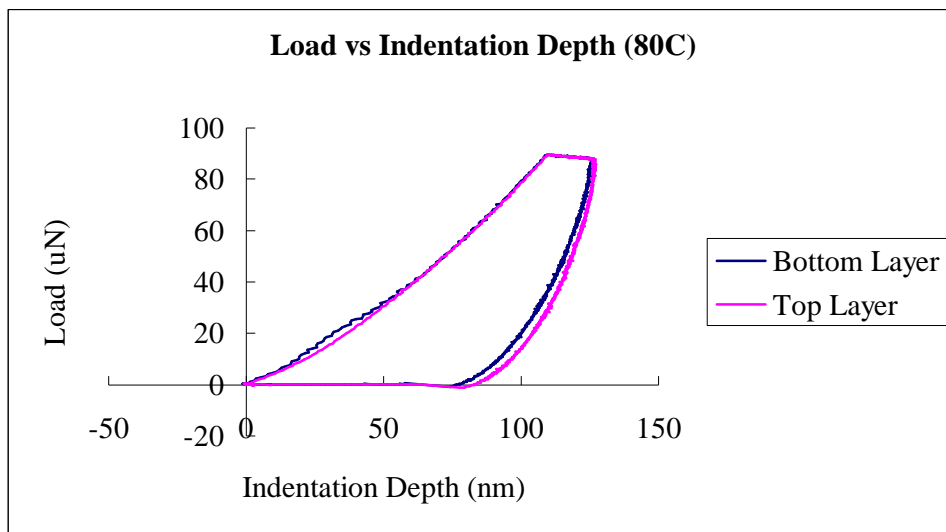


Figure 4.25 Comparisons between the top and bottom layers of the fractured surface of NCs subject to 80 °C sonication temperature

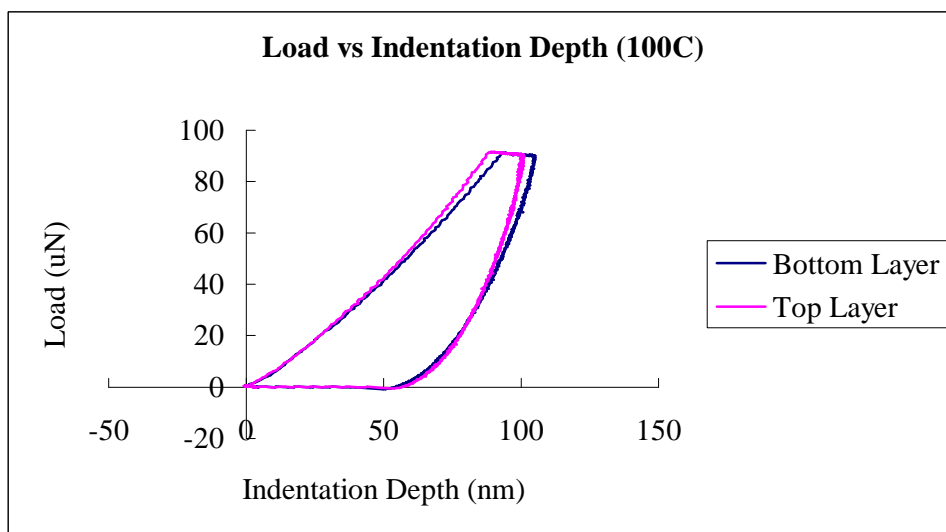


Figure 4.26 Comparisons between the top and bottom layers of the fractured surface of NCs subject to 100 °C sonication temperature

In Fig. 4.24, the nanoindentation depth increases drastically in the top layer of the NC sample when comparing with the bottom layer of the NC sample. The result



shows that the mechanical resistance of penetration of external force on the top surface of the NCs with 40°C sonication temperature treatment is much less than the bottom layer. In Figs. 4.25 and 4.26, NCs with sonication temperature 80°C and 100°C respectively, the nanoindentation depths of the top layer in each sample are almost the same as the one in the bottom layer. This concludes that the hardness of the two NCs with 80°C and 100°C sonication temperature are evenly distributed throughout the entire sample whereas in the NCs with 40°C sonication temperature, the hardness increases from top to bottom of the entire sample.

Fig. 4.27 shows the relative elastic modulus of the three NC samples calculated from the nanoindentation experiments where each testing point was separated by a length of 0.05 mm starting from the bottom portion to the top portion of the specific sample.

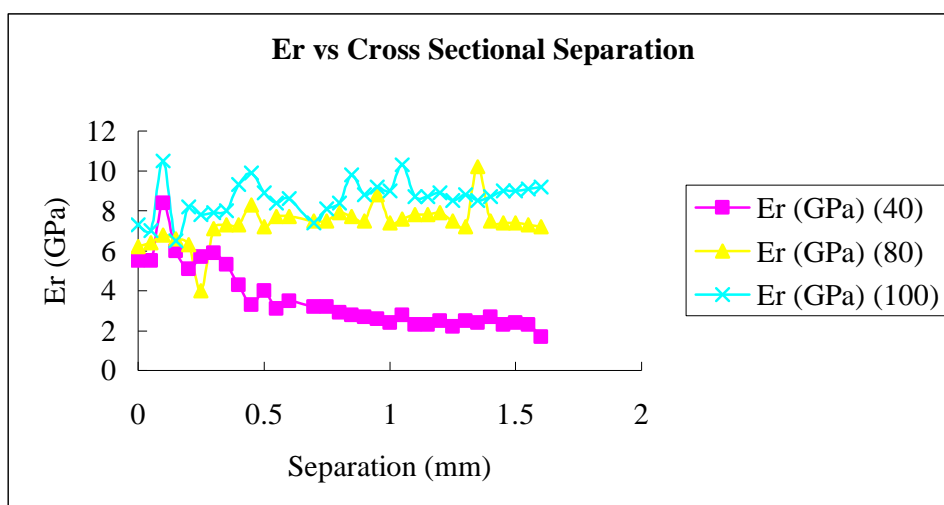


Figure 4.27 Relative elastic modulus of NCs subject to different sonication temperature treatments

The results showed that at 40°C sonication temperature, the relative elastic modulus decreases from bottom layer to the top layer of the NC sample. However, in the 80°C and 100°C sonication temperature samples, the values of relative elastic modulus are almost the same when comparing with the top and bottom layers of the NC samples. The phenomenon is due to the effect of gravity on the nanoclay clusters inside the NCs during curing in the mold. Before the NCs completely cured, the mobility of the nanoclay clusters inside the composites depends on the effect of gravity as it is the only source that causes movement when a stationary object has weight. Therefore, the nanoclay clusters are pulled downwards under gravity in an incompletely cured NCs. Nevertheless,



the curing time of epoxy resin is different if the surrounding temperature changes. At higher temperatures, the curing time of the epoxy resin must be faster than lower temperatures. As a result, at the NC sample with 40°C sonication temperature, the nanoclay clusters inside have much more time to settle to the bottom by gravity and hence there are more nanoclay clusters situated at the bottom layer of the NCs so the relative elastic modulus decreases gradually from bottom to top layer of the NC sample with 40°C sonication temperature. At higher temperature, the effect of gravity on the nanoclay clusters is limited as the curing time is faster and the nanoclay clusters can remain in a well dispersed location when cured. Thus, the relative elastic moduli of NCs are stable in the 80°C and 100°C sonication temperature samples.

There is a region with fluctuating relative elastic modulus extremely close to the bottom boundaries in all of the three NC samples as shown in Fig. 4.27. This is due to the boundary adhesion effects between the surface of the mold and surface of the NCs. Nanoclay clusters tend to concentrate near the bottom boundaries where their movements are blocked. Therefore, there is a thin layer with sudden increase of relative elastic modulus near the bottom boundaries of the three NC samples.



5. THEORETICAL ANALYSIS

In this chapter, theoretical analyses of the mechanical properties of NCs are illustrated and modeled mathematically. Proofs are given for the optimization of mechanical properties of NCs at different wt.% of nanoclays.

5.1 MICRO-HARDNESS AND WEAR RESISTANCE

A mathematical model of micro-hardness and wear resistance of NCs with different wt. % of nanoclays is developed in this section. Since micro-hardness and wear resistance of NCs are closely related to each other, therefore, they are modeled together in this section.

Fig. 5.1 shows the average hardness of different NC samples. By adding nanoclays into epoxy resin, the micro-hardness of the NCs increases proportionally with the nanoclay content up to 4 wt.%. By Zhang et al., the correlations between the inter-particle distances, diameters of the nanoparticles and wt.% of the nanoparticles in nanocomposites can be explained by Eq. (5.1).

$$\tau = d \left[\sqrt[3]{\left(\frac{\pi}{6\varphi_p} \right) - 1} \right] \quad (5.1)$$

where τ is the inter-particle distance, d is the particle diameter and φ_p is the filler content.

In this project, τ , d and φ_p represent the inter-cluster distance, the diameter of the nanoclay clusters and the nanoclay content respectively. As the micro-hardness of the NCs increases in proportion to the content of nanoclays, the diameter of the nanoclay clusters increases while the inter-cluster distance between them decreases accordingly, the micro-hardness of the NCs can be modeled as,

$$H = H_i + k_H \left(\frac{\varphi_p d}{\tau} \right) \quad (5.2)$$

where H is the micro-hardness of the NCs, k_H is the micro-hardness proportional constant and H_i is the micro-hardness of pure epoxy. Thus, Eq. (5.1) can then be rewritten as,

$$\frac{d}{\tau} = \frac{1}{\left[\sqrt[3]{\left(\frac{\pi}{6\varphi_p}\right) - 1} \right]} \quad (5.3)$$

Substituting Eqs. (5.3) into (5.2), the micro-hardness of the NCs can be determined by,

$$H = H_i + \frac{k_H \varphi_p}{\left[\sqrt[3]{\left(\frac{\pi}{6\varphi_p}\right) - 1} \right]}$$

and can be further modified into Eq. (5.4),

$$H = H_i + k_H \left[\frac{1.817 \sqrt[4]{\varphi_p}}{\left(\sqrt[3]{\pi} - 1.817 \sqrt[3]{\varphi_p}\right)} \right] \quad (5.4)$$

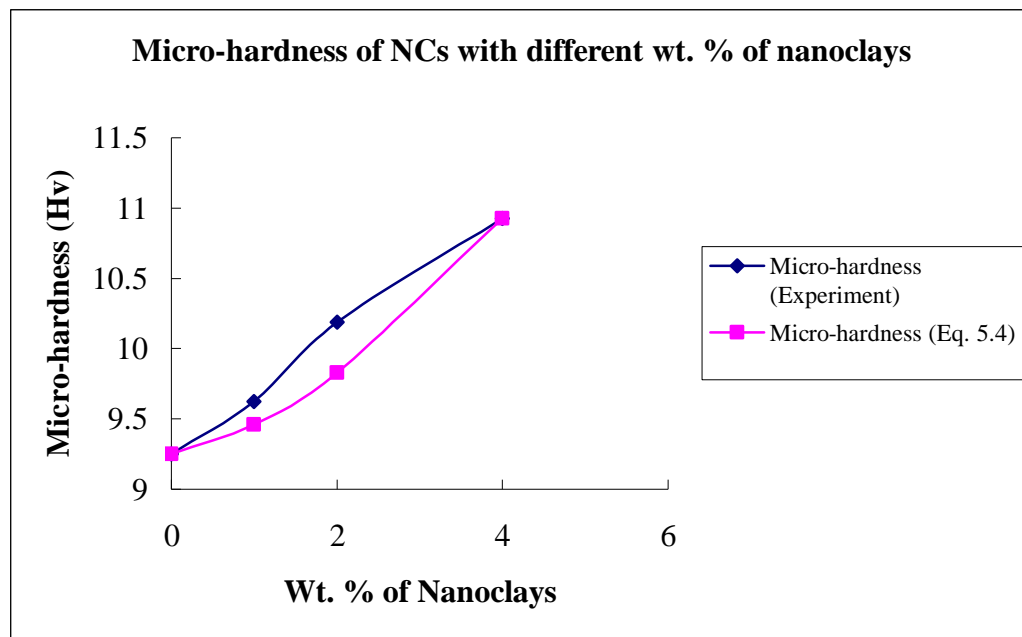


Figure 5.1 Micro-hardness of NCs with different wt. % of nanoclays

Fig. 5.2 shows the test results of the wear resistance of the NC samples. The higher the wear index, the lower the wear resistance and vice versa. Therefore, NC-4 has the highest wear resistance. As the wear resistance of the NCs increases in proportion to the nanoclay content, the wear resistance of the NCs can be co-related to the diameter of the nanoclay clusters and the inter-cluster distance from the argument as stated in Eq. (5.2) by,

$$W = W_i - k_w \left(\frac{\phi d}{\tau} \right) \tag{5.5}$$

where W is the wear resistance of the NCs, k_w is the wear resistance proportional



constant and W_i is the wear resistance of pure epoxy.

Substituting Eqs. (5.3) into (5.5), the wear resistance of the NCs can be determined by,

$$W = W_i - \frac{k_w \phi_p}{\left[\sqrt[3]{\frac{\pi}{6\phi_p}} - 1 \right]}$$

and can be further modified into Eq. (5.6),

$$W = W_i - k_w \left[\frac{1.817 \sqrt[4]{\phi_p}}{\sqrt[3]{\pi} - 1.817 \sqrt[3]{\phi_p}} \right] \quad (5.6)$$

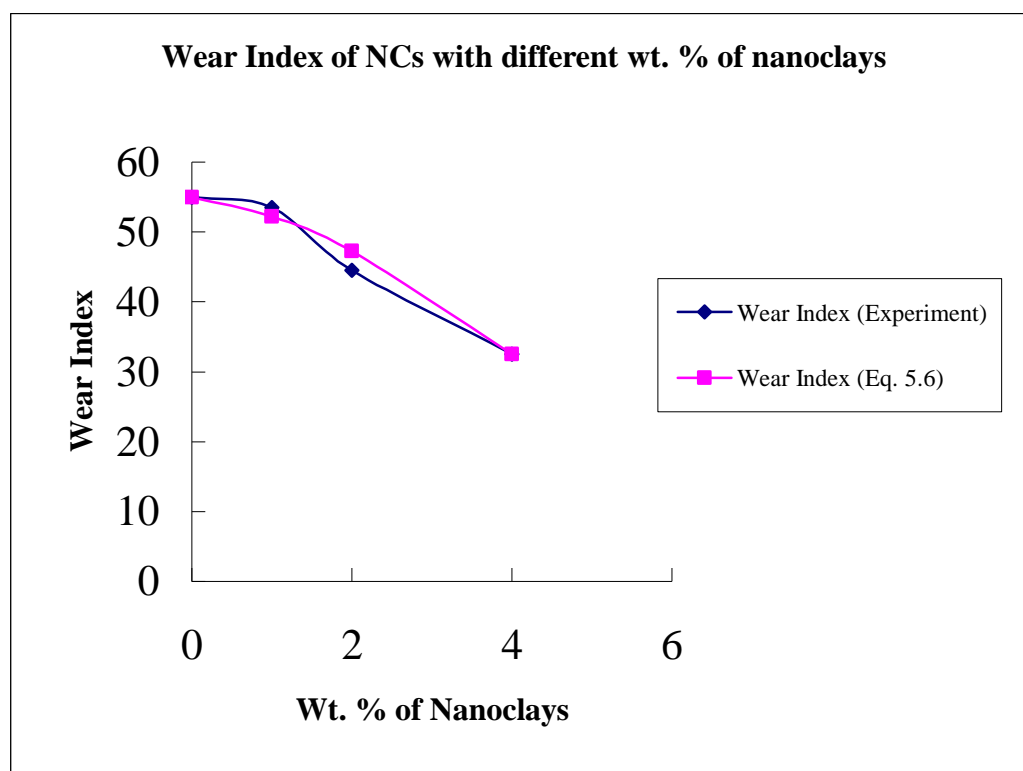


Figure 5.2 Wear index of NCs with different wt.% of nanoclays

The mathematical predictions of micro-hardness and wear resistance of the NCs are based on the empirical data with the nanoclay content from 0-4 wt.% and the condition of fully intercalation of nanoclay platelets inside nanoclay clusters. In Figs. 5.1 and 5.2, the mathematical predictions of micro-hardness and wear index of the NCs with different nanoclay contents are compared with experimental results respectively. It shows that these mathematical models are valid for the micro-hardness and wear index estimation once the nanoclay content is known.

5.2 CREEP MECHANISM

Creep of materials has a significant impact on the manufacturing of high precision industrial products. All of the engineering materials would be deformed at various creeping rates with a constant uniaxial loading at a specified temperature. The aircraft industry has applied NCs on the surface of aircraft body for the purpose of enhancing heat resistance and improving mechanical properties without inducing any weight penalty. The automobile manufacturing companies also have employed NCs on the body of automobiles in order to fulfill the shock absorption during serious collisions. Therefore, creep of the NCs is becoming a major considering factor and should be controlled carefully to avoid any engineering discrepancies.

Nanoindentation is a newly invented technique for the determination of localized material properties that was introduced by Oliver and Pharr in 1992. Elastic modulus, nano-hardness and contact stiffness of a material can be determined by nanoindentation nanoscopically. Fig. 5.3 shows a typical nanoindentation profile for determination of localized mechanical properties in polymer composites.

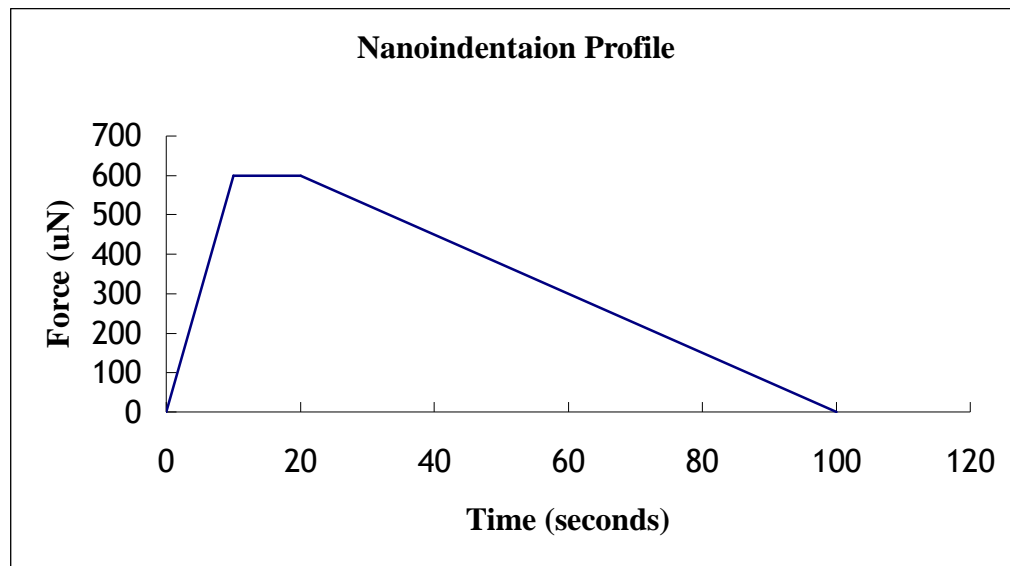


Figure 5.3 Nanoindentation profile

This technique makes use of creating a permanently plastically deformed surface on a material being tested. Based on the force applied on the surface and the indentation depth of the indent, relative elastic modulus (E_r) can be obtained by the equations given as,

$$A_c = f(h_c) \quad (5.7)$$

$$E_r = \frac{\left(\frac{\sqrt{\pi}}{2}\right)}{\left(\frac{S}{\sqrt{A_c}}\right)} \quad (5.8)$$



where h_c is the contact height, A_c is the contact surface area between the nanoindenter and the material surface and S is the contact stiffness that is the slope of the unloading portion in the nanoindentation profile as shown in Fig. 5.3.

Numerous researches were conducted in investigating the mechanical properties of pure elements and nanocomposites by nanoindentation. Nanoindentation has also been employed to evaluate the depth of the coatings on polymer-ceramic nanocomposites by depth sensing indentation. Shen et al. began to study the morphologies of nylon 66/nanoclay composites by nanoindentation. Apart from visualizing the localized mechanical properties, nanoindentation can also be used to investigate the localized creep effect from the holding portion of the nanoindentation profile as shown in Fig. 5.3. From the definition of creep, the elongation of the materials from its original position after a constant applied force at thermally stable environment is called creep. In nanoindentation, the degree of creeping can also be measured by holding the applied force of the nanoindenter constant with respect to the deformation of the materials being tested. The advantages of using nanoindentation to measure creep are time economic as the time for conducting an indent is far less than the novel creep

testing techniques. Moreover, nanoindentation can measure creep within an infinitesimal small area, hence, localized creep can be easily obtained instead of creeping of the whole structure. As a result, nanoindentation was employed in the study of creep mechanism of the NCs in this project.

5.2.1 KELVIN-VOIGT CREEP MODEL

Fig. 5.4 shows the schematic diagram of the Kelvin-Voigt model. In the Kelvin-Voigt model, a purely elastic spring is connected in parallel with a purely viscous damper.

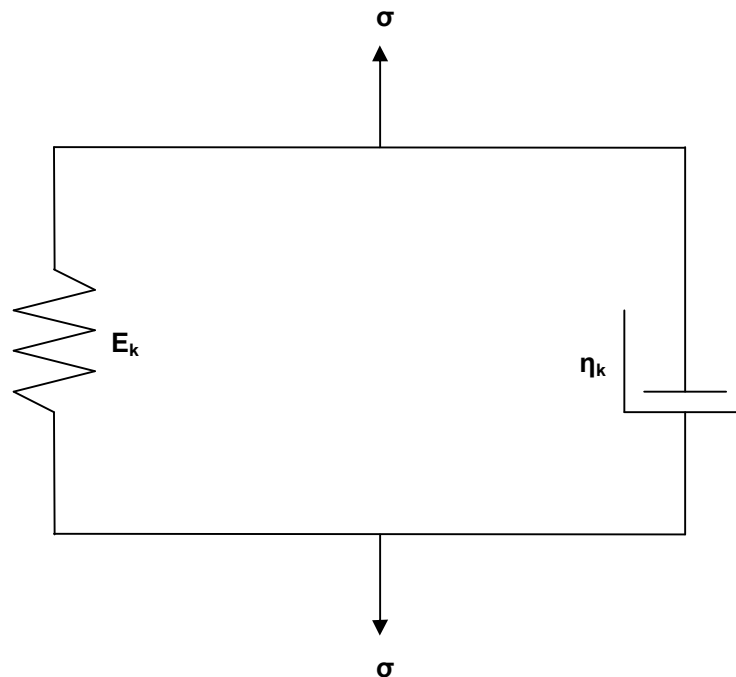


Figure 5.4 Kelvin-Voigt model

E_k and η_k are the modulus of elasticity and viscosity coefficient respectively. By applying the stress at the two ends of the model, the stress of the whole model should be the addition of the stress on the damper and the spring while the elongation should be the same. Hence,

$$\varepsilon_{tot} = \varepsilon_D = \varepsilon_E \quad (5.9)$$

$$\sigma_{tot} = \sigma_D + \sigma_E \quad (5.10)$$

where ε_D and ε_E are the strains of the damper and the spring respectively.

By taking the time derivative of Eq. (5.10),

$$\frac{d\sigma_{tot}}{dt} = \frac{d\sigma_D}{dt} + \frac{d\sigma_E}{dt} \quad (5.11)$$

Therefore, Eq. (5.11) can be further written as,

$$\sigma = E\varepsilon + \eta\dot{\varepsilon} \quad (5.12)$$

From Fig. 5.4 and Eq. (5.12), the Kelvin-Voigt creep model contains an elastic element and a viscous element connects in series. It describes a material possesses both viscoelastic and absolute elastic properties where they do not interfere with each other. When estimating the stress relaxation process in the creep experiment, it can give a perfect estimation. Hence, the model should not



be used to describe a material consists of only one uniformly distributed element. However, in the process of nanoindentation of NCs with intercalated nanoclay clusters, the model can be used to estimate the nanoscopic creep behavior of NCs. Fig. 5.5 shows the three different stages of nanoindentation of the NCs with intercalated nanoclay clusters. During nanoindentation, the creep behavior is measured in the holding region of the test. It does not need to consider the unloading region where the stress is released gradually as the change of the contact area during nanoindentation is the only controlling factor of the result. In this project, the creep behavior of NCs with different wt.% of nanoclays was investigated by nanoindentation. The nanoindentation data were used to interpret by the Kelvin-Voigt creep model in order to develop the relationship between the macroscopic and nanoscopic visualization of creep mechanism of NCs.

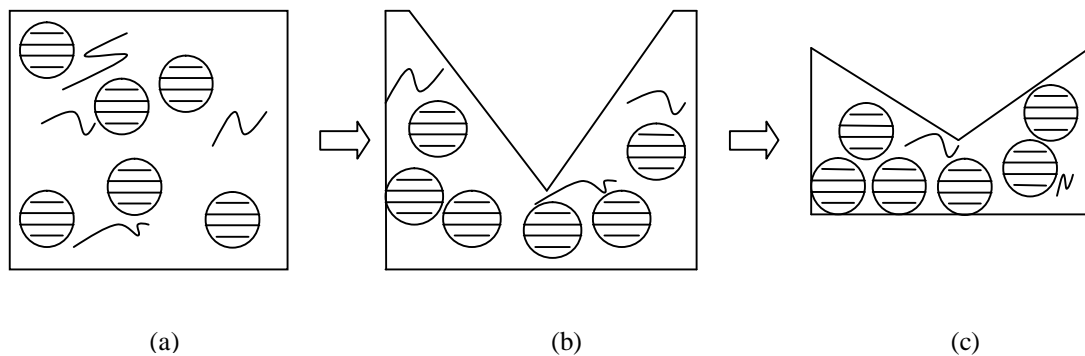


Figure 5.5 Three different stages of nanoindentation of NCs. (a) before nanoindentation; (b) during nanoindentation and (c) after nanoindentation due to creep effect

5.2.2 NANOINDENTATION CREEP MODEL

NC samples with different wt. % of nanoclays were tested on the localized creep effects with constant holding load during nanoindentation. Fig. 5.3 shows the nanoindentation profile during the experiment. The load was held at 600 μN for 10s throughout the experiment.

Fig. 5.6 shows the creeping strain of different NC samples with respect to time during load holding of the nanoindentation profile. Strain2, strain4, strain6 and strain8 in Fig. 5.6 represent the creeping strain at 2 wt.%, 4 wt.%, 6 wt.% and 8 wt.% of nanoclays respectively.

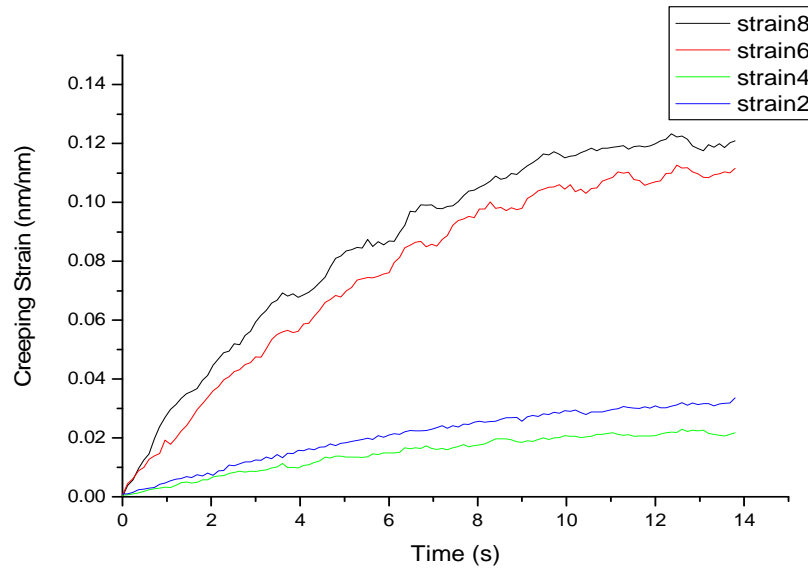


Figure 5.6 Creeping strain of different wt.% of NCs

The creeping strain at each data collecting point can be calculated by Eq. (5.13).

$$\varepsilon = \frac{(h_l - h_c)}{h_c} \quad (5.13)$$

where h_l and h_c are the instantaneous localized penetration depth at each specified data collecting point and contact depth at that nanoindentation point respectively.

As the indentation depth was changed on each data collection point with the load holding constant, the instantaneous creeping strain can be obtained by comparing

with the final contact depth of the indent after the indentation.

The creeping strains of the NC-2 and NC-4 had a huge difference with NC-6 and NC-8. The NC-4 had the lowest creeping strain compared to the other wt. % of nanoclays. This was due to the maximum mechanical reinforcement by the intercalated nanoclay clusters in the NCs at 4 wt. % of nanoclays. As the Vickers micro-hardness was proven to be maximum at 4 wt.% of nanoclays in Chapter 5, therefore, the creeping strain should be the lowest among the other NC samples.

Creeping strain of the NCs can be described by Eq. (5.14) experimentally.

$$\varepsilon = \varphi \exp\left(\frac{-t}{\omega}\right) + \kappa \quad (5.14)$$

where φ , ω and κ are constants.

The constants can be obtained by fitting the strain vs time curve with Eq. (5.14).

Figs. 5.7(a) to 5.7(d) show the fitted results of NCs with 2 wt.%, 4 wt.%, 6 wt.% and 8 wt.% nanoclays respectively.

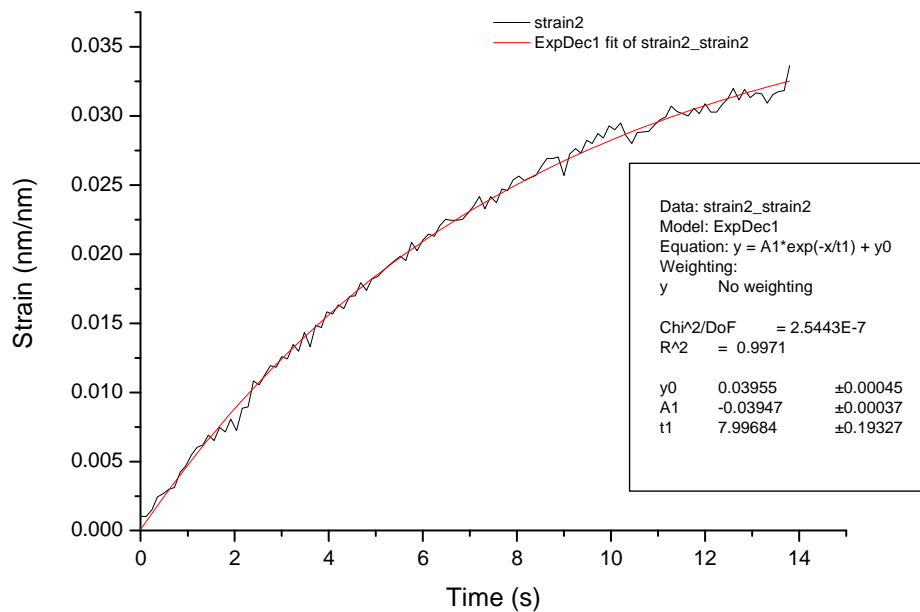


Figure 5.7(a) Result of fitted ϵ vs t curve of 2 wt.% NCs

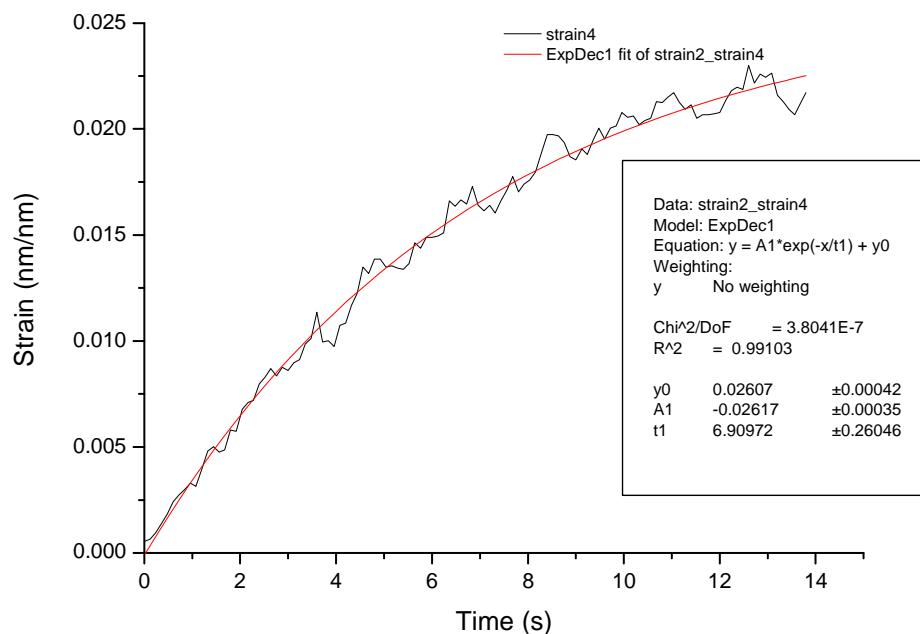


Figure 5.7(b) Result of fitted ϵ vs t curve of 4 wt.% NCs

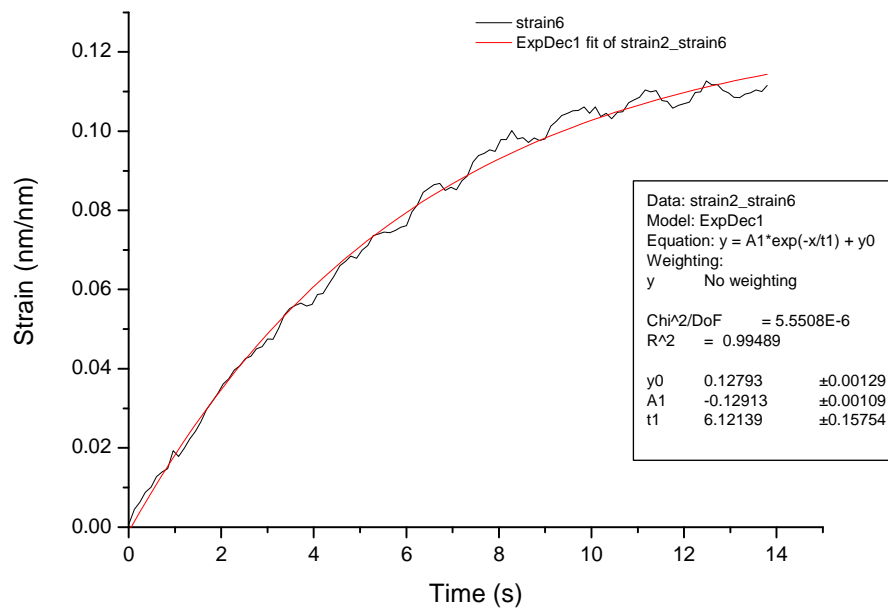


Figure 5.7(c) Result of fitted ϵ vs t curve of 6 wt.% NCs

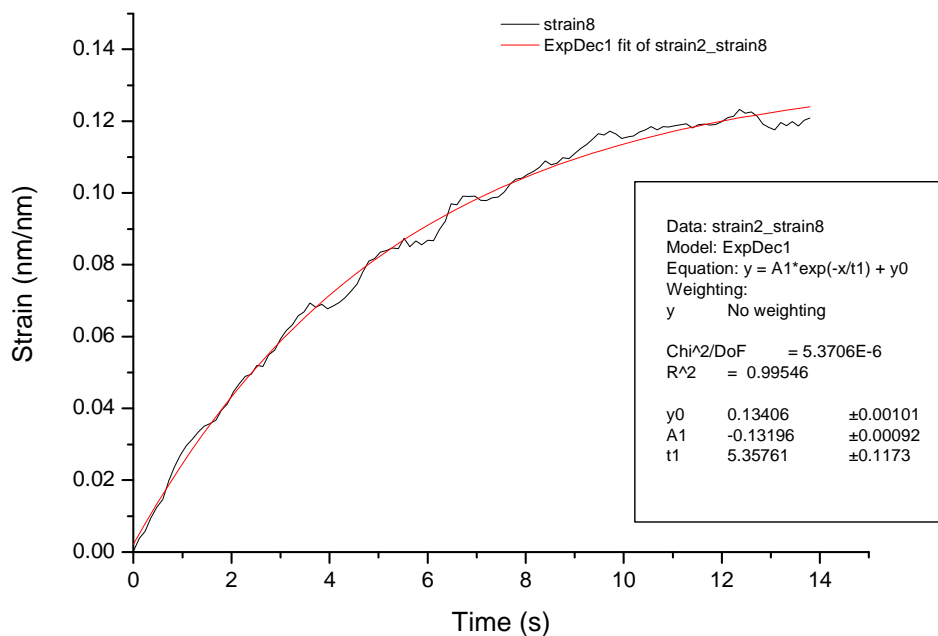


Figure 5.7(d) Result of fitted ϵ vs t curve of 8 wt.% NCs

By differentiating Eq. (5.14) with respect to time,

$$\dot{\varepsilon} = -\left(\frac{\varphi}{\omega}\right)\exp\left(\frac{-t}{\omega}\right) \quad (5.15)$$

Substituting Eqs. (5.14) and (5.15) into Eq. (5.12),

$$\begin{aligned} \sigma &= E\left[\varphi\exp\left(-\frac{t}{\omega}\right) + \kappa\right] - \frac{\eta\varphi}{\omega}\exp\left(-\frac{t}{\omega}\right); \\ \sigma &= \varphi\exp\left(-\frac{t}{\omega}\right)\left[E - \frac{\eta}{\omega}\right] + E\kappa \end{aligned} \quad (5.16)$$

Before the indenter touches the NC samples, i.e. $t = 0$, the exponential part of Eq. (5.16) dominates the mechanical properties of NCs. During nanoindentation in progress, i.e. $t > 0$, the domination of the exponential part decreases gradually with time elapsed. If the load continues to hold for a certain period of time, i.e. $t \rightarrow \infty$, the stress will reach a constant value. Fig. 5.5 shows the three different stages of nanoindentation schematically. As the indenter continues deforming the surfaces of the NCs, there is less free volume for the intercalated nanoclay clusters in the NCs to live in. At the load holding region of the nanoindentation process where the creep mechanisms of the NCs is measured, the density of intercalated nanoclay clusters surrounding the indenter surface is greater than the



other regions of the NCs as the concentrated stress at the indent forced the epoxy matrix to deform and the distances between intercalated nanoclay clusters are diminished. The exponential part of Eq. (5.16) describes the behavior of viscoelastic epoxy matrix during nanoindentation completely while the linear part of Eq. (5.16) can represent the behavior of intercalated nanoclay clusters in the NCs. When the nanoindentation process continues, the effect of the viscoelastic behavior of the epoxy matrix on the creep mechanism decreases while the NCs tends to be more elastic at the end of the load holding region in which the intercalated nanoclay clusters density is maximized. If time goes to infinity in Eq. (5.16),

$$\sigma = E\kappa \quad (5.17)$$

Eq. (5.17) can be compared to the elastic stress-strain relationship $\sigma = E\varepsilon$, hence,

$$\kappa \approx \varepsilon \quad (5.18)$$

Fig. 5.8 shows the creeping strain variation of the NCs with different wt.% of

nanoclays. The creeping strain of the NCs is minimized at NC-4 with constant loading. This deduces that the hardness of the NCs is the maximized at 4 wt.% of nanoclay content. Hence, the obtained results support the maximized hardness at 4 wt.% as obtained in Chapter 4. Accompanying with the nanoindentation results, the degree of creeping of NCs is also minimized at 4 wt.% of nanoclay content.

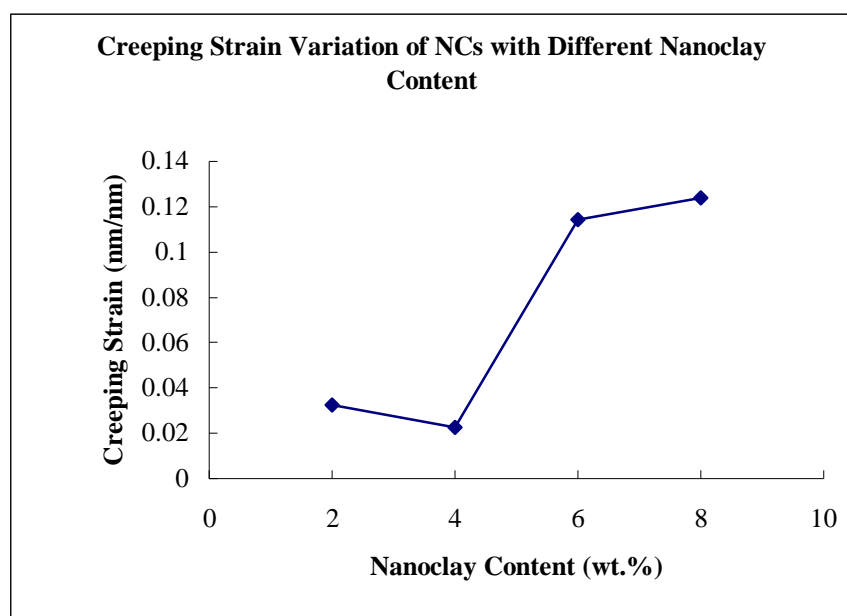


Figure 5.8 Creeping strain variation of NCs at different nanoclay content



5.3 THERMO-MECHANICAL MIXING ENERGY

In the manufacturing process of NCs, the degree of mixing between nanoclays and epoxy resin is significant to govern their mechanical properties. The effect on the mechanical properties in relation to the curing kinetics and gelation mechanism of the NCs has been studied. However, the mixing mechanism before curing is also an important factor for improving the mechanical properties of the resultant NCs. This issue has not yet been investigated comprehensively to date. The amount of free energy that nanoclays have inside pre-cured epoxy resin is the determining factor for the degree of mixing between nanoclays and epoxy resin. According to Flory's principle, the free energy in a binary mixture consists of two parts; they are interaction entropy and energy accordingly. Mechanical properties of specific NCs can be easily estimated with the free energy of the mixture of nanoclays and epoxy resin is known. The importance of developing the relationship between mechanical properties and molecular structure of pre-cured NCs is when their sets of manufacturing conditions are known, for instance, wt. % of nanoclays, duration of mechanical stirring and sonication, and temperature for curing process, the degree of mechanical property enhancement can be estimated before production. Thus, the economic efficiency in both the



use of materials and time consumption can be improved for both industrial and academic production of NCs.

5.3.1 ENTROPY OF THE MIXTURE

Assuming there are no volume changes during the mixing process between nanoclays and epoxy resin, i.e. the total volume of the mixture can be calculated by summing up of the volume of the nanoclays, W_N , and the volume of epoxy resin, W_E , based on the rule of mixture. The volume fractions of the nanoclays and epoxy resin inside the NCs can be determined by

$$\phi_N = \frac{W_N}{W_N + W_E} \quad \text{and} \quad \phi_E = \frac{W_E}{W_N + W_E} = 1 - \phi_N \quad (5.19)$$

The entropy S is determined by the product of the Boltzmann constant k and the natural logarithm of Ω ways to arrange the molecules in the lattice:

$$S = k \ln \Omega \quad (5.20)$$

In a homogenous mixture of nanoclays and epoxy resin, each molecule has:

$$\Omega_{NE} = n \quad (5.21)$$

possible states, where n is the total number of lattice sites of combined system.

The number of states Ω_N of each particle of nanoclays inside NCs before mixing is equal to the number of lattice sites occupied by nanoclays:

$$\Omega_N = n\phi_N \quad (5.22)$$

For a single particle of nanoclays, the entropy change on mixing is,

$$\begin{aligned} \Delta S_N &= k \ln \Omega_{NE} - k \ln \Omega_N = k \ln \left(\frac{\Omega_{NE}}{\Omega_N} \right) \\ \Delta S_N &= k \ln \left(\frac{1}{\phi_N} \right) = -k \ln \phi_N \end{aligned} \quad (5.23)$$

Hence, the entropy change is always positive as the volume fraction must be less than unity ($\phi_N < 1$) and ($\Delta S_N = -k \ln \phi_N > 0$). Fig. 5.9 shows the variation of entropy with different volume fraction of nanoclays. Thus, the entropy of the NC mixture decreases when the nanoclay content increases.

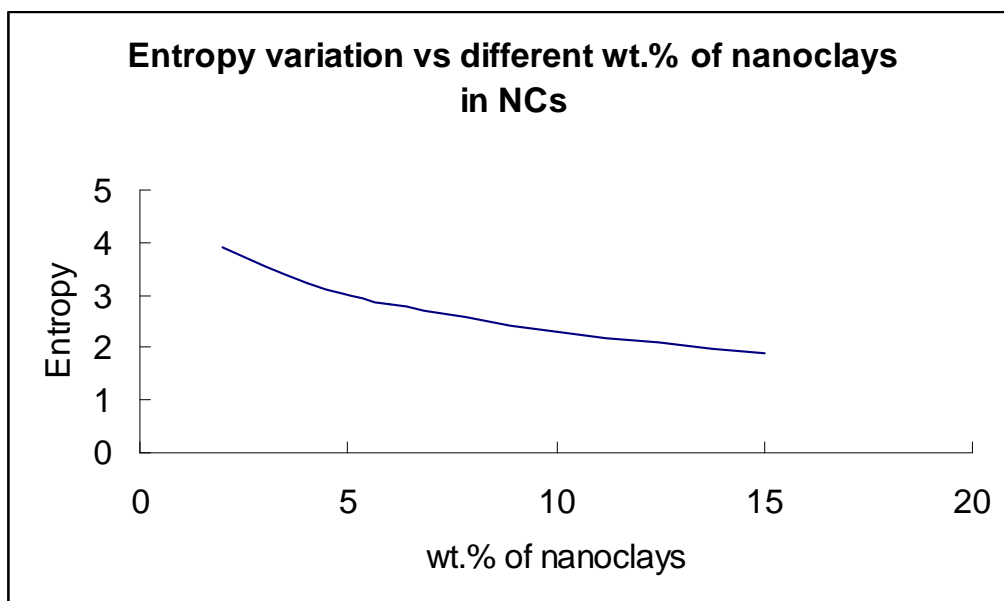


Figure 5.9 Entropy variation of NCs with different wt.% of nanoclays

For the entropy change in epoxy during the mixing process is similar and thus the entropy contributions from nanoclays and epoxy resin are added together:

$$\Delta S_{tot} = n_N \Delta S_N + n_E \Delta S_E = -k(n_N \ln \phi_N + n_E \ln \phi_E) \quad (5.24)$$

Let N_N and N_E be the numbers of lattice sites occupied by the nanoclays and epoxy resin, respectively. Then the entropy mixing per lattice site in NCs is:

$$\Delta \bar{S}_{tot} = -k \left[\frac{\phi_N}{N_N} \ln \phi_N + \frac{\phi_E}{N_E} \ln \phi_E \right] \quad (5.25)$$

5.3.2 INTERACTION ENERGY OF THE MIXTURE

The interfacial surface energy is an important characteristic for efficient mechanical property enhancement. In regular solution theory, the energy of mixing is represented by three pairwise interaction energies. In terms of nanoclays and epoxy resin, the interaction energies between nanoclay/nanoclay, nanoclay/epoxy and epoxy/epoxy interfaces are u_{NN} , u_{NE} and u_{EE} respectively. The probability of nanoclays being a neighbor with another nanoclays is ϕ_N in the lattice and $1 - \phi_N$ for the neighbor being an epoxy resin molecule. The weighted sum of interaction energies for nanoclays (U_N) and epoxy resin (U_E):

$$U_N = u_{NN}\phi_N + u_{NE}\phi_E, \text{ and} \quad (5.26)$$

$$U_E = u_{NE}\phi_N + u_{EE}\phi_E \quad (5.27)$$

Let z be the coordination number of nearest neighbors in each lattice site of a regular lattice. That is, $z = 4$ for a square lattice and $z = 6$ for a cubic lattice.

Hence, the average interaction energy of nanoclays with z neighbours is zU_N . However, the average energy per nanoclays is $zU_N/2$ as every pairwise action is counted twice. The corresponding energy per site occupied by epoxy resin is $zU_E/2$. Let n be the total number of sites occupied by the NCs. Thus, the number of sites occupied by nanoclays and epoxy resin is $n\phi_N$ and $n\phi_E$ respectively. The total interaction energy of the mixture can be given by:

$$U = \frac{zn}{2} [U_N\phi_N + U_E\phi_E] \quad (5.28)$$

Replacing the weight fraction of nanoclays by $\phi = \phi_N = 1 - \phi_E$, the total interaction energy of the nanoclays and epoxy resin with n lattice sites can be modeled by:

$$U = \frac{zn}{2} \{ [u_{NN}\phi + u_{NE}(1-\phi)]\phi + [u_{NE}\phi + u_{EE}(1-\phi)](1-\phi) \} \quad (5.29)$$

$$U = \frac{zn}{2} [u_{NN}\phi \cdot \phi + 2u_{NE}\phi(1-\phi) + u_{EE}(1-\phi) \cdot (1-\phi)]$$

The interaction energy per site in nanoclays before mixing is $zu_{NN}/2$. The total number of nanoclays is $n\phi$, hence the total energy of nanoclays before mixing is:

$$\frac{zn}{2} u_{NN}\phi \quad (5.30)$$

and the total energy of epoxy resin before mixing is:

$$\frac{zn}{2} u_{EE}(1-\phi) \quad (5.31)$$

As a result, the total energy of the mixture of nanoclays and epoxy resin by summing up the energies of the two pure components is:

$$U_0 = \frac{zn}{2} [u_{NN}\phi + u_{EE}(1-\phi)] \quad (5.32)$$

The energy change when mixing is:

$$\begin{aligned} U - U_0 &= \frac{zn}{2} [u_{NN}\phi_2 + 2u_{NE}\phi(1-\phi) + u_{EE}(1-\phi)_2 - u_{NN}\phi - u_{EE}(1-\phi)] \\ U - U_0 &= \frac{zn}{2} [u_{NN}(\phi_2 - \phi) + 2u_{NE}\phi(1-\phi) + u_{EE}(1 - 2\phi + \phi_2 - 1 + \phi)] \\ U - U_0 &= \frac{zn}{2} [u_{NN}\phi(\phi - 1) + 2u_{NE}\phi(1-\phi) + u_{EE}\phi(\phi - 1)] \\ U - U_0 &= \frac{zn}{2} \phi(1-\phi)(2u_{NE} - u_{NN} - u_{EE}) \end{aligned} \quad (5.33)$$

The energy change on mixing per site is:

$$\Delta \bar{U}_{tot} = \frac{U - U_0}{n} = \frac{z}{2} \phi(1-\phi)(2u_{NE} - u_{NN} - u_{EE}) \quad (5.34)$$



From the definition of Flory interaction parameter χ , where the difference in the interaction energies between nanoclays and epoxy resin is:

$$\chi \equiv \frac{z}{2} \frac{(2u_{NE} - u_{NN} - u_{EE})}{kT} \quad (5.35)$$

By using the Flory interaction parameter, the energy of mixing per lattice site is:

$$\Delta \bar{U}_{tot} = \chi \phi (1 - \phi) kT \quad (5.36)$$

Combining with the entropy of mixing between the nanoclays and epoxy resin, the Helmholtz free energy of mixing per lattice site is:

$$\begin{aligned} \Delta \bar{F}_{tot} &= \Delta \bar{U}_{tot} - T \Delta \bar{S}_{tot} \\ \Delta \bar{F}_{tot} &= kT \left[\frac{\phi}{N_N} \ln \phi + \frac{1-\phi}{N_E} \ln(1-\phi) + \chi \phi (1-\phi) \right] \end{aligned} \quad (5.37)$$

5.3.3 MATHEMATICAL OPTIMIZATION

According to Eq. (5.37) as the experimental temperature and the testing materials were the same throughout the experiment, the only parameter that was changed was the wt.% of nanoclays in NCs. Therefore, Eq. (5.37) can be further simplified as:

$$\Delta \bar{F}_{tot} \approx \phi \ln \phi + (1 - \phi) \ln(1 - \phi) + \phi(1 - \phi) \quad (5.38)$$

By taking negative logarithm to both sides,

$$-\log(\Delta \bar{F}_{tot}) \approx -\log[\phi \ln \phi + (1 - \phi) \ln(1 - \phi) + \phi(1 - \phi)] \quad (5.39)$$

Let α and H be the NCs reaction efficiency factor with reference to micro-hardness and Vicker's micro-hardness respectively. By relating the Vickers micro-hardness to the Helmholtz free energy approximation of the NCs in Eq. (5.39),

$$\alpha = \frac{H}{-\log(\overline{\Delta F_{tot}})} \approx \frac{H}{-\log[\phi \ln \phi + (1-\phi) \ln(1-\phi) + \phi(1-\phi)]} \quad (5.40)$$

Fig. 5.10 shows the plot for the reaction efficiency factor with the change in nanoclay contents in the NCs.

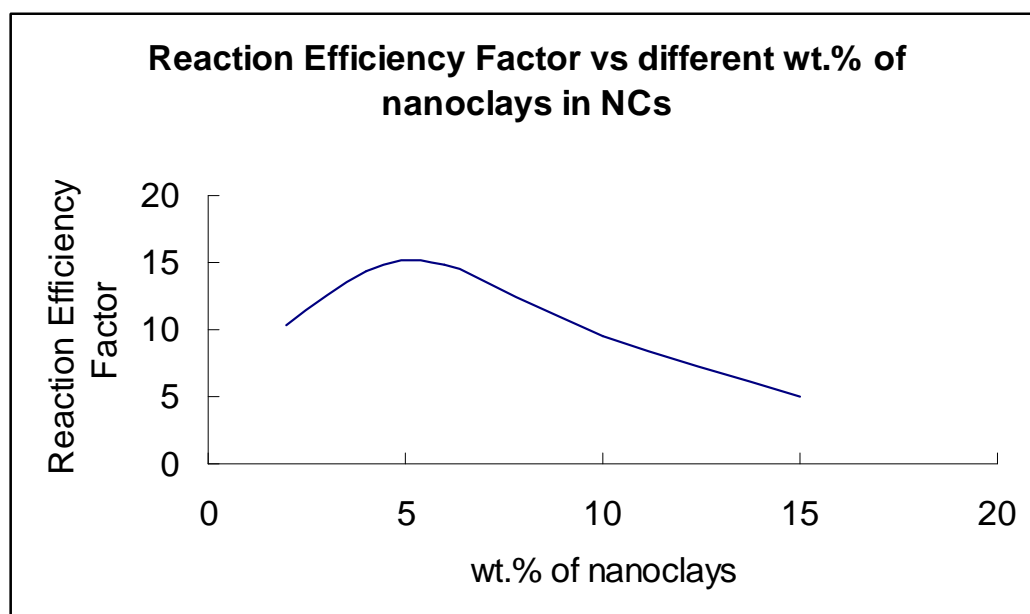


Fig. 5.10 Reaction efficiency factor of NCs with different wt.% of nanoclays

The reaction efficiency of the NCs is maximized at the range of 4 wt.% - 6 wt.% of nanoclay contents with the most sufficient free energy for the nanoclays to interact with the epoxy resin and disperse throughout the NC samples. The proposed reaction efficiency factor agrees with the experimental results obtained



from the Vickers micro-hardness test. The reaction efficiency factor can relate the free energy in the pre-cured NC mixtures with the micro-hardness performance of the cured NCs. Furthermore, from the Flory's principle and Eq. (5.40), the free energy during mixing of nanoclays and epoxy resin plays an important role of micro-hardness enhancement of NCs.



5.4 FORMATION OF NANOCCLAY CLUSTERS

In Chapter 4, SEMs show that there are many nanoclay clusters inside NCs. Nevertheless, the reasons for the natural tendency to form clusters in NCs has not been figured out previously. In this section, based on the nucleation theory, the relationship between the formation and size of nanoclay clusters in NCs is explained in detail.

Nanoclay content and sonication time are fixed at 4 wt.% and 20 minutes respectively in this study. The only variable is the sonication temperature. Three types of samples were fabricated in this study; they were NCs with 40°C, 80°C and 100°C preheating for 5 minutes before ultrasound sonication. In Chapter 5, the SEMs showed that the size of nanoclay clusters increase while the number of nanoclay clusters decrease when the sonication temperature increases. This result proves that when the viscosity of the epoxy resin decrease with the increase in sonication temperature, nanoclays tend to form larger clusters due to the less restraining force by the surrounding epoxy resin. They can be flow around easily with the aid of sonication that provides extra kinetic energy for the nanoclays. The significance of increasing the kinetic energies of the nanoclays is to



overcome interfacial tension between the nanoclay clusters formed and the epoxy matrix. There are several papers review on the classic nucleation of clusters in liquids in supersaturated vapor by Abraham, Zettlemoyer and LaMer, which was developed by Volmer, Becker and Doring and further modified by Frenkel and Zeldovich explained the increase of surface energy or interfacial tension when the size of clusters increase. For a cluster containing n atoms, the surface energy $\sigma A(n)$ is given by:

$$4\pi\sigma\left(\frac{3vn}{4\pi}\right)^{\frac{2}{3}} \quad (5.41)$$

where σ is the interfacial tension per unit area, $A(n)$ is the surface area of the cluster, and v is the volume per molecule in the bulk liquid. By applying Eq. (5.41) to the case of nanoclay clusters in epoxy resin, n corresponds to the number of nanoclays inside a nanoclay cluster. When the nanoclay cluster increases in size, the nanoclays inside the cluster increase. Hence, n will increase in Eq. (5.41) and result in increasing the interfacial tension between the nanoclay cluster and the surrounding epoxy resin. Nevertheless, if the interfacial tension continues to build up on the surface of the nanoclay clusters when their sizes

increase, it causes the nanoclays more difficult to adhere on the surface of the nanoclay clusters. Therefore, the change of viscosity of epoxy resin due to the alteration of sonication temperature plays an important role in the growing of nanoclay cluster sizes. The size of the nanoclay clusters depends on the viscosity of the epoxy resin by altering the sonication temperature, thus, Eq. (5.41) need to be further modified for describing the interfacial tension between the nanoclay clusters and the epoxy resin. As the increase in nanoclay cluster size is directly proportional to the sonication temperature and inversely proportional to the viscosity of epoxy resin, the relationship between the sonication temperature, the viscosity of epoxy resin and the nanoclay cluster sizes can be approximate by Eq. (5.42). Consider a nanoclay cluster with radius r and has n nanoclays inside,

$$r = kT \left[\frac{1}{\frac{d\rho}{dT}} \right] \quad (5.42)$$

where k is a constant, T is the sonication temperature and ρ is the viscosity of epoxy resin. Eq. (5.42) describes the phenomenon of increasing the sonication temperature, the viscosity of epoxy resin decreases and the nanoclay cluster size increases. Differentiating both sides of Eq. (5.42) by d/dt , the rate of increase of

the radius of the nanoclay cluster can be obtained.

$$\frac{dr}{dt} = k \left(\frac{dT}{dt} \right) \left[\frac{1}{\left(\frac{d\rho}{dT} \right)} \right] \quad (5.43)$$

$$\frac{dr}{dt} = k \left(\frac{dT}{dt} \right) \left(\frac{dT}{d\rho} \right) \quad (5.44)$$

Rewriting Eq. (5.42),

$$r = k \left(\frac{dT}{d\rho} \right) \quad (5.45)$$

Assuming the nanoclay clusters are spherical in shape, the change of the surface area A of a nanoclay cluster is given by:

$$A = 4\pi \left[k \left(\frac{dT}{d\rho} \right) \right]^2 \quad (5.46)$$

As the interfacial tension equal to $\sigma A(n)$ as stated in Eq. (5.41), combining with Eq. (5.46), the interfacial tension is given by,

$$\sigma A = \sigma 4\pi \left[k \left(\frac{dT}{d\rho} \right) \right]^2 \quad (5.47)$$

$$\sigma A = \sigma 4\pi \left[k \left(\frac{1}{\frac{d\rho}{dT}} \right) \right]^2 \quad (5.48)$$

In Eq. (5.48), if the change of viscosity of epoxy resin is huge from 40°C to 100°C, $d\rho/dT$ becomes large in Eq. (5.48) and results in decreasing the interfacial tension between the nanoclay clusters and epoxy resin. This is the reason for the increase in nanoclay cluster sizes when increasing the sonication temperature since the interfacial tension between the nanoclay clusters and the epoxy resin decrease and facilitates the adhesion of free nanoclays onto the surface of nanoclay clusters. Furthermore, increase in sonication temperature also provides addition of kinetic energy for the free nanoclays to move and increase the chance to adhere on the surfaces of nanoclay clusters. If the change of viscosity with respect to sonication temperature is zero, for example, in solids or cured NCs, the interfacial tension as predicted by Eq. (5.48) becomes infinity and hence the size of nanoclay clusters cannot be changed in cured NCs.



6. CONCLUSION

In this project, mechanical properties of the inclusion of intercalated nanoclay clusters in NCs have been investigated in detail. Since uneven pressure can be easily introduced into NC mixtures during manufacturing processes, such as extrusion and injection molding of engineering products, intercalated nanoclay clusters are readily formed in NC products. However, there was a lack of investigation on the mechanical properties of NCs with intercalated nanoclay clusters in recent research. Mathematical and theoretical models seldom address the formation of nanoclay clusters and the mixing mechanisms inside the NC mixtures. With the extraordinary growth of importance of NCs in modern engineering structures, the need of understanding and interpreting different internal structures of NCs is growing enormously. For this reason, this project was focused on the mechanical properties of NCs with intercalated nanoclay clusters that has not previously been studied elsewhere. Vickers micro-hardness, wear resistance and creep behavior of NCs with intercalated nanoclay clusters are reported here. Theoretical analyses on the mechanical properties, interaction energy in the NC mixtures and the formation of nanoclay clusters in NCs are also proposed for the facilitation of understanding and analyzing the maximized



mechanical properties of the NCs at 4 wt.% of nanoclays.

Firstly, Vickers micro-hardness and wear resistance of NCs at different amount of nanoclays were tested in this project with different nanoclay content. It was found that the micro-hardness and wear resistance of the NCs increased with nanoclay content. Based on the experimental results and SEM analysis, the size of the intercalated nanoclay clusters reached a crucial limit and therefore the reinforcing function of the nanoclays decreased. Vickers micro-hardness and wear resistance increased with the content of nanoclays increased up to 4 wt.% of nanoclays. A mathematic correlation of micro-hardness and wear resistance of the NCs with the diameters of intercalated nanoclay clusters and inter-cluster distance is also proposed. This can aid the understanding of the infrastructure inside the NCs for everyday engineering applications. The formation of intercalated nanoclay clusters in NC surface coatings on engineering products is accurately modeled instead of only considering ideally exfoliated NCs in many laboratory studies.

Secondly, this project examined the dispersion effect by ultrasound sonication on the NC mixtures before curing. Maximum micro-hardness of the NCs at 4 wt.%



of nanoclays was achieved when they were sonicated for 10 minutes. The existence of the optimum micro-hardness at a specific sonicating time was explained with the aid of SEM and XRD. The experimental results found that different ultrasound sonication times indeed affected the size of the nanoclay clusters. Nevertheless, the interplanar distance between the nanoclay platelets was not as strongly influenced by the sonication effect.

Thirdly, this project studied the formation of nanoclay clusters and their size in NCs by the modified nucleation theory of clusters. Based on the deduction of the modified nucleation theory of clusters in which the effects of sonication temperature and viscosity of epoxy resin were taken into consideration, the increase in size of nanoclay clusters at higher sonication temperature was due to the decrease of interfacial tension between the surfaces of nanoclay clusters and the surrounding epoxy resin. Accompanying the increase of kinetic energy of the nanoclays in NCs at higher temperature, the probability for free nanoclays to adhere on the surface of a nanoclay cluster greatly increased. Hence, nanoclay clusters appear larger at higher sonication temperature.

Furthermore, the results obtained by nanoindentation found that the relative



elastic modulus of NCs decreased from the bottom to the top portion of the NC samples due to the effect of gravity on the nanoclay clusters. Based on the experimental results, this was caused by the sonication temperatures that played an important role in the curing time of NCs. At higher temperature, the distribution of nanoclay clusters were more even than at lower temperature as gravity needed less time to pull down the nanoclay clusters than it did at lower temperature. The distributions of nanoclay clusters were still well dispersed at higher sonication temperature at the time of curing, so the relative elastic modulus remained stable.

Moreover, this project also demonstrates the relationship between Helmholtz free energy and Vickers micro-hardness of NCs at different nanoclay content. The Helmholtz free energy in the NC mixtures was maximized when the Vickers micro-hardness of NCs was maximized simultaneously. This shows that the mechanical properties of cured NCs was closely related to the mixing conditions when the NCs was in the pre-cure state, and hence, the degree of free energy was the energy source to provide the mobility for nanoclays to move around the epoxy resin in order to promote dispersion of nanoclays inside the NCs. The reaction efficiency factor (α) was established in the project in order to estimate



the micro-hardness of the NCs at different wt.% of nanoclays from their Helmholtz free energy in their pre-cure state. With the aid of α , it can prove that the mixing conditions before curing play a significant role in the preparation of the NCs.

Finally, creep of NCs at different nanoclay contents was measured by the load holding mechanism in nanoindentation. The novel Kelvin-Voigt creep model was proven to describe the creep mechanism of NCs during nanoindentation with only intercalated nanoclay clusters inside. At the beginning stage of nanoindentation, the viscoelastic behavior of epoxy matrix in NCs dominated. When the time elapsed, the elastic behavior of the intercalated nanoclay clusters in the NCs became significant. As time approached infinity, the degree of creeping was determined by the intercalated nanoclay clusters. As a result, the creeping strain of NCs with different nanoclay content can be readily obtained by using the mathematical model in this project. The creeping strain of the NCs was minimized at 4 wt.% of nanoclays.

In conclusion, this project studied the mechanical properties of NCs with intercalated nanoclay clusters. It demonstrated the theoretical analysis of the



formation and mixing energy of nanoclay clusters. It is a comprehensive study of NCs with intercalated nanoclay clusters and provides a research platform and milestone for the practical and academic understanding and interpretation of nanoclay clusters in NCs .



REFERENCES

Abraham F. F., Homogeneous Nucleation Theory, 1974 (New York: Academic)

Ahn H. S., Julthongpiput D., Kim D. I. and Tsukruk V. V., Dramatic enhancement of wear stability in oil-enriched polymer gel nanolayers, *Wear*, **255**, 801 – 807 (2003)

Alexandre M and Dubois P., Polymer-layered silicate nanocomposites: preparation, properties and uses of a new class of materials, *Mater Sci Eng* 2000;**28**:1–63.

Avila A. F., Soares M. I., Neto A. S., A study on nanostructured laminated plates behavior under low-velocity impact loadings, *International Journal of Impact Engineering*, **34**, 28-41 (2007)

Bhiwankar N. N. and Weiss R. A., Melt intercalation/exfoliation of polystyrene–sodium-montmorillonite nanocomposites using sulfonated polystyrene ionomer compatibilizers, *Polymer*, **47**, 19, 6684-6691 (2006)



Bradley S. F., Application of carbon nanotubes for human space exploration, *Proceedings of nanospace 98*.

Bradley S. F., Processing of carbon nanotubes for revolutionary space applications, *AIAA-2000-5345* 2000.

Briscoe B. J., Fiori L., and Pelillo E., Nano-indentation of polymeric surfaces, *J. Phys. D Appl. Phys.*, **31**, 2395 (1998).

Chen C. and Curliss D., Processing and morphological development of montmorillonite epoxy nanocomposites, *Nanotechnology*, **14** (2003) 643 - 648.

Dasari A., Yu Z. Z., Mai Y. W., Hu G. H., Varlet J., Clay exfoliation and organic modification on wear of nylon 6 nanocomposites processed by different routes, *Comp. Sci. and Tech.*, **65**, 2314 – 2328 (2005)

Dietsche F, Thomann Y, Thomann R and Mulhaupt R., Translucent acrylic nanocomposites containing anisotropic nano-particle derived from intercalated layered silicates, *J Appl Polym Sci* ,**75**, 396 – 405 (2000)



Duquesne S., Jama C., Le Bras M., Delobel R., Recourt P. and Gloaguen J. M.,
Elaboration of EVA–nanoclay systems—characterization, thermal behaviour and
fire performance, *Compos Sci Technol*, **63**, 1141. (2003)

Flory P. J., *Principles of Polymer Chemistry*, Cornell University Press, Ithaca,
NY (1953)

Frenkel J., *Kinetic Theory of Liquids*, ch 7, 1955 (New York: Dover)

Giannelis E. P., Polymer layered silicate nanocomposites, *Adv Mater*, **8**, 29–35.
(1996)

Haque A., Shamsuzzoha M., Hussain F. and Dean D., S2-Glass/Epoxy Polymer
Nanocomposites: Manufacturing, Structures, Thermal and Mechanical Properties,
Journal of Composite Materials, **37**, 1821 – 1837 (2003)

Ho M. W., Lam C. K., Lau K. T., Ng D. H. L. and Hui D., Mechanical properties
of epoxy-based composites using nanoclays, *Composite Structures*, **75**, 415-421
(2006)



Isik I., Yilmazer U. and Bayram G., Impact modified epoxy/montmorillonite nanocomposites: synthesis and characterization, *Polymer*, **44**, 6371 – 6377 (2003)

Jia Q. M., Zheng M., Xu C. Z. and Chen H. X., The mechanical properties and tribological behavior of epoxy resin composites modified by different shape nanofillers, *Polym. Adv. Tech.*, **17**, 168 – 173 (2006)

Ke Y., Long C. and Qi Z., Crystallization, properties, and crystal and nanoscale morphology of PET-clay nanocomposites, *J Appl Polym Sci*, **71**, 1139–46 (1999)

Kojima Y., Usuki A., Kawasumi M., Okada A., Fukushima Y. and Kurauchi T., Mechanical properties of nylon 6-clay hybrid, *J Mater Res*, **8**, 1185 (1993)

Kortaberria G., Solar L., Jimeno A., Arruti P., Gómez C. and Mondragon I., Curing of an epoxy resin modified with nanoclay monitored by dielectric spectroscopy and rheological measurements, *Journal of Applied Polymer Science*, **102**, 5927-5933 (2006)



LAM C. K., Cheung H. Y., Lau K. T., Zhou L. M., Ho M. W. and Hui D., Cluster size effect in hardness of nanoclay/epoxy composites, *Composites Part B: Engineering*, **36**, 263 – 269 (2005)

LAM C. K. and Lau K. T., The effect of thermo-mechanical mixing energy to the mechanical performance of a nanoclay/polymer composite, *Composites Part A: Applied Science and Manufacturing*, 2007; Submitted.

LAM C. K. and Lau K. T., Tribological behavior of nanoclay/epoxy composites, *Materials Letters*, 2007; In press.

LAM C. K. and Lau K. T., Optimization Effect of Micro Hardness by Nanoclay Clusters in Nanoclay/Epoxy Composites, *Journal of Thermoplastic Composite Materials*, 2007; Accepted.

LAM C. K. and Lau K. T., Enhancement of Hardness and Wear Resistance of Epoxy-based Materials using Clay Nanoparticles, *HKIE Transactions*, 2007; **14**(1): In press.



LAM C. K. and Lau K. T., Localized elastic modulus distribution of nanoclay/epoxy composites by using nanoindentation, *Composite Structures*, **75**, 553-558 (2006)

LAM C. K., Lau K. T., Cheung H. Y. and Ling H. Y., Effect of ultrasound sonication in nanoclay clusters of nanoclay/epoxy composites, *Materials Letters*, **59**, 1369 – 1372 (2005)

LAM C. K., Lau K. T. and Zhou L. M., Nano-mechanical creep properties of nanoclay/epoxy composite by nano-indentation, *Key Engineering Materials*, **334-335**, 685-688 (2007)

Lamer V. K. and Dinegar R. H., *J. Am. Chem. Soc.*, **72**, 4847 (1950)

Lau K. T., Effectiveness of using carbon nanotubes as nano-reinforcements for advanced composite structures, *Carbon*, **40**, 1605–6 (2002)

Lau K. T., Micro-hardness and flexural properties of carbon nanotube composites, *Proc ICCE* **9** (2002)



Lau K. T., Chan W. L., Shi S. Q. and Zhou L. M., Interfacial bonding behaviour of embedded SMA wire in smart composites: micro-scale observation. *Mater Des*, **23**, 265–70 (2002)

Lau K. T. and Hui D., The revolutionary creation of advanced materials: carbon nanotube composites, *Compos Part B Eng*, **33**, 263–77 (2002)

Lau K. T., Poon C. K., Yam L. H. and Zhou L. M., Bonding behaviour at a NiTi/epoxy interface: SEM observation and theoretical study, *Mater Sci Forum*, **394–395**, 527–30 (2002)

LeBaron P. C., Wang Z. and Pinnavaia T. J., Polymer-layered silicate nanocomposites: an overview, *Appl Clay Sci*, **15**, 11–29 (1999)

Li M., Palacio M. L., Carter C. B. and Gerberich W. W., Indentation deformation and fracture of thin polystyrene films, *Thin Solid Films*, **416**, 174 (2002)

Liu T., Lim K. P., Tjiu W. C., Pramoda K. P. and Chen Z. K., Preparation and characterization of nylon 11/organoclay nanocomposites, *Polymer*, **44**, 3529 –



3535 (2003)

Liu W. P., Hoa S. V. and Pugh M., Fracture toughness and water uptake of high-performance epoxy/nanoclay nanocomposites, *Composites Science and Technology*, **65**, 2364-2373 (2005)

Miyoshi K., Pohlchuck B., Street K. W., Zabinski J. S., Sanders J. H., Voevodin A. A. and Wu R. L. C., Sliding wear and fretting wear of diamondlike carbon-based, functionally graded nanocomposite coatings, *Wear*, **225 – 229**, 65 – 73 (1999)

Ng C. B., Schadler L. S. and Siegel R. W., Synthesis and mechanical properties of TiO₂-epoxy nanocomposites, *Nanostruct Mater*, **12**, 507–510 (1999)

Oliver W. C. and Pharr G. M., An improved technique for determining hardness and elastic modulus using load and displacement sensing indentation experiments, *J. Mater. Res.*, **7**, 1564 - 1583 (1992)



Payne J. A., Strojny A., Francis L. F. and Gerberich W. W., Indentation measurements using a dynamic mechanical analyzer, *Polym. Eng. Sci.*, **38**, 1529 (1998).

Pharr G. M., Oliver W. C. and Brotzen F. R., On the generality of the relationship among contact stiffness, contact area, and elastic modulus during indentation, *J. Mater. Res.*, **7**, 613 – 617 (1992)

Pollet E., Delcourt C., Alexandre M. and Dubois P., Transesterification catalysts to improve clay exfoliation in synthetic biodegradable polyester nanocomposites, *European Polymer Journal*, **42**, 1330-1341 (2006)

Pope C., Making Space, *Professional Eng*, **15**, 22–23 (2002)

Qi B., Zhang Q. X., Bannister M. and Mai Y. W., Investigation of the mechanical properties of DGEBA-based epoxy resin with nanoclay additives, *Composite Structures*, **75**, 514-519 (2006)

Qian D., Dickey E. C., Andrews R. and Rantell T., Load transfer and



deformation mechanism in carbon nanotube–polystyrene composites, *Appl Phys Lett*, **76**, :2868 – 2870 (2000)

Rice B. P., Chen C. G., Cloos L. and Curliss D., Carbon fibre composites: organoclay-aerospace epoxy nanocomposites, *SAMPE J*, **37**, 7–9 (2001)

Sandler J., Shaffer M. S. P., Prasse T., Bauhofer W., Schutle K. and Windle A. H., Development of a dispersion process for carbon nanotubes in an epoxy matrix and the resulting electrical properties. *Polymer*, **40**, 5967 – 5971 (1999)

Schadler L. S., Giannaris S. C. and Ajayan P. M., Load transfer in carbon nanotube epoxy composites, *Appl Phys Lett*, **73**, 3842–3844 (1998)

Shen L., Liu T. and Lv P., Polishing effect on nanoindentation behavior of nylon 66 and its nanocomposites, *Polymer Testing*, **24**, 746 – 749 (2005)

Shen L., Phang I. Y., Chen L., Liu T. and Zeng K., Nanoindentation and morphological studies on nylon 66 nanocomposites. I. Effect of clay loading, *Polymer*, **45**, 3341 – 3349 (2004)



Shen L., Phang I. Y., Liu T. and Zeng K., Nanoindentation and morphological studies on nylon 66/organoclay nanocomposites. II. Effect of strain rate, *Polymer*, **45**, 8221 – 8229 (2004)

Shi L., Sun C., Gao P., Zhou F. and Liu W., Mechanical properties and wear and corrosion resistance of electrodeposited Ni–Co/SiC nanocomposite coating, *Appl. Surf. Sci.*, **252**, 3591- 3599 (2006)

Siddiqui N. A., Woo R. S. C., Kim J. K., Leung C. C. K. and Munir A., Mode I interlaminar fracture behavior and mechanical properties of CFRPs with nanoclay-filled epoxy matrix, *Composites Part A: Applied Science and Manufacturing*, **38**, 449-460 (2007)

Sinha Ray S. and Okamoto M., Polymer/layered silicate nanocomposites: a review from preparation to processing, *Prog Polym Sci*, **28**, 1539–1641. (2003)

Song M., Hourston D. J., Yao K. J., Tay J. K. H. and Ansarifard M. A., High performance nanocomposites of polyurethane elastomer and organically modified layered silicate, *J Appl Polym Sci*, **90**, 3239–3243 (2003)



Sun J., Francis L. F., Gerberich W. W., Mechanical properties of polymer-ceramic nanocomposite coatings by depth-sensing indentation, *Polym. Eng. Sci.*, **45**, 207 (2005)

Ton-That M. T., Ngo T. D., Ding P., Fang G., Cole K. C. and Hoa S. V., Epoxy nanocomposites: Analysis and kinetics of cure, *Polymer Engineering and Science*, **44**, 1132-1141 (2004)

Timmerman J. F., Hayes B. S. and Seferis J. C., Nanoclay reinforcement effects on the cryogenic microcracking carbon fibre/epoxy composites, *Compos Sci Technol*, **62**, 1249 – 1258 (2001)

Tsai J. L. and Sun C. T., Effect of Platelet Dispersion on the Load Transfer Efficiency in Nanoclay Composites, *Journal of Composite Materials*, **38**, 567 – 579 (2004)

Vaia R. A., Jandt K. D., Kramer E. J., Giannelis E. P., Microstructural evolution of melt intercalated polymer-organically modified layered silicates nanocomposites, *Chem Mater*, **8**, 2628 – 2635 (1996)



VanLandingham M. R., Villarrubia J. S., Gutherie W. F. and Meyers G. F.,
Macromol. Symp., **167**, 15 (2001)

Veprek S., The search of novel superhard materials, *J Vacuum Sci Technol*, **A17**,
2401–2420 (1999)

Veprek S. and Argon A. S., Towards the understanding of mechanical properties
of super- and ultrahard nanocomposites, *J Vacuum Sci Technol*, **B20**, 650–664
(2002)

Veprek S. and Jilek M., Superhard composite coating: from basic science toward
industrialization, *Pure Appl Chem*, **74**, 475–481 (2002)

Wang L., Gao Y., Xue Q., Liu H. and Xu T., Effects of nano-diamond particles on
the structure and tribological property of Ni-matrix nanocomposite coatings, *Mat.
Sci. and Eng. A*, **390**, 313 – 318 (2005)

Wetzel B., Hauptert F., Friedrich K., Zhang M. Q. and Rong M. Z., Impact and
wear resistance of polymer nanocomposites at low filler content, *Polym Eng Sci*,



42, 1919 – 1927 (2002)

Wetzel B., Hauptert F. and Zhang M. Q., Epoxy nanocomposites with high mechanical and tribological performance, *Compos Sci Technol*, **63**, 2055 – 2067 (2003)

Yang F., Yngard R. and Nelson G. L., Flammability of Polymer-Clay and Polymer-Silica Nanocomposites, *Journal of Fire Sciences*, **23**, 209 – 226 (2005)

Yang Z., Dong B., Huang Y., Liu L., Yan F. Y. and Li H. L., Enhanced wear resistance and micro-hardness of polystyrene nanocomposites by carbon nanotubes, *Mat. Chem. and Phys.*, **94**, 109 – 113 (2005)

Yano K., Usuki A., Okada A., Kurauchi T. and Kamigaito O., Synthesis and properties of polyimide-clay hybrid, *J. Polym. Sci.: Part A: Polym. Chem.*, **31**, 2493 (1993)

Zeldovich J. B., *Acta Physicochim.*, **18**, 1 (1943)



Zettlemoyer A. C., *Nucleation Phenomena*, 1969 (New York: Dekker)

Zhang H., Zhang Z., Friedrich K. and Eger C., Property improvements of in situ epoxy nanocomposites with reduced interparticle distance at high nanosilica content, *Acta Materialia*, **54**, 1833 – 1842 (2006)

Zhou L. M., Mai Y. W. and Baillie C., Interfacial debonding and fibre pullout stresses: part V. A methodology for evaluation of interfacial properties, *J Mater Sci*, **29**, 5541 – 5550 (1994)

Zhou L. M., Ye L. and Mai Y. W., Techniques for evaluating interfacial properties of fibre matrix composites, *Key Eng Mater*, **104–107**, 549–600 (1995)



APPENDIX

A selection of published papers arising from the Doctor of Philosophy thesis is attached for reference.

1. **LAM CK**, Cheung HY, Lau KT, Zhou LM, Ho MW and Hui D. Cluster size effect in hardness of nanoclay/epoxy composites. *Composites Part B: Engineering*, 2005; **36**(3), 263 – 269.
2. **LAM CK**, Lau KT, Cheung HY and Ling HY. Effect of ultrasound sonication in nanoclay clusters of nanoclay/epoxy composites. *Materials Letters*, 2005; **59**(11), 1369 – 1372.
3. **LAM CK** and Lau KT. Localized elastic modulus distribution of nanoclay/epoxy composites by using nanoindentation. *Composite Structures*, 2006; **75**(1-4): 553-558.
4. **LAM CK**, Lau KT and Zhou LM. Nano-mechanical creep properties of nanoclay/epoxy composite by nano-indentation. *Key Engineering Materials*, 2007; **334-335**: 685-688.
5. **LAM CK** and Lau KT. Tribological behavior of nanoclay/epoxy composites. *Materials Letters*, 2007; **61**(18): 3863-3866.



Cluster size effect in hardness of nanoclay/epoxy composites

Chun-Ki Lam^a, Hoi-yan Cheung^a, Kin-tak Lau^{a,*}, Li-min Zhou^a, Man-wai Ho^b, David Hui^b

^aDepartment of Mechanical Engineering, The Hong Kong Polytechnic University, Hung Hom, Kowloon, Hong Kong, China

^bDepartment of Mechanical Engineering, University of New Orleans, New Orleans, LA 70148, USA

Received 10 March 2004; revised 16 April 2004; accepted 28 September 2004

Available online 19 November 2004

Abstract

The mechanical and thermal properties of nanoclay polymer composites have been experimentally investigated over the last decade. Most of the research has been focused mainly on the control of their interplanar structures, which govern the global properties of the composites. In reality, these structures (both exfoliated and intercalated patterns) are hardly achieved through the use of conventional manufacturing process for plastic products. Different sizes of clusters mixed by nanoclays and matrix would be easily formed, particularly in the extrusion of polymer-based components. This paper experimentally studied the hardness and interlaminar shear properties of nanoclay/epoxy composites with different amount of nanoclay content, which formed different sizes of nanoclay/epoxy clusters after mixing in an extruder. The results showed that the micro-hardness of the composites could be enhanced when a small amount of nanoclay was added into the epoxy. However, there was an optimal limit in which the hardness was dropped by continuously increasing the nanoclay content. Microscopic observation on the fracture surfaces showed that the size of the clusters varied with the amount of nanoclays used in the composites. Although previous literatures have reported that the use of nanoclays in polymer-based composites could enhance their mechanical properties, the interlaminar shear test indicated that the short beam shear strength of the composites decreased after adding the nanoclays into the matrix.

© 2004 Elsevier Ltd. All rights reserved.

Keywords: B. Hardness; Product development

1. Introduction

Recently, the developments on mechanical, bio-medical engineering and aeronautical components have been miniaturised into different scale levels. Due to the increasing need of micro/nano-sized devices and structural members in the nano-tech and space industries, the development of new advanced materials, which are able to sustain their strength in any extreme temperature and chemical environments without being mechanically, chemically or thermally degraded and to be manufactured to high degree of defect-free properties, particularly for space and automotive applications becomes a new challenge in the current decade.

In past few years, National Aeronautics and Space Administration (NASA) and John Space Centre (JSC) have

driven breakthrough technologies to expand human exploration of space [1]. One of the most important focuses in achieving this goal is to develop new materials, which possess strength-to-weight ratio that far exceeds any of today's materials. Nanocomposites have emerged as very efficient strategy to upgrade properties of synthetic polymers to the level where performance of these nanocomposites largely exceed the ones of conventional composites. Veprek and Argon [2], Veprek and Jilek [3] and Veprek [4] have found that nanocomposites exhibit superior hardness and elastic properties, and high level of thermal stability. Carbon nanotube and nanoclay composites have been recognised as the best nano-fillers for the composites to fulfil aforementioned requirements [5–7]. Successful use of nanotube/polymer and nanotube/metal composites in space applications is highly dependent on the structural integrity and mechanical performances of the composites in extreme low temperature, heat and radiation, and vacuum environments, particularly for reusable launch vehicles [8,9]. However, many literatures have reported that the nanotubes

* Corresponding author. Tel.: +86 852 2766 7730; fax: +86 852 2365 4703.

E-mail address: mmktlau@

(K.-t. Lau).

have a poor bonding strength to aerospace-used polymer matrices because of their perfect hexagonal atomic architecture on the nanotubes' surface [10–13]. It has been proofed that a good bonding strength between internal reinforcements and matrix is one of the dominant factors that attribute the outstanding mechanical properties of advanced composite structures [14–17]. Adding chemical catalysts to enhance the bonding strength of composite systems may damage the carbon–carbon bond that attributes to extraordinary mechanical and electrical properties of nanotubes.

Recent researches have found that commercial organo-clays (layered silicates such as montmorillonite which has a fairly large aspect ratio, hereafter called 'nanoclays') could be used to make aerospace epoxy nanocomposites, which possess excellent mechanical strength and low coefficient of thermal expansion with relatively low cost and ease of fabrication [18,19]. Companies such as Nanocor, Southern Clay Products and Zhejiang Fenfong Clay Chemicals Co. in the US, Japan and China have patented technologies for production of nanoclays. Several polymer companies both in the US and Japan are producing nylon nanocomposites for automotive and packaging applications. A few weight percentages of nanoclays with a thickness of about 1 nm in polymer boots the heat distortion temperature by 80 °C making possible structural applications under conditions where the pristine polymer would normally fail [19–21]. The existence of silicate platelets inhibits the polymer chain rotation that influences the mechanical and thermal properties of the nanocomposites. In some extents, these platelets could inhibit the crack propagation due to the formation of micro-voids when the nanocomposites are under-stressed, thus increasing the fracture toughness [22]. Alexandre and Dubois [19] and Lau et al. [23] have proofed that the mechanical and thermal properties of composites could be modulated by nano-fabrication process of intermetallic compounds. A latest literature also revealed that intercalated and exfoliated morphologies of nanoclay/polymer composites are highly affected by the manufacturing time and temperature, which in turn influenced the cross-linking interaction of polymer. The amount of nanoclays inside the polymer also appeared different with mechanical, thermal and electrical properties of nano-composites. The permeability of water, oxygen and other gases of the nanoclay composites also decreased making these composites ideal for building up advanced composite fuel tanks for tomorrow's reusable launch vehicles. Timmerman et al. [24] clearly demonstrated that the number of transverse cracking of carbon fibre/epoxy laminates as a response to cryogenic cycling was significantly reduced when nanofillers were used. The development of these polymer-based nanocomposite materials enables to make advanced structures with high strength and thermal stability. It thus minimises the risk of geometrical and thermal distortions due to the changes of ambient temperature and therefore maintains the aerodynamic profiles of the structures. Due to

layered silicate nanocomposites achieving composite properties at much lower volume fraction of reinforcements, they avoid many of the costly and cumbersome fabrication techniques common to conventional fibre-reinforced polymer materials [18].

An appropriate addition of a small amount of nanoclays, typically in the range of 3–5 wt%, could provide an efficient upgrade on the mechanical and thermal performances of conventional polymer-based composites [25,26]. In an industrial point of view, these lightest particles could be effectively used to produce high stiffness and thermal stability structural components with having low cost and no subsection to weight penalty. Recently, many product manufacturing organisations and commercial companies have started to deeply investigate the possibility of producing this type of nanocomposites in order to fabricate plastic products with high strength and low thermal distortion [27–29]. However, these properties are highly dependent on the dispersion property and interplanar arrangements of nanoclays inside the composites [30].

It has been reported that the impact and wear resistance, as well as fracture toughness of advanced composites, could be improved by mixing an optimal amount of nanoclays [31–33]. The optimal amount of the nanoclays in the composites is dependent on the particle size and shape, homogeneity, dispersion property and interfacial bonding properties between the particles and matrix. Practically, both exfoliated and intercalated planar structures can only be found in laboratory studies, which is in fact difficultly achieved during product moulding processes. To the best knowledge of the authors to date, no detailed report has been published presently to study the dispersion properties of nanoclays in polymer-based materials after extrusion. Practically, the formation of micro-size nanoclay/polymer clusters always appears in the composite. These clusters, in turn, would influence the intrinsic material and mechanical properties of the composites. To look at the cluster size effects to the properties of the composites, micro-hardness and interlaminar shear tests were conducted in this work. Different amounts of nanoclays were added into epoxy-based resin to form nanoclay/epoxy composites. The micro-hardness of testing samples was examined by using micro-hardness tester (Vicker type). The microscopic observation on the fractured surface of these samples was also conducted to measure the cluster size and study their effect to the hardness of the composites. An interlaminar shear test was also carried out to investigate the short beam shear properties that have not been discussed previously elsewhere of the composites. The effect co-relating to the size of nanoclay/epoxy clusters was also discussed in this paper.

2. Experimental investigation

Araldite GY 251 epoxy resin and hardener HY 956 in the ratio of 5:1 were used to form base polymer materials.

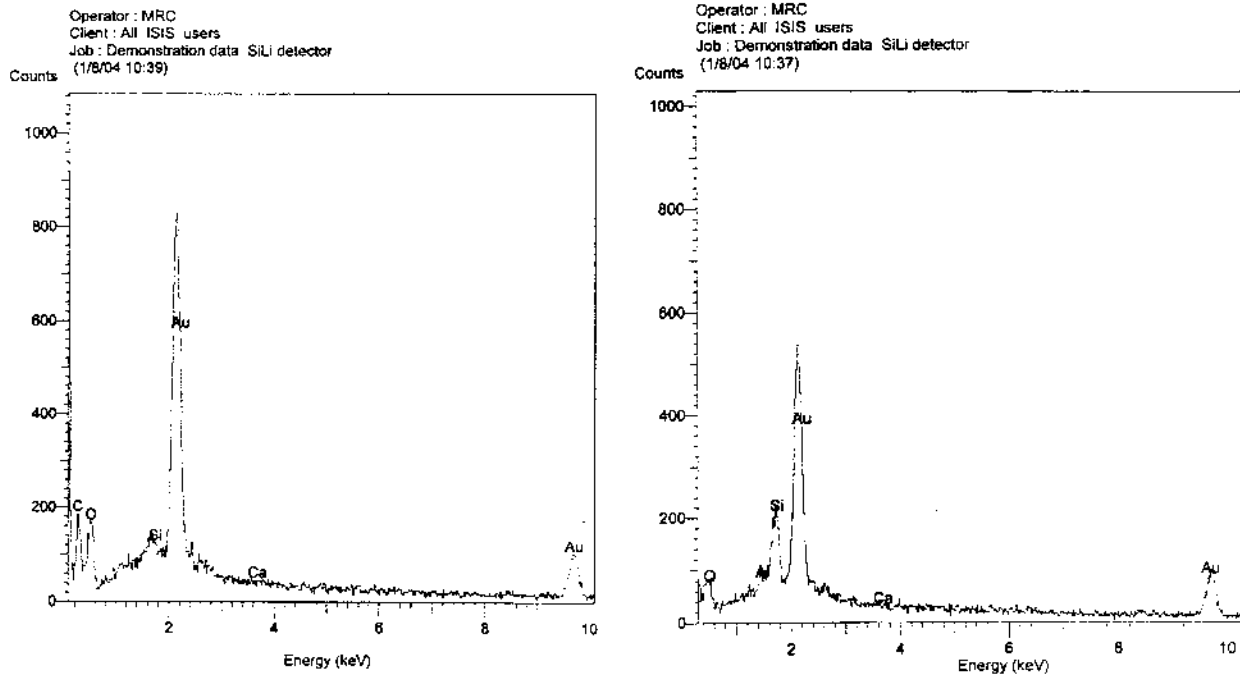


Fig. 1. Diagrams captured from EDX: location away from the cluster (left) and the center of the cluster (right).

Nanoclay particles (SiO_2 , Nanolin DK1 series from the Zhejiang FH Nanoclay Chemical Technology Company) were then added into the materials to form nanoclay/epoxy nanocomposites. The mean diameter, density and moisture content of the nanoclays were 25 nm, less than 3% and 0.45 g/cm^3 with more than 95% of SiO_2 , respectively. At the beginning of the nanocomposite manufacturing process, the predetermined amount of nanoclays was added into the resin by mechanical stirring and followed by sonication for 1 h at room temperature in order to provide a uniformly dispersed nanoclay/epoxy uncured mixture. The hardener was then added into the mixture by appropriate ratio followed by mechanical stirring and afterward vacuuming for another 24 h. This step was to remove air-bubbles that were trapped inside the nanocomposites before curing. Six types of sample were made in this study; they were pure epoxy (0 wt% nanoclay content), and nanocomposites with 2, 4, 6, 10 and 15 wt% of nanoclays.

Micro-hardness test was conducted to all samples and a total of 10 indentation points were measured on the samples' surface. Micro-hardness tester (FM-7E) of the Future-Test Corporation from Tokyo, Japan was used in the test. To increase the accuracy of measurement, all samples' surfaces were well polished using high-grade sandpapers prior to the test. To observe the dispersion and mixing properties of the nanoclays in the nanocomposites with different amounts of nanoclay content, all samples were broken into two pieces by undergoing a bending test. The fractured surfaces were then examined by using Leica Stereoscan 440 model scanning electron microscopy (SEM). X-ray spectroscopy (EDX) was also used to verify the validity of the location of the nanoclay particles (Fig. 1).

Since most of the previous study was mainly focused on the tensile and bending strengths of nanotube/polymer composites, the interfacial shear properties of these composites have not yet been investigated elsewhere. In our work, similar samples as for the micro-hardness test were also made for interlaminar shear test to investigate the short beam shear strength of the nanocomposites and study the effect to their cluster sizes. The size of the samples was $10 \text{ mm} \times 10 \text{ mm} \times 2 \text{ mm}$.

3. Results and discussion

Table 1 shows the experimental measurements of micro-hardness of the nanocomposites with different nanoclay

Table 1
Results of the micro-hardness measurements at different nanoclay compositions

Hardness (Hv)	0%	2%	4%	6%	10%	15%
1	9.9	10.8	11.7	11.7	8.2	1.5
2	9.2	11.6	12.9	10.4	5.1	1.5
3	9.6	10.1	11.9	11.1	5.5	2.3
4	9.4	11.9	14.4	10.9	6.2	3.5
5	9.5	12.3	12.8	12.9	6.1	5.1
6	10.1	11.8	12.7	12.5	6.1	2.9
7	10.6	10.1	12.1	10.9	4.8	3.2
8	11.4	12.2	13.1	11.8	5.3	2.6
9	10.5	12	13	12	6.1	2.2
10	10.6	11.3	12.9	10.2	6.3	2
Average	10.08	11.41	12.75	11.44	5.97	2.68
Maximum	11.4	12.3	14.4	12.9	8.2	5.1
Minimum	9.2	10.1	11.7	10.2	4.8	1.5

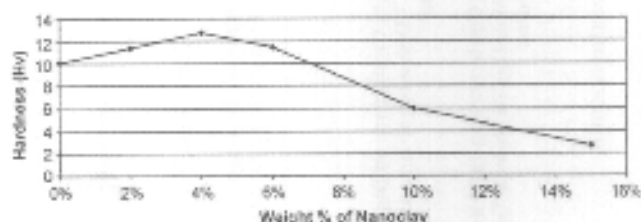


Fig. 2. Average value of the micro-hardness test at different weight % of nanoclay.

contents. An average hardness was calculated by 10 indentation measurements and a plot of the results of each type of samples is shown in Fig. 2. At the beginning, it is obvious that the hardness increases with increasing nanoclay content. The maximum hardness was measured where the nanoclay content reached 4 wt%. A decline of the hardness also appears on further increasing the nanoclay content; the hardness decreases in a drastic manner from 12.75 Hv (4 wt% of nanoclay) to 2.68 Hv (15 wt% of nanoclay). In most previous literatures, it has been indicated that adding a small amount of nanoclays into polymer-based materials could potentially enhance their strength, like hardness of the current samples with the nanoclay content less than 4 wt%. However, it is also reasonable to believe that it should have an optimal limit since the physical properties between these nano-structural materials and matrix are different. In the current study, it was demonstrated that the hardness was dropped if the amount of the nanoclays was beyond 4 wt%. Besides, for the sample with more nanoclay content, the time required for solidification was also longer as well as the surface of the sample was relatively soft compared with other samples with lower nanoclay contents. It was suspected that the nanoclays might retard the chemical reaction, and so cause incomplete curing process of the composites. For all samples with high nanoclay content, the matrix might not be fully cured. By looking at the trend presented in Fig. 2, it is worthwhile to study in detail the physical mechanism that governs this contrary effect in hardness of the nanocomposites.

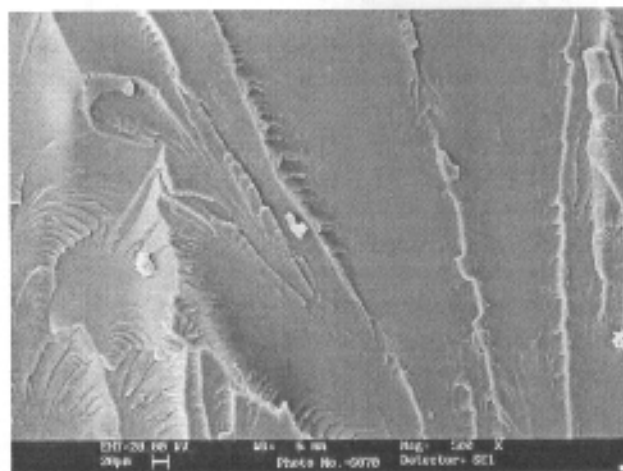


Fig. 3. SEM photograph of pure epoxy.

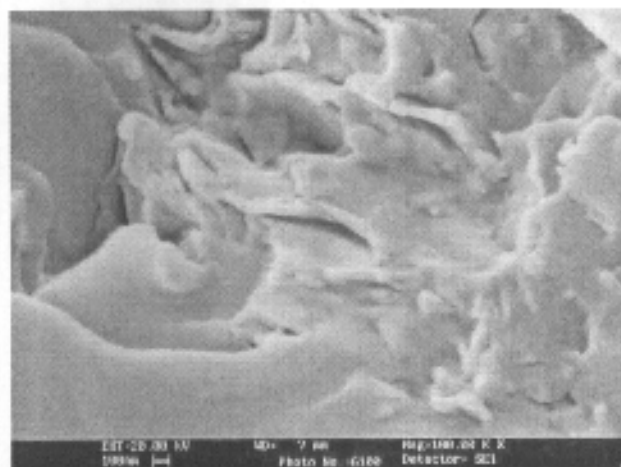


Fig. 4. SEM photograph of 4 wt% of nanoclay/epoxy composite.

In Figs. 3 and 4, morphological observations on the fractured surfaces of the nanoclay/epoxy samples are shown. It is obvious that clusters were formed in the sample with 4 wt% nanoclay particles. The average diameter of the clusters measured throughout the whole sample at different locations was about 125 nm. The clusters were evenly distributed throughout the sample, which reflected that those small nanoparticles intended to agglomerate with each other. This phenomenal observation denoted that those nanoclay particles could not be easily dispersed although it was subjected to sonication. This might be due to the fact that the viscosity of the room temperature cured resin could not be low enough to allow the diffusion of monomers into planar structures of the nanoclay particles. This agglomeration may be caused during the curing process of the composites. The nanoclay particles moved toward others and partly bonded with epoxy matrix to form clusters. The size of the clusters was dependent on the amount of nanoclay particles inside the uncured matrix.

In Fig. 5, a micrograph of the sample with 15 wt% of nanoclay particles is also shown. Comparing with Fig. 4,

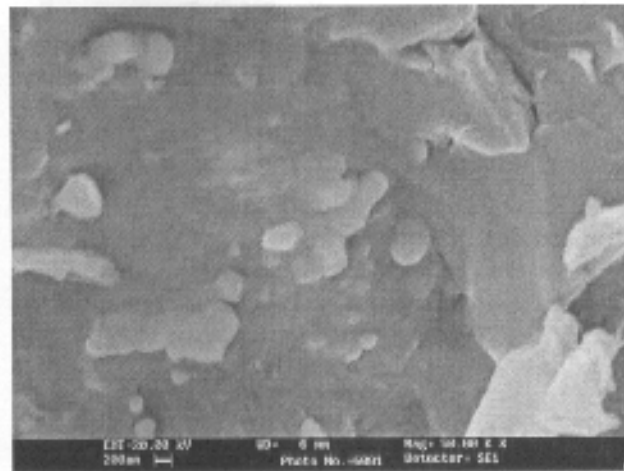


Fig. 5. SEM photograph of 15 wt% of nanoclay/epoxy composite.

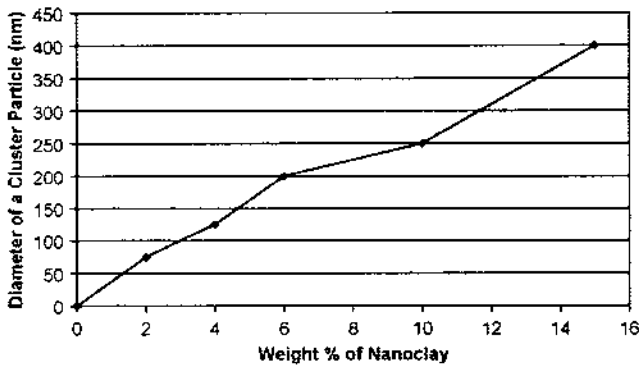


Fig. 6. Variation of the cluster size at different wt% of nanoclay.

the size of the clusters was apparently bigger than that of the one with only 4 wt% nanoclay particles. The diameter of the sample with 15 wt% of nanoclay particles measured from the SEM was about 400 nm. In fact, this phenomenon is explainable. As the wt% of the nanoclay particles increases, the free volume allows for nanoclay particles to move around would be decreased. Therefore, the mechanical stirring and ultrasonic separation techniques cannot be effectively used to separate the agglomerations of the nanoclays, as higher the wt% of nanoclay particles in the epoxy resin, the less the free volume for each nanoclay particles to live in. At the same time, the cross-link density of the nanocomposites then increased and it therefore resulted in increasing the tendency for the nanoclay particles to form pairs or clusters [10]. As the amount of nanoclay particles increases in the composites, the inertia for the nanoclay particles to form agglomeration is also increased. Therefore, larger clusters of nanoclay would be easily formed. The average cluster sizes of nanocomposites with different amounts of nanoclay particles are plotted in Fig. 6. The cluster size increased with increasing the wt% of the nanoclay particles.

In Fig. 7, there is a long plastic yielding zone appearing in a pure epoxy sample after the interlaminar shear test. From the long yielding zone of the pure epoxy, it is obvious that the fracture energy consumption and toughness of the pure epoxy are quite high. However, it is apparently different compared with others after adding nanoclay

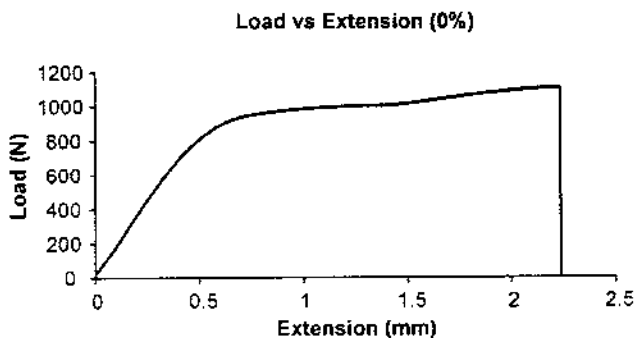


Fig. 7. Load–deflection curve extracted from the interlaminar shear test of pure epoxy.

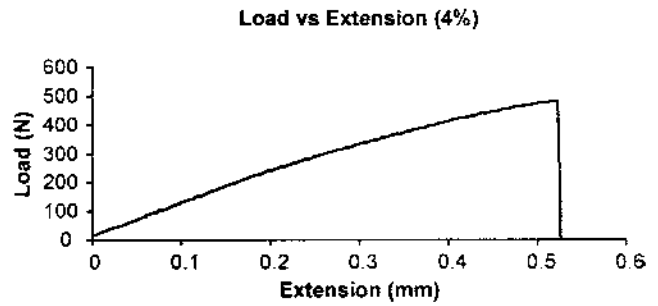


Fig. 8. Load–deflection curve extracted from the interlaminar shear test of nanocomposites with 4 wt% of nanoclay particles.

particles. In Figs. 8 and 9, the load–deflection relationships captured during the interlaminar shear test of nanoclay/epoxy samples are shown. In these figures, it is obvious that the ductility of the epoxy-based samples dropped after mixing with nanoclay particles. In Fig. 8, no plastic deformation of a nanocomposite with 4 wt% of nanoclays is shown. However, for another sample with 15 wt% of nanoclays, the sample became softer and the short beam shear strength is also lower than the one with 4 wt% of nanoclay particles and pure epoxy.

Although Section 2 shows that the hardness of nanoclay/epoxy composites could be enhanced and the maximum hardness could be achieved by adding 4 wt% nanoclays into epoxy composites, the results from the interlaminar shear strength test showed that the short beam shear strength of all nanoclay/epoxy composites decreased. In the 4 wt% of nanoclay sample, there were more tiny nanoclay clusters as shown in Fig. 4. These tiny nanoclay clusters of about 125 nm in diameter would squeeze into the polymer chains of the epoxy and loosen the interaction between them. In addition, from the crack surface of the sample, the clusters' shape appeared like a sphere. From the mirror-like interface between the nanoclay clusters and the epoxy, it reflects that the interfacial bonding strength between the nanoclay clusters and the epoxy was weak. As a result, when there is an external force applied, debond at the interface between the nanoclays and matrix would easily occur. Hence, the short beam shear strength of the epoxy decreased with

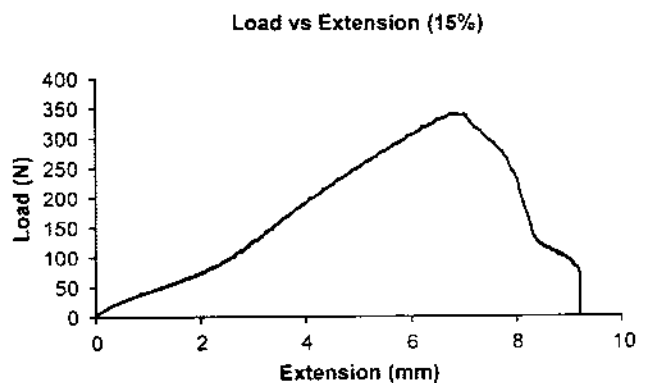


Fig. 9. Load–deflection curve extracted from the interlaminar shear test of nanocomposites with 15 wt% of nanoclay particles

nanoclay added. At 15 wt% of nanoclay, the load–deflection behaviour appeared in a strange way as shown in Fig. 9. It does not possess a clear fracture point after the maximum load appears. This is due to the fact that the amount of nanoclay content has been greatly increased and the mechanical behaviour is determined by the nanoclay particles interaction rather than the epoxy–nanoclay interface mechanisms. The epoxy now acts like ‘glue’ between the nanoclay particles. As the cluster size becomes larger, the breaking paths of the applied load become rougher and in a ‘zig–zag’ manner. Hence, the fracture toughness of the 15 wt% of nanoclay becomes higher and more difficult to fracture than the pure epoxy. Thus, the micro-hardness of the 15 wt% of nanoclay sample was much lower than the other samples as the deformability of the 15 wt% of nanoclays was the highest. Therefore, it becomes obvious to understand the trend of the micro-hardness behaviour as shown in Fig. 2 and the existence of the optimal amount of the addition of nanoclay.

According to the results obtained from the micro-hardness test, the cluster size attributed the properties of the nanocomposites. Increasing the amount of the nanoclay particles in the nanocomposites represents that the quantity of the nano-reinforcements increases, and therefore the overall strength is also increased. However, it would have an optimal limit since the size of the cluster increases and subsequently the total number of the clusters, as nano/micro-reinforcements are decreased. The distance between these nano-size or micro-size clusters is also decreased which eventually reduces the effectiveness of strengthening the nanocomposites. This is an important aspect since most of previous literatures were mainly focused on the production of exfoliated and intercalated nanoclay structures for nanocomposites. The effect due to the formation of clusters is normally neglected. However, in real practice, it is extremely difficult to control the nano-structures of the nanoclay particles in the general product manufacturing process. Although the formation of clusters, in some points would induce adverse effects to the product, the use of appropriate amount of nanoclay particles, which produce a pre-determined size of clusters after the manufacturing process, may give optimal mechanical and thermal properties to the whole structures.

4. Conclusion

This paper studies the hardness of nanoclay/epoxy composites with different amounts of nanoclay particles. The influence of the hardness due to the formation of clusters is also explained in the paper. Microscopic observation using SEM was conducted to measure the cluster size of the nanocomposites. It was found that the hardness of the nanocomposites increased with increasing nanoclay content. However, it was also seen that there was an optimal limit. This might be due to the size of the clusters

reaching a crucial limit and therefore the reinforcing function of the nanoclays decreased. Interlaminar shear test showed the short beam shear strength of the epoxy decreased after adding few percents of nanoclay particles. A shiny surface of the clusters, captured from the fractured samples also revealed that a weak bonding interfacial existed between the cluster and matrix, which led to a poor short beam strength of the composites. However, it would not affect the hardness of the composites during different stress transfer mechanisms between the hardness and shear properties of materials. Further work is under processing to study in detail the mechanical and thermal properties of nanoclay/polymer composites due to formation of clusters.

Acknowledgements

This project was supported by the Hong Kong Polytechnic University Grants (G-T 936 and G-T 861). The work was also funded by the Graduate Enhancement Funds, University of New Orleans.

References

- [1] Bradley SF. Application of carbon nanotubes for human space exploration. *Proceedings of nanospace 98*.
- [2] Veprek S, Argon AS. Towards the understanding of mechanical properties of super- and ultrahard nanocomposites. *J Vacuum Sci Technol* 2002;B20(2):650–64.
- [3] Veprek S, Jilek M. Superhard composite coating: from basic science toward industrialization. *Pure Appl Chem* 2002;74(3):475–81.
- [4] Veprek S. The search of novel. Superhard materials. *J Vacuum Sci Technol* 1999;A17(5):2401–20.
- [5] Lau KT, Hui D. The revolutionary creation of advanced materials: carbon nanotube composites. *Compos Part B Eng* 2002;33:263–77.
- [6] Lau KT. Micro-hardness and flexural properties of carbon nanotube composites. *Proc ICCE* 2002;9.
- [7] Rice BP, Chen CG, Cloos L, Curliss D. Carbon fibre composites: organoclay-aerospace epoxy nanocomposites. *SAMPE J* 2001;37(5):7–9.
- [8] Bradley SF. Processing of carbon nanotubes for revolutionary space applications. *AIAA-2000-5345* 2000.
- [9] Pope C. Making Space. *Professional Eng* 2002;15(11):22–3.
- [10] Lau KT. Effectiveness of using carbon nanotubes as nano-reinforcements for advanced composite structures. *Carbon* 2002;40:1605–6.
- [11] Schadler LS, Giannaris SC, Ajayan PM. Load transfer in carbon nanotube epoxy composites. *Appl Phys Lett* 1998;73(26):3842–4.
- [12] Sandier J, Shaffer MSP, Prasse T, Bauhofer W, Schulte K, Windle AH. Development of a dispersion process for carbon nanotubes in an epoxy matrix and the resulting electrical properties. *Polymer* 1999;40:5967–71.
- [13] Qian D, Dickey EC, Andrews R, Rantell T. Load transfer and deformation mechanism in carbon nanotube–polystyrene composites. *Appl Phys Lett* 2000;76(20):2868–70.
- [14] Zhou LM, Mai YW, Baillie C. Interfacial debonding and fibre pullout stresses: part V. A methodology for evaluation of interfacial properties. *J Mater Sci* 1994;29:5541–50.
- [15] Zhou LM, Ye L, Mai YW. Techniques for evaluating interfacial properties of fibre matrix composites. *Key Eng Mater* 1995;104–107:549–600.

- [16] Lau KT, Poon CK, Yam LH, Zhou LM. Bonding behaviour at a NiTi/epoxy interface: SEM observation and theoretical study. *Mater Sci Forum* 2002;394–395:527–30.
- [17] Lau KT, Chan WL, Shi SQ, Zhou LM. Interfacial bonding behaviour of embedded SMA wire in smart composites: micro-scale observation. *Mater Des* 2002;23:265–70.
- [18] LeBaron PC, Wang Z, Pinnavaia TJ. Polymer-layered silicate nanocomposites: an overview. *Appl Clay Sci* 1999;15:11–29.
- [19] Alexandre M, Dubois P. Polymer-layered silicate nanocomposites: preparation, properties and uses of a new class of materials. *Mater Sci Eng* 2000;28:1–63.
- [20] Giannelis EP. Polymer layered silicate nanocomposites. *Adv Mater* 1996;8(1):29–35.
- [21] Vaia RA, Jandt KD, Kramer EJ, Giannelis EP. Microstructural evolution of melt intercalated polymer-organically modified layered silicates nanocomposites. *Chem Mater* 1996;8:2628–35.
- [22] Dietsche F, Thomann Y, Thomann R, Mulhaupt R. Translucent acrylic nanocomposites containing anisotropic nano-particle derived from intercalated layered silicates. *J Appl Polym Sci* 2000;75:396–405.
- [23] Lau KT, Ho MW, Hui D. The nano-fabrication and characterisation of aluminium-based intermetallic compounds and metal matrix composite materials. Submitted for publication; 2002.
- [24] Timmerman JF, Hayes BS, Seferis JC. Nanoclay reinforcement effects on the cryogenic microcracking carbon fibre/epoxy composites. *Compos Sci Technol* 2001;62:1249–58.
- [25] Ke Y, Long C, Qi Z. Crystallization, properties, and crystal and nanoscale morphology of PET-clay nanocomposites. *J Appl Polym Sci* 1999;71:1139–46.
- [26] Song M, Hourston DJ, Yao KJ, Tay JKH, Ansarifard MA. High performance nanocomposites of polyurethane elastomer and organically modified layered silicate. *J Appl Polym Sci* 2003;90:3239–43.
- [27] Kojima Y, Usuki A, Kawasumi M, Okada A, Fukushima Y, Kurauchi T, et al. Mechanical properties of nylon 6-clay hybrid. *J Mater Res* 1993;8:1185.
- [28] Yano K, Usuki A, Okada A, Kurauchi T, Kamigaito O. Synthesis and properties of polyimide-clay hybrid. *J Polym Sci: Part A: Polym Chem* 1993;31:2493.
- [29] Duquesne S, Jama C, Le Bras M, Delobel R, Recourt P, Gloaguen JM. Elaboration of EVA-nanoclay systems—characterization, thermal behaviour and fire performance. *Compos Sci Technol* 2003;63:1141.
- [30] Sinha Ray S, Okamoto M. Polymer/layered silicate nanocomposites: a review from preparation to processing. *Prog Polym Sci* 2003;28:1539–641.
- [31] Wetzel B, Hauptert F, Zhang MQ. Epoxy nanocomposites with high mechanical and tribological performance. *Compos Sci Technol* 2003;63:2055–67.
- [32] Wetzel B, Hauptert F, Friedrich K, Zhang MQ, Rong MZ. Impact and wear resistance of polymer nanocomposites at low filler content. *Polym Eng Sci* 2002;42:1919–27.
- [33] Ng CB, Schadler LS, Siegel RW. Synthesis and mechanical properties of TiO₂-epoxy nanocomposites. *Nanostruct Mater* 1999;12:507–10.



Effect of ultrasound sonication in nanoclay clusters of nanoclay/epoxy composites

Chun-ki Lam, Kin-tak Lau*, Hoi-yan Cheung, Hang-yin Ling

Department of Mechanical Engineering, The Hong Kong Polytechnic University, Hung Hom, Kowloon, Hong Kong, China

Received 23 September 2004; accepted 14 December 2004

Available online 18 January 2005

Abstract

Ultrasound sonication has been widely used in the exfoliation of nanoclay platelets. Nevertheless, the existence of absolutely exfoliated nanoclay composites is impossible in reality. Regions of intercalated nanoclay platelets can be easily formed and agglomerate as tiny clusters. Different sizes of clusters mixed by nanoclays and matrix would be easily formed, particularly in the extrusion of polymer-based components. The effects of ultrasound sonication in these intercalated nanoclay clusters will be detailedly discussed in this paper. The hardness of nanoclay/epoxy composites samples made under different ultrasound sonication time will be examined to compare their mechanical performances. X-ray diffraction (XRD) technique will also be employed to investigate the interplanar distance between the nanoclay platelets in different samples. Scanning electron microscopy (SEM) will also be used to investigate the clusters distribution inside the composites. The results show that there exists an optimum ultrasound sonication time where the mechanical properties of the composites are mostly enhanced. The cluster sizes of nanoclay change with different sonicating time, whereas the interplanar distance without being altered.

© 2005 Elsevier B.V. All rights reserved.

Keywords: Nanocomposites; Hardness; Ultrasound Sonication

1. Introduction

The enhanced mechanical properties of nanoclay/polymer nanocomposites with a relatively light weight compared with conventional polymer-based composites have attracted the focus of researchers in the last decade. A relatively small amount of nanoclays, typically in the range of 3–5 wt.% [1,2], is enough for the enormous improvements in the mechanical and thermal properties of the nanoclay/polymer nanocomposites. Industries and manufacturing sectors enjoy the economic benefits of the effective production of this improved structural component with small amount of nanoclay required. Investigations on the product developments of the nanoclay/polymer nanocomposites have began explosively in major manufacturing

industries in the world [3–5]. Nevertheless, these improved mechanical properties are mainly depended on the fine dispersion of nanoclay platelets inside the nanoclay/polymer nanocomposites. Ultrasound sonication of pre-mixed nanoclay/polymer samples is always being used in assistance of the dispersion or exfoliation of the nanoclay platelets [6]. Fully exfoliated nanoclay/polymer nanocomposites are expected after the ultrasound sonication process. However, entirely exfoliated or intercalated nanoclay structures are seldom found in the plastic moulding process in reality, they can only be successfully implemented in laboratory studies. Small clusters of micro- or nanosize in diameter of nanoclays are often formed in the composites instead and they would influence the mechanical properties of the nanoclay/polymer nanocomposites. However, the effectiveness of ultrasound sonication in the dispersion of nanoclay platelets inside the nanoclay clusters of the composites has not yet been studied elsewhere.

* Corresponding author. Tel.: +86 852 2766 7730; fax: +86 852 2365 4703.

E-mail address: mmktlau@polyu.edu.hk (K. Lau).

In this paper, nanoclay/epoxy composites with the same amount of nanoclay content were made subjected to different ultrasound sonicating times. Micro-hardness test (Vicker type) was employed to investigate the mechanical properties of the composites. X-ray diffraction (XRD) and scanning electron microscopy (SEM) were used to study the interplanar distance between the nanoclay platelets and examine the surface morphology of fractured samples, respectively.

2. Experimental investigation

Araldite GY 251 epoxy resin mixed with hardener HY 956 in the ratio of 5:1 to form base materials and nanoclay particles (SiO_2 , Nanolin DK1 series from the Zhejiang FH Nanoclay Chemical Technology Company) were then added into the materials to form nanoclay/epoxy nanocomposites. The mean diameter, density and moisture content of the nanoclays were 25 nm, less than 3% and 0.45 g/cm^3 with more than 95% of SiO_2 , respectively. At the beginning of the nanocomposite manufacturing process, 4% of the nanoclay was added into the resin by hand stirring and followed by different sonicating time, namely, 5 min, 10 min, 15 min, 30 min and 60 min at room temperature. The hardener was then added into the mixtures by mechanical stirring and followed by vacuuming for another 24 h for curing. Under microscopic observation, the nanoclay platelets were formed after interacting with the epoxy. Micro-hardness test was conducted to all samples and a total of 10 indentation points were measured on the samples' surface. Micro-hardness tester (FM-7E) of the Future-Test Corporation from Tokyo, Japan was used in the test. To increase the accuracy of measurement, all sample's surfaces were well polished using high-grade sandpapers prior to the test. To observe the dispersion properties of the nanocomposites with different amount of nanoclay content, some samples were broken into two pieces by a simple three-point bending test and the fractured surfaces were examined by using Leica Stereoscan 440 model scanning electron microscopy (SEM). XRD examinations were also conducted on the different sonicating samples by using the Philips PW 1830 X-ray Generator ($\text{Cu K} \alpha$, $\lambda=0.154 \text{ nm}$).

3. Results and discussion

Fig. 1 shows the micro-hardness of the nanocomposites containing 4 wt.% of nanoclay prepared at different sonicating times. An average hardness was calculated by 10 indentation measurements. As observed in the figure, there is an optimum hardness at the nanoclay/epoxy nanocomposite with 10 min sonicating time. The micro-hardness of the nanoclay sample is decreasing from 10.6 Hv (pure epoxy) to 9.03 Hv (5 min sonicating time). Further increasing the sonication time beyond the optimum point, the micro-hardness decreases gradually from 12.05 Hv (10

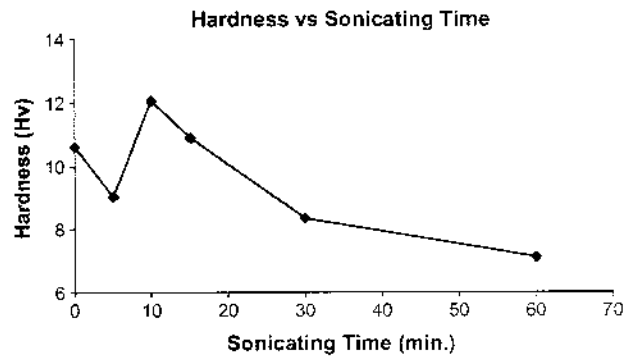


Fig. 1. Micro-hardness of the nanoclay composites at different sonicating times at 4 wt.% of nanoclay content.

min sonicating time) to 7.09 Hv (60 min sonicating time). From the trend of the micro-hardness value in nanoclay/epoxy nanocomposite samples with different sonicating times, the time for the ultrasound sonication must be adequately controlled in order to achieve the maximum mechanical performance of the composites. At any sonicating time lower or higher than the optimum value, the micro-hardness will be adversely affected and may be even worse than the original pure epoxy sample.

In Figs. 2–4, SEM photographs of fractured samples with 5 min, 10 min and 15 min sonicating time are shown, respectively. It is obvious that nanoclay clusters were formed in all of the samples. In Fig. 2, a micrograph of the sample with 5 min sonicating time is shown. The size of the nanoclay cluster is about 100 nm in diameter and they are separated from each other with a long distance. A SEM micrograph of the sample with 10 min sonicating time is shown in Fig. 3. Comparing with the cluster size in Fig. 2, the size of the nanoclay clusters have been reduced drastically to 10 nm in diameter. The distances between each cluster are shorter. Hence, the surface area for the interaction between the nanoclay clusters and the epoxy has been increased and provided the better reinforcement in micro-hardness of the nanoclay sample. Fig. 4 shows that the size of the nanoclay clusters increases again and the distance between the clusters is also increased. Therefore, the mechanical performance of the nanoclay composites is decreased with applying longer sonication time during the composite manufacturing process.

In Fig. 5, the XRD spectrums of each of the samples are shown. There exists only one common peak at $2\theta=20$ with the maximum intensity. Thus, by the use of the Bragg's formula, the interplanar distance between nanoclay platelets is approximately equal to 0.225 nm. That means the sonicating time variation would not influence the exfoliation of the nanoclay platelets as always expected by most of the researchers. The only difference with sonicating time varying is the changing of cluster size.

According to the results obtained, ultrasound sonication can aid the enhancement of the mechanical properties in the nanoclay/epoxy nanocomposites with properly control-



Fig. 2. SEM of the nanoclay composite with 5 min sonicating time at 4 wt.% of nanoclay content.

ling the sonicating time. Ultrasound sonication is a form of vibration that provides energy for the nanoclay platelets to escape from the surrounding restraining force. Extra energy is given to the nanoclay platelets to move around when sonicating the nanoclay/polymer mixture. If there is not enough energy given to the polymer/nanoclay mixture, the nanoclay platelets cannot escape the restraining force within the nanoclay clusters; thus, the aid for dispersion is limited. On the other hand, if too much energy is given to the nanoclay platelets to move around, then the frequency of collision between each single nanoclay platelets will be increased. The chance for each single platelet to tangle up and react to form a larger nanoclay cluster would be increased. Hence, the dispersion mechanism may be adversely affected with too much energy given to the nanoclay platelets. Therefore, an optimum sonicating time must be achieved in order to have the maximum dispersion ability. Nevertheless, if there are clusters of nanoclay formed, as shown in Fig. 5, the interplanar distance of the nanoclay platelets would not be affected by the ultrasound sonication. Instead, the size of the nanoclay clusters are

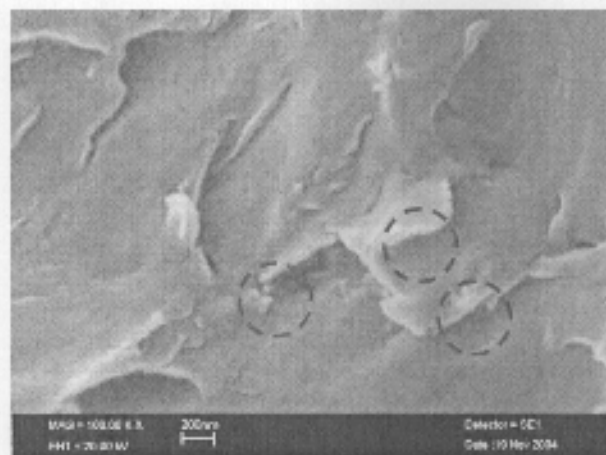


Fig. 3. SEM of the nanoclay composite with 10 min sonicating time at 4 wt.% of nanoclay content.

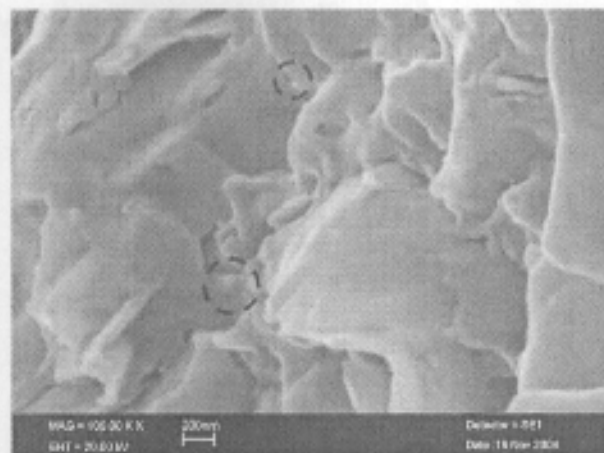


Fig. 4. SEM of the nanoclay composite with 15 min sonicating time at 4 wt.% of nanoclay content.

reduced in accompany with the increase of the number of nanoclay clusters when the optimum sonicating time is reached. Therefore, the surface area for the interaction between the nanoclay clusters and the epoxy is increased and provides the maximum reinforcement. If further increasing the sonicating time beyond the optimum value, the size of the nanoclay clusters will start growing and therefore the number of the nanoclay clusters will then decrease. Thus, the surface area for the interaction between the nanoclay clusters and the epoxy is reduced and the mechanical properties of the composites are adversely affected.

4. Conclusion

This paper presents the ultrasound sonication effect on the dispersion properties and platelet arrangement of nano-

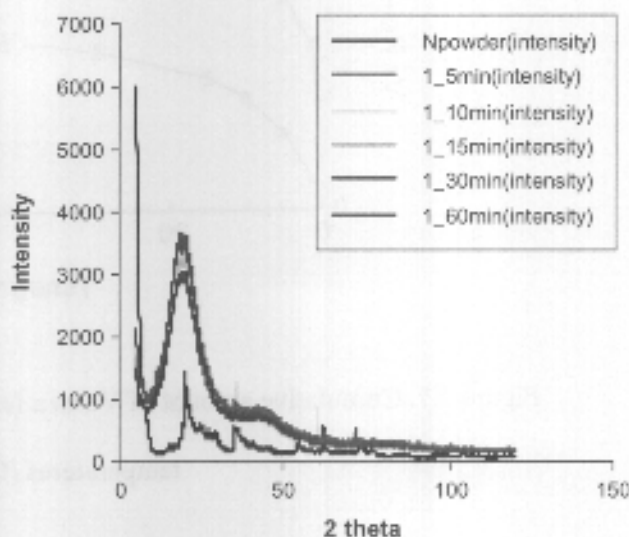


Fig. 5. XRD spectrum of different sonicating times at 4 wt.% of nanoclay content.

clay/epoxy composites. Micro-hardness test of the composites with different ultrasound sonication times was conducted. Optimum micro-hardness of 4 wt.% nanoclay content occurs at 10 min sonicating time. The existence of the optimum micro-hardness at a specific sonicating time is also explained in this paper. With the aids of SEM and XRD on the fractured samples, it was found that different ultrasound sonication times indeed affect the size of the nanoclay clusters. Nevertheless, the interplanar distance between the nanoclay platelets was less influenced by the sonication effect. By using XRD, the interplanar distance between nanoclay platelets was approximately equal to 0.225 nm for all the sonicating samples. Exfoliation of the nanoclay platelets inside the nanoclay clusters cannot be done by simple ultrasound sonication. Further work is still on going to detailedly study the mechanical of nanoclay/polymer composites due to the formation of clusters and the interaction between the platelets and matrix inside the clusters using nanoindentation technique.

Acknowledgement

This project was supported by the Hong Kong Polytechnic University Grants (G-T 936 and G-T 861).

References

- [1] Y. Ke, C. Long, Z. Qi, *J. Appl. Polym. Sci.* 71 (1999) 1139–1146.
- [2] M. Song, D.J. Hourston, K.J. Yao, J.K.H. Tay, M.A. Ansarifard, *J. Appl. Polym. Sci.* 90 (2003) 3239–3243.
- [3] C. Chen, D. Curliss, *Nanotechnology* 14 (2003) 643–648.
- [4] T. Liu, K.P. Lim, W.C. Tjiu, K.P. Pramoda, Z.K. Chen, *Polymer* 44 (2003) 3529–3535.
- [5] S. Duquesne, C. Jama, M. Le Bras, R. Delobel, P. Recourt, *J.M. Gloaguen, Comput. Sci. Tech.* 63 (2003) 1141.
- [6] I. Isik, U. Yilmazer, G. Bayram, *Polymer* 44 (2003) 6371–6377.



Localized elastic modulus distribution of nanoclay/epoxy composites by using nanoindentation

Chun Ki Lam, Kin Tak Lau *

Department of Mechanical Engineering, The Hong Kong Polytechnic University, Hung Hom, Kowloon, Hong Kong, China

Available online 30 May 2006

Abstract

The enhancement of mechanical properties by the use of nanoclay platelets in epoxy resin has been extensively investigated through numerous experimental techniques recently. Elastic modulus was obtained mainly from the tensile test of bone-like nanoclay/epoxy specimens. The results from the tensile test have only showed the globalized mechanical properties of composites and their localized elastic modulus distribution has been neglected. Despite the orientation and the degree of exfoliation of nanoclay platelets inside nanoclay/epoxy composites, the localized elastic modulus is important for the understanding of the distribution of agglomerations of nanoclay platelets. The elastic modulus of nanoclay/epoxy composite samples made under different sonication temperatures would be examined by nanoindentation to compare their localized mechanical behaviors. Scanning electron microscopy (SEM) would also be employed to study the distribution of the nanoclay clusters throughout the composites. The results showed that the elastic modulus varied throughout the composites and the nucleation theory of clusters was modified to explain the behavior of nanoclay agglomerations under different sonication temperatures in which the viscosity of the epoxy resin was varied. The gravitational effect was significant to cause the non-uniform distributions of nanoclay clusters at low sonication temperature.

© 2006 Elsevier Ltd. All rights reserved.

Keywords: Nanocomposites; Elastic modulus; Nanoindentation

1. Introduction

Numerous researches found out that the elastic modulus, micro-hardness, other mechanical properties and thermal retardation properties of nanoclay/polymer composites can be effectively improved by using a small fraction of nanoclay content inside the composites in the last decade [1,2]. Wear resistance, fracture toughness and the reduction of water absorption ability of polymer-based matrix were significantly improved by adding a small amount of nanoparticles [3–5]. Major manufacturing companies and product innovation firms have been investigating the possibilities for nanoclays to strengthen their products since mechanical properties were highly enhanced without any increase of the total weight [6,7]. It is well known that the addition of small

amount of nanoclays or nanoparticles into polymer matrix can greatly improve their globalized mechanical properties. Globalized mechanical properties of nanoclay/polymer are mainly studied by the use of bulk material testing techniques. In common practice for instance, axial tensile test is used to study the elastic modulus of various nanoclay/polymer composites. Nevertheless, the localized mechanical properties of nanoclay/polymer composites were an important characteristic for studying the integrity, internal properties and uniformity of the composites. It is because intermolecular micro-voids will generally exist in composites under stress. In the bulk material properties testing of the composites containing nanoclays, Dietsche et al. [8] showed that the fracture toughness was increased by adding nanoclay particles into the composites due to the blockage of crack propagation initiated by the micro-voids between the nanoclay particles. But at the nanoscopic point of view, the existence of micro-voids in the nanoclay/polymer composites will increase the possibility of fracture as the

* Corresponding author. Tel.: +852 27667730; fax: +852 23654703.
E-mail address: mmktlau@polyu.edu.hk (K.T. Lau).

micro-voids are the origins of cracking. Cracks will propagate through the weakest path in the composites where micro-voids or debonding situate. Hence, investigations on the localized mechanical behaviors of nanoclay/polymer composites are significant for manufacturing an infrastructure that minimizes the risk of void formation.

Nanoindentation is a newly invented technique for the determination of localized material properties that was introduced by Oliver and Pharr in 1992 [9]. Elastic modulus, nano-hardness and contact stiffness of a material can be determined by nanoindentation nanoscopically [9,10]. Fig. 1 shows a typical nanoindentation profile for determination of localized mechanical properties in polymer composites. The technique makes use of creating a permanently plastically deformed surface on a material being tested. From the force applied on the surface and the indentation depth of the indent, relative elastic modulus can be obtained by the equations given as:

$$A_c = f(h_c) \quad (1)$$

$$E_r = (\sqrt{\pi}/2)/(S/\sqrt{A_c}) \quad (2)$$

where h_c is the contact height that different from the maximum indentation height as shown in Fig. 2, A_c is the contact surface area between the nanoindenter and the material surface and S is the contact stiffness that is the slope of the unloading portion in the nanoindentation profile as shown in Fig. 1.

Numerous researches conducted in investigating the mechanical properties of pure elements and Shen et al. [11–13] has studied the morphologies of nylon 66/nanoclay composites by nanoindentation. To the best knowledge of the authors, there were no nanoindentation testings focusing on the localized mechanical properties of nanoclay clusters distribution for nanoclay/epoxy composites.

In this paper, the elastic modulus of nanoclay clusters throughout the cross-section of nanoclay/epoxy composites prepared under different sonication temperatures will be studied by using nanoindentation technique. The nano-

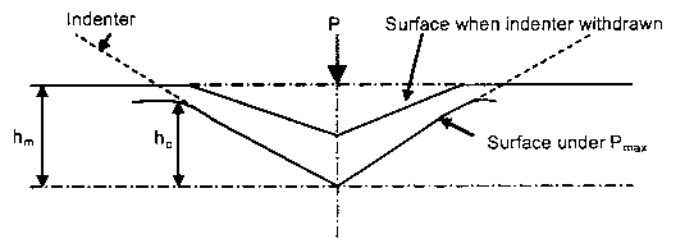


Fig. 2. Schematic diagram of nanoindentation parameters.

clay content and the sonication time were fixed throughout the experiment while the sonication temperatures varied in order to visualize the distribution of nanoclay clusters under different sonication temperatures. By the different sonication temperatures, the viscosity of the epoxy resin will be different. The higher the sonication temperature, the lower the viscosity of epoxy resins. Nanoindentation was employed to study the localized mechanical properties of the composites as the diameters of nanoclay clusters were only several hundred nanometers. Scanning electron microscopy (SEM) was used to study the morphologies of the cross-sectionally cut surface of the nanoclay/epoxy composites in order to visualize the distribution of nanoclay clusters. X-ray spectroscopy (EDX) was used to identify the locations of the nanoclay clusters.

2. Experimental investigation

2.1. Materials

Nanoclay particles (SiO_2 Nanolin DK1 series from the Zhejiang FH Nanoclay Chemical Technology Company) were used as nano-reinforcements for this study. The mean diameter, density and moisture content of the nanoclays were 25 nm, 0.45 g/cm^3 and more than 95% of SiO_2 , respectively. The epoxy resin and hardener selected for this study were araldite GY 251 and hardener HY 956 respectively. They were mixed in a ratio of 5 to 1 parts by weight.

2.2. Sample preparation

Nanoclay/epoxy composite samples were fabricated by using mechanical mixing process with nanoclay content fixed at 4 wt.%. The 4 wt.% of nanoclay content was used in order to achieve maximized mechanical strength of the composites reinforced by nanoclay clusters as studied by Lam et al. [14]. Nanoclays were dispersed in the epoxy resin at 4 wt.% of nanoclays. The mixture was hand stirred for 10 min until the epoxy resin and the nanoclays were well mixed at room temperature. Ultrasound sonication was employed to further disperse the nanoclays in the epoxy resin. Before sonicating the samples, each of them was subjected to a different level of preheating process in order to study the dispersion effect of the localized elastic modulus at different temperatures. Three types of samples were fabricated in this study; they were composites with 40°C ,

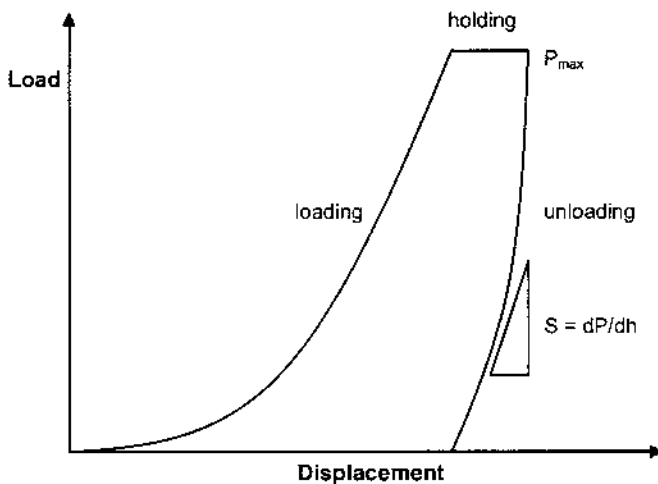


Fig. 1. The loading profile of nanoindentation.

80 °C and 100 °C preheating for 5 min before ultrasound sonication. After the preheating, the samples were sonicated. The sonication time was fixed at 20 min for all the samples in order to ensure the maximized mechanical performance [15]. Hardener was added into the sonicated mixtures by hand stirring and followed by vacuuming for 24 h at room temperature for curing. All of the composites samples were subjected to fine polishing by SiC papers and followed by diamond paste polishing to 6 μm accuracy before nanoindentation in order to ensure the reliability of the results obtained.

2.3. Measurements

To study the surface morphology of the composites under different sonicating temperatures, scanning electron microscopy (SEM) was used to examine the fractured surfaces of the samples. The fractured surfaces of the samples were obtained by cutting the freshly fabricated samples cross-sectionally and followed by fine polishing to 6 μm accuracy. SEM photographs were obtained by examining the distribution of nanoclay clusters at different regions of the samples. The SEMs of the top layer and the bottom layer of the cured composites were used to compare the effects of sonicating temperature and as well as gravitational effect on the allocation of the nanoclay clusters. Under the gravitational effect, the nanoclay particles were settled to the bottom of the specimens. Leica Stereoscan 440 model SEM machine was employed for the examinations.

The nanoindentation data were obtained on a Hysitron Triboindenter at room temperature. A Berkovich nanoindenter head was used for the nanoindentation experiments. The elastic modulus was measured from the bottom to the top layer of the fractured surfaces of different samples. Each composite sample were subject to one set of nanoindentation. Relative elastic moduli (E_r) were obtained for each set of data of the nanoindented samples. The loading time, holding time, unloading time and maximum indentation force (P_{max}) are 10 s, 10 s, 40 s and 100 μN for all testing samples. The separation distance between each nanoindentation point was 0.05 mm.

3. Results and discussion

3.1. Surface morphology

Fig. 3 shows the surface morphologies of the fractured surfaces of composites treated at different sonicating temperatures. Fig. 4 shows the EDX examinations on both circled and non-circled regions in Fig. 3. It shows an obvious increase in Si content in the circled regions and thus nanoclays agglomerate in the circled regions. The size of nanoclay clusters increases while the number of nanoclay clusters decrease when the sonicating temperatures increase. This result proves that when the viscosity of the epoxy resin decrease with the increase in sonicating temperatures, nanoclays tended to form larger clusters or agglomerations due to the less restraining force by the surrounding

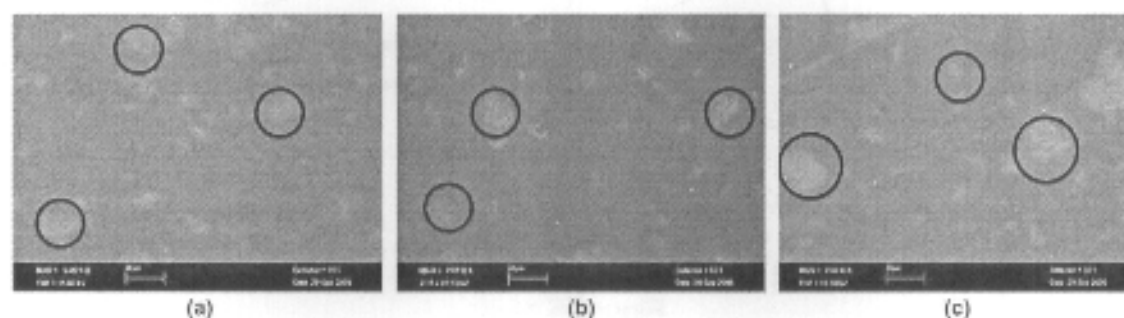


Fig. 3. Surface morphologies of the fractured surface of nanoclay/epoxy composites with different sonicating temperatures, (a) 40 °C (b) 80 °C and (c) 100 °C.

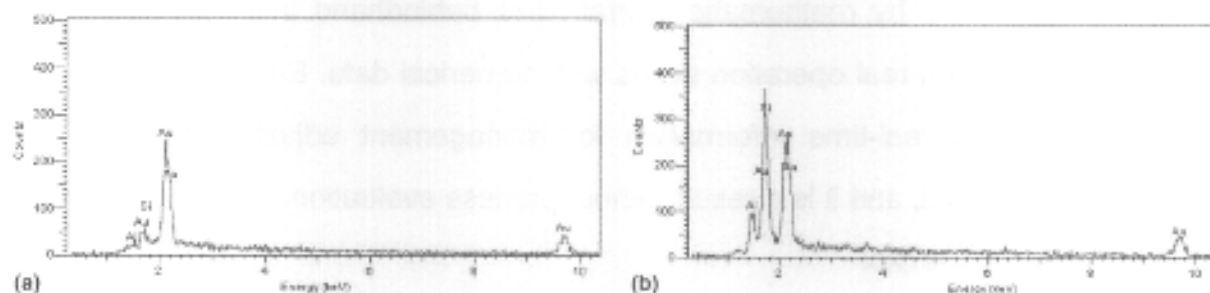


Fig. 4. EDX examinations on the fractured surfaces of nanoclay/epoxy composites. (a) non-circled regions and (b) circled regions.

epoxy resin. They can be flown around easily with the aid of sonication that provided extra kinetic energy for the nanoclays. The significance of increasing the kinetic energies of the nanoclays is to overcome interfacial tension between the nanoclay clusters formed and the epoxy matrix. There are several papers review on the classic nucleation of clusters in liquids in supersaturated vapor by Abraham [16], Zettlemoyer [17] and Lamer [18], which was developed by Volmer, Becker and Doring and further modified by Frenkel [19] and Zeldovich [20] explained the increase of surface energy or interfacial tension when the size of clusters increase. For a cluster containing n atoms, the surface energy is given by:

$$\sigma A(n) = 4\pi\sigma(3v/4\pi)^{2/3}n^{2/3} \quad (3)$$

where σ is the interfacial tension per unit area, $A(n)$ is the surface area of the cluster, and v is the volume per molecule in the bulk liquid. By applying Eq. (3) to the case of nanoclay clusters in epoxy resin, n corresponds to the number of nanoclay particles inside a nanoclay cluster. When the nanoclay cluster increases in size, the nanoclay particles inside the cluster will increase. Hence, n will increase in Eq. (3) and result in increasing the interfacial tension between the nanoclay cluster and the surrounding epoxy resin. Nevertheless, if the interfacial tension continues to build up on the surface of the nanoclay clusters when their sizes increase, it will cause the nanoclay particles more difficult to adhere on the surface of the nanoclay clusters. Therefore, the change of viscosity of epoxy resin due to the alteration of sonication temperatures plays an important role in the growing of nanoclay cluster sizes. The size of the nanoclay clusters depends on the viscosity of the epoxy resin by altering the sonication temperatures, thus, Eq. (3) needs to be further modified for describing the interfacial tension between the nanoclay clusters and the epoxy resin. As the increase in nanoclay cluster size is directly proportional to the sonication temperature and inversely proportional to the viscosity of epoxy resin approximately, the relationship between the sonication temperatures, the viscosity of epoxy resin and the nanoclay cluster sizes can be described by Eq. (4). Considering a nanoclay cluster with radius r and have n nanoclay particles inside,

$$r = kT[1/(d\rho/dT)] \quad (4)$$

where k is a constant, T is the sonication temperature and ρ is the viscosity of epoxy resin. Eq. (4) describes the phenomenon of increasing the sonication temperature, the viscosity of epoxy resin will be decreased and the nanoclay cluster size will be increased. Differentiating both sides of Eq. (4) by d/dt , the rate of increase of the radius of the nanoclay cluster can be obtained.

$$dr/dt = k(dT/dt)[1/(d\rho/dT)] \quad (5)$$

$$dr/dt = k(d^2T/dt^2 d\rho) \quad (6)$$

Integrating Eq. (6) with respect to time,

$$r = k(dT/d\rho) \quad (7)$$

Assuming the nanoclay clusters are spherical in shape, the change of the surface area " A " of a nanoclay cluster is given by:

$$A = 4\pi[k(dT/d\rho)]^2 \quad (8)$$

As the interfacial tension equal to $\sigma A(n)$ as stated in Eq. (3), combining with Eq. (8), the interfacial tension is given by:

$$\sigma A = \sigma 4\pi[k(dT/d\rho)]^2 \quad (9)$$

$$\sigma A = \sigma 4\pi[k(1/(d\rho/dT))]^2 \quad (10)$$

In Eq. (10), if the change of viscosity of epoxy resin is huge from 40 °C to 100 °C, $d\rho/dT$ becomes large in Eq. (10) and results in decreasing the interfacial tension between the nanoclay clusters and epoxy resin. This is the reason for the increase in nanoclay cluster sizes when increasing the sonication temperatures since the interfacial tension between the nanoclay clusters and the epoxy resin decrease and facilitates the adhesion of free nanoclay particles onto the surface of nanoclay clusters. Furthermore, increase in sonication temperature also provides addition of kinetic energy for the free nanoclay particles to move and increase the chance to adhere on the surfaces of nanoclay clusters. If the change of viscosity with respect to sonication temperature is 0, for example, in solids or composites, the interfacial tension as predicted by Eq. (10) will become infinity and hence the size of nanoclay clusters will not change in cured nanoclay/epoxy composites.

4. Nanoindentation

Figs. 5–7 show the comparisons of the nanoindentation profiles between the bottom surfaces and the top surfaces of the composites with different sonication temperature treatments, namely, 40 °C, 80 °C and 100 °C, respectively. The comparisons of the behavior of the difference in the nanoindentation depth of the loading portion are significant as the deeper the nanoindentation depth in the loading portion, the softer the material is. In Fig. 5, the nanoindentation depth increases drastically in the top surface of the composite when comparing with the bottom surface of the composite. The result shows that the mechanical resis-

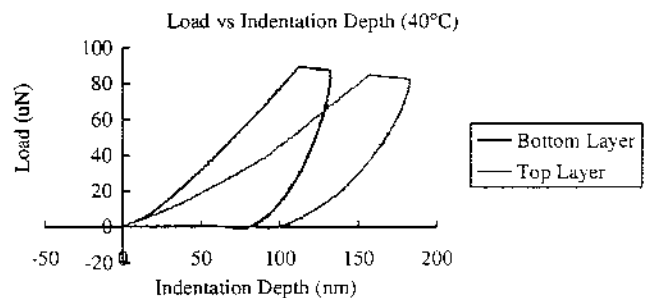


Fig. 5. Comparisons between the top and bottom layers of the fractured surface of nanoclay/epoxy composites subject to 40 °C sonication temperature.

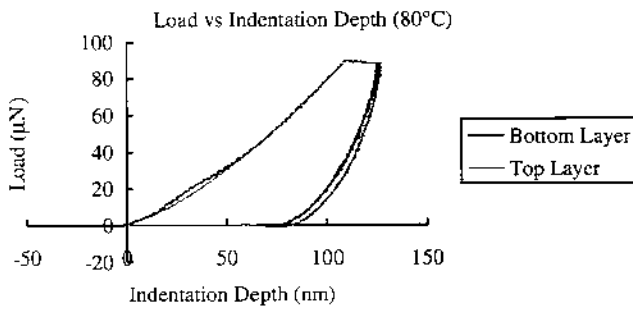


Fig. 6. Comparisons between the top and bottom layers of the fractured surface of nanoclay/epoxy composites subject to 80 °C sonication temperature.

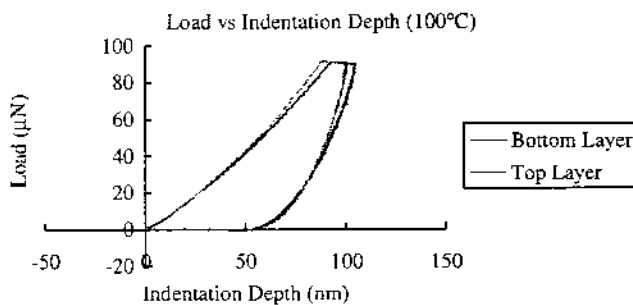


Fig. 7. Comparisons between the top and bottom layers of the fractured surface of nanoclay/epoxy composites subject to 100 °C sonication temperature.

tance of penetration of external force on the top surface of the composite with 40 °C sonication temperature treatment is much less than the bottom surface. In Figs. 6 and 7, composites with sonication temperatures at 80 °C and 100 °C, respectively, the nanoindentation depths of the top surface in each sample are almost the same as the one in the bottom surface. This concludes that the hardness of the composites with 80 °C and 100 °C sonication temperatures are evenly distributed throughout the entire sample whereas in the composite with 40 °C sonication temperature, the hardness decreases from bottom surface to the top surface of the entire sample.

Fig. 8 shows the relative elastic modulus of the composites with different sonication temperatures from the nanoindentation experiments where each nanoindentation point is separated by a length of 0.05 mm starting from

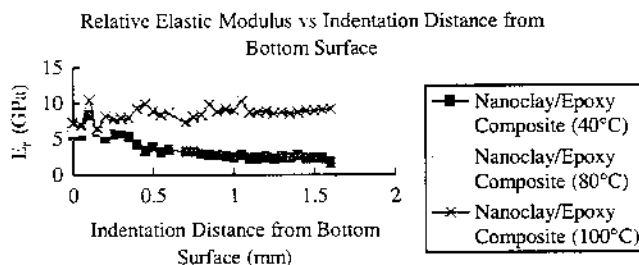


Fig. 8. Relative elastic modulus of nanoclay/epoxy composites subject to different sonication temperature treatments.

the bottom surface to the top surface of the specific sample. The results show that at 40 °C sonication temperature, the relative elastic modulus will decrease from bottom surface to the top surface of the composites. However, at 80 °C and 100 °C sonication temperatures, the values of relative elastic modulus of the composites are almost the same when comparing the top and bottom surfaces of the composites. The phenomenon is due to the gravitational effect on the nanoclay clusters inside the composites during curing. Before the composites completely cured, gravitational effect plays an important role in the distribution of nanoclay clusters. Under the gravitational effect, nanoclay clusters tend to settle to the bottom surface in the semi-cured composites. Nevertheless, the curing time of epoxy resin is different if the temperature changes. At higher temperatures, the curing time of the epoxy resin must be faster than lower temperatures. As a result, at the composite with 40 °C sonication temperature, nanoclay clusters inside have much more time to settle to the bottom surface of the composite by the gravitational effect. Hence there are more nanoclay clusters situated at the bottom layer of the composite so the relative elastic modulus will decrease gradually from bottom to top surfaces of the composite sample with 40 °C sonication temperature. At higher temperatures, the gravitational effect on the nanoclay clusters is limited as the curing time is fast and the nanoclay clusters will remain in a well dispersed location when cured. Thus, the relative elastic moduli of the composites are stable at 80 °C and 100 °C sonication temperatures.

5. Conclusion

This paper studies the nanoclay cluster sizes by the modified explanation of nucleation theory of clusters and the distribution of nanoclay clusters at different sonication temperatures, namely, 40 °C, 80 °C and 100 °C in polymer-based composites. The nanoclay cluster size increases with the sonication temperature increases as shown by SEM. By the deduction of the modified nucleation theory of clusters in which the effects of sonication temperature and viscosity of epoxy resin are newly inserted, the increase in size of nanoclay clusters at higher sonication temperatures is due to the decrease of interfacial tension between the surfaces of nanoclay clusters and the surrounding epoxy resin. Moreover, accompany with the increase of kinetic energy for the nanoclay particles at higher temperatures, the probability for free nanoclay particles to adhere on the surface of a nanoclay cluster is greatly increased. Hence, nanoclay clusters appear larger in size at higher sonication temperatures. From the results obtained by nanoindentation on the cross-section of nanoclay/epoxy composites, it was found that the relative elastic modulus decreases from bottom surface to the top surface of the composites due to the gravitational effect of the nanoclay clusters. The sonication temperatures play an important role in the mixing process of nanoclay/epoxy composites. At higher temperatures, the distribution of nanoclay clusters

will be more even than at lower temperatures as higher temperatures may cause a relatively fast curing time, it therefore builds viscous barriers, i.e. semi-cured resin, among nanoclay clusters and results in avoiding the sinking of clusters to the bottom surface. The distributions of nanoclay clusters are still well dispersed at higher sonication temperatures samples, so the relative elastic modulus remains stable.

Acknowledgement

This project was supported by the Hong Kong Polytechnic University Research Grants (G-T936 and G-T861).

References

- [1] Ke Y, Long C, Qi Z. *J Appl Polym Sci* 1999;71:1139–46.
- [2] Song M, Hourston DJ, Yao KJ, Tay JKH, Ansarifard MA. *J Appl Polym Sci* 2003;90:3239–43.
- [3] Wetzel B, Haupt F, Zhang MQ. *Comp Sci Tech* 2003;63:2055–67.
- [4] Wetzel B, Haupt F, Friedrich K, Zhang MQ, Rong MZ. *Polym Eng Sci* 2002;42:1919–27.
- [5] Ng CB, Schadler LS, Siegel RW. *Nanostruct Mater* 1999;12:507–10.
- [6] Kojima Y, Usuki A, Kawasumi M, Okada A, Fukushima Y, Kurauchi T, Kamigaito O. *J Mater Res* 1993;8:1185.
- [7] Kojima Y, Usuki A, Okada A, Kurauchi T, Kamigaito O. *J Polym Sci Part A Polym Chem* 1993;31:2493.
- [8] Dietsche F, Thomann Y, Thomann R, Mulhaupt R. *J Appl Polym Sci* 2000;75:396–405.
- [9] Oliver WC, Pharr GM. *J Mater Res* 1992;7:1564–83.
- [10] Pharr GM, Oliver WC, Brotzen FR. *J Mater Res* 1992;7:613–7.
- [11] Shen L, Liu T, Lv P. *Polym Test* 2005;24:746–9.
- [12] Shen L, Phang IY, Chen L, Liu T, Zeng K. *Polymer* 2004;45:3341–9.
- [13] Shen L, Phang IY, Liu T, Zeng K. *Polymer* 2004;45:8221–9.
- [14] Lam CK, Cheung HY, Lau KT, Zhou LM, Ho MW, Hui D. *Comp Struct Part B Eng* 2005;36:263–9.
- [15] Lam CK, Lau KT, Cheung HY, Ling HY. *Mat Lett* 2005;59:1369–72.
- [16] Abraham FF. *Homogeneous nucleation theory*. New York: Academic; 1974.
- [17] Zettlemoyer AC. *Nucleation phenomena*. New York: Dekker; 1969.
- [18] Lamer VK, Dinegar RH. *J Am Chem Soc* 1950;72:4847.
- [19] Frenkel J. *Kinetic theory of liquids*. New York: Dover; 1955 [Chapter 7].
- [20] Zeldovich JB. *Acta Physicochim* 1943;18:1.

Nano-mechanical Creep Properties of Nanoclay/Epoxy Composite by Nanoindentation

Chun Ki Lam¹, Kin Tak Lau² and Li Min Zhou³

Department of Mechanical Engineering, The Hong Kong Polytechnic University, Hung Hom, Kowloon, Hong Kong

¹me.cklam@polyu.edu.hk, ²mmktlau@polyu.edu.hk, ³mmlmzhou@polyu.edu.hk

Keywords: Nanoindentation; Creep; Stress Exponent

Abstract. Mechanical properties of nanoclay/epoxy composites (NC) have been studied by various experimental setups in bulk form recently. Creep mechanism of the NC is an important manufacturing criterion for the aircraft industry. In this paper, nanoindentation was employed to investigate the nano-mechanical creep effects on different wt. % of nanoclay contents in epoxy matrix. Creep behaviors of the nanoclay/epoxy composites with different wt. % of nanoclay contents were modeled by the power-law creep equation. Neglecting the temperature effects on creep, the stress exponents of tested composites were estimated.

Introduction

Nanoindentation is a newly invented technique for the determination of localized material properties that was introduced by Oliver and Pharr in 1992 [1]. Elastic modulus, nano-hardness and contact stiffness of a material can be determined by nanoindentation nanoscopically [1,2]. Fig. 1 shows a typical nanoindentation profile for determination of localized mechanical properties in polymer composites.

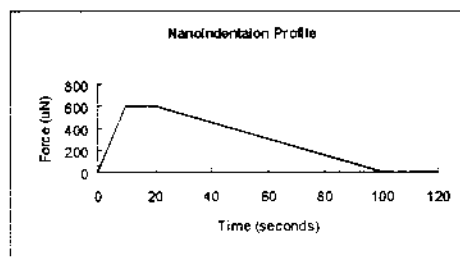


Fig. 1 Nanoindentation Profile

The technique makes use of creating a permanently plastically deformed surface on a material being tested. From the force applied on the surface and the indentation depth of the indent, relative elastic modulus can be obtained by the equations given as, $A_c = f(h_c)$ and $E_r = (\sqrt{\pi}/2)/(S/\sqrt{A_c})$, where h_c is the contact height, A_c is the contact surface area between the nanoindenter and the material surface and S is the contact stiffness that is the slope of the unloading portion in the nanoindentation profile as shown in Fig. 1.

Numerous research conducted in investigating the mechanical properties of pure elements and nanocomposites by nanoindentation. Nanoindentation has also been employed to evaluate the depth of the coatings on polymer-ceramic nanocomposites by depth sensing indentation [3-7]. Shen et al. [8-10] has begun to study the morphologies of nylon 66/nanoclay composites by nanoindentation. Apart from visualizing the localized mechanical properties, nanoindentation can also investigate the localized creep effect from the holding portion of the nanoindentation profile. From the definition of creep, the elongation of the materials from its original position after a constant applied force at thermally stable environment is called creep. In nanoindentation, the degree of creeping can also be measured by holding the applied force of the nanoindenter constant with respect to the deformation of the materials being tested. The advantages of using nanoindentation to measure creep are time

economic as the time for conducting an indent is far less than the novel creep testing techniques. Moreover, nanoindentation can measure creep within an infinitesimal small area, hence, localized creep can be easily obtained instead of creeping of the whole structure. As a result, for composite structures, especially in nanocomposites, nanoindentation can detect the changing creep behavior within the nanocomposites as the reinforcement at each separate point by the nanoparticles/nanofibres is varying. To the best knowledge of the authors, the localized creep behavior of NC has not been studied before. In this paper, creep behavior of NC with different wt. % of nanoclay will be investigated by nanoindentation.

Experimental Investigation

Materials. Nanoclay particles (SiO₂ Nanolin DK1 series from the Zhejiang FH Nanoclay Chemical Technology Company) were used as nano-reinforcements for this study. The mean diameter, density and moisture content of the nanoclay were 25 nm, 0.45 g/cm³ and more than 95% of SiO₂, respectively. The epoxy resin and hardener selected for this study were araldite GY 251 and hardener HY 956 respectively. They were mixed in a ratio of 5 to 1 parts by weight.

Sample Preparation. NC samples were fabricated by using mechanical mixing process with different amount of nanoclay contents, 2 wt.% (NC-2), 4 wt.% (NC-4), 6 wt.% (NC-6) and 8 wt.% (NC-8). The predetermined amount of nanoclay was dispersed in the epoxy resin. The mixture was hand stirred for 10 minutes until the epoxy resin and the nanoclay were well mixed at room temperature. Ultrasound sonication was employed to further disperse the nanoclay in the epoxy resin. The sonication time was fixed at 20 minutes for all the samples in order to ensure the maximized mechanical performance [11]. Hardener was added into the sonicated mixtures by hand stirring and followed by vacuuming for 24 hours at room temperature for curing. The nanoindentation specimens were made by cutting the sample to 18mm x 3mm x 3mm by size before polishing. All of the composites samples were subjected to fine polishing by SiC papers and followed by diamond paste polishing to 6 μm accuracy before nanoindentation in order to ensure the reliability of the results obtained.

Measurements. Nanoindentation was carried on a Hysitron Triboindenter at room temperature. A Berkowich nanoindenter head was used for the nanoindentation experiments. The loading time, holding time, unloading time and the maximum load (P_{max}) were 10s, 10s, 80s and 600μN respectively. The holding time was fixed at 10s for all the samples in order to compare the creep behavior. Each specimen was indented three times and took the average result.

Results and Discussions

Nanoindentation. NC samples with different wt. % of nanoclay were tested on the localized creep effects with constant holding load during nanoindentation. Fig. 1 shows the nanoindentation profile during the experiment. The load was held at 600 μN for 10s throughout the experiment.

Fig. 2 shows the creeping strain of different NC samples with respect to time during load holding of the nanoindentation profile.

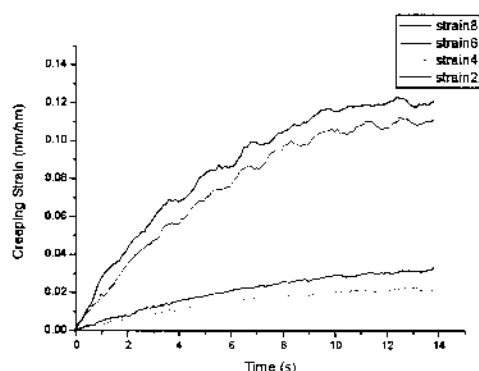


Fig. 2 Creeping strain of different wt. % of nanoclay/epoxy composites

The creeping strain at each data collecting point can be calculated by (1).

$$\varepsilon = (h_1 - h_c)/h_c \quad (1)$$

where h_1 and h_c are the instantaneous localized penetration depth at each specified data collecting point and contact depth at that nanoindentation point respectively.

As the indentation depth was changing on each data collection point with the load holding constant, the instantaneous creeping strain can be obtained by comparing with the final contact depth of the indent after the indentation.

The creeping strain of the NC-2 and NC-4 were having a huge difference with NC-6 and NC-8. The NC-4 has the lowest creeping strain compared to the other wt. % of nanoclay. This was due to the maximum mechanical reinforcement by the nanoclay clusters in the nanoclay/epoxy composites at 4 wt. % of nanoclay by Lam et. al [11,12].

Creeping strain of NC can be described by (2) experimentally.

$$\varepsilon = A \exp(-t/B) + C \quad (2)$$

where A, B and C are constants. The constants can be obtained by fitting the strain vs time curve with equation (2). Differentiate equation (2) with respect to time,

$$\dot{\varepsilon} = -(A/B) \exp(-t/B) \quad (3)$$

Neglecting the effect of temperature, the steady state uniaxial creeping mechanism can be described by the power law relationship between the strain rate and the stress during creeping.

$$\dot{\varepsilon} = K\sigma^n \quad (4)$$

where K is a constant and n is the stress exponent of the nanoclay/epoxy composites. The localized stress with time varying during testing is determined by,

$$\sigma = P_{(\text{at each data collecting point})}/A_{(\text{contact area})} \quad (5)$$

K and n can be obtained by fitting the strain rate vs stress curve with equation (4). Table 1 shows the stress exponent of different wt.% of NC obtained from the fitting results by equation (4).

Table 1 Stress exponent of the nanoclay/epoxy composites with different wt. % of nanoclay

	2%	4%	6%	8%
Stress Exponent	7.31	7.58	11.87	13.95

When there is a constant force added on the surface of NC-2 and NC-4, the nanoclay clusters within the composites will be altered from its original position and block the creeping path of the epoxy matrix. Whereas the stress exponent of NC-6 and NC-8 show an apparent difference with NC-2 and NC-4, the reinforcement by the nanoclay clusters are negligible in those samples.

Conclusions

In this paper, the localized creep mechanisms of the NC with different wt. % of nanoclay were studied by nanoindentation. Mathematical interpretations of the nanoindentation results were made and the stress exponents of the NC with different wt. % of nanoclay were obtained. An optimum creeping

strain was obtained from 4 wt. % of nanoclay content. Below the optimum point of the creeping strain, the stress exponent showed that dislocation creep will occur as the nanoclay clusters within the composites will be altered from its original position and blocked the creeping path of the epoxy matrix. When the amount of nanoclay increased, the total free volume for each nanoclay particles to live in will be reduced gradually and the tendency for the nanoclay particles to form pairs or aggregates will be enhanced. Thus, larger nanoclay clusters can be readily found in the NC samples with a higher wt. % of nanoclay content. In the nanoclay content above the optimum value, creeping strain will increase rapidly as the reinforcement mechanisms between the nanoclay clusters and the epoxy matrix were deteriorated by the oversized nanoclay clusters and the decrease of interacting surface area.

Acknowledgement

This project was supported by the Hong Kong Polytechnic University Grant (GT-861).

References

- [1] W. C. Oliver and G. M. Pharr, *J. Mater. Res.*, 7 (1992) 1564-1583.
- [2] G. M. Pharr, W. C. Oliver and F. R. Brotzen, *J. Mater. Res.*, 7 (1992) 613-617.
- [3] M. R. VanLandingham, J. S. Villarrubia, W. F. Guthrie, and G. F. Meyers, *Macromol. Symp.*, 167 (2001) p. 15
- [4] B.J. Briscoe, L. Fiori, and E. Pelillo, *J. Phys. D Appl. Phys.*, 31 (1998) p. 2395.
- [5] J. Sun, L. F. Francis, W. W. Gerberich, *Polym. Eng. Sci.*, 45 (2005) p. 207.
- [6] M. Li, M. L. Palacio, C. B. Carter, and W. W. Gerberich, *Thin Solid Films*, 416 (2002) p.174.
- [7] J. A. Payne, A. Strojny, L. F. Francis, and W. W. Gerberich, *Polym. Eng. Sci.*, 38 (1998) p.1529.
- [8] L. Shen, T. Liu, P. Lv, *Polymer Testing*, 24 (2005) 746-749.
- [9] L. Shen, I. Y. Phang, L. Chen, T. Liu, K. Zeng, *Polymer*, 45 (2004) 3341-3349.
- [10] L. Shen, I. Y. Phang, T. Liu, K. Zeng, *Polymer*, 45 (2004) 8221-8229.
- [11] C. K. Lam, K. T. Lau, H. Y. Cheung, H. Y. Ling, *Mat. Lett.*, 59 (2005), 1369-1372.
- [12] C. K. Lam, H. Y. Cheung, K. T. Lau, L. M. Zhou, M. W. Ho, D. Hui, *Comp. Struct. Part B: Engineering*, 36 (2005) 263 - 269.

Tribological behavior of nanoclay/epoxy composites

Chun Ki Lam, Kin Tak Lau*

Department of Mechanical Engineering, The Hong Kong Polytechnic University, Hung Hom, Kowloon, Hong Kong, China

Received 17 September 2006; accepted 21 December 2006

Available online 18 January 2007

Abstract

This paper aims to discuss the mechanical performance of nanoclay/epoxy composites (NCs) through micro-hardness and abrasive tests. It was found that the hardness and wear resistance of NCs increased with increasing nanoclay content of up to 4 wt.%. The improvement of mechanical properties of the NCs by increasing nanoclay content is explained by the degree of agglomeration of nanoclay clusters inside the NCs through SEM and XRD investigations. A mathematical interpretation for the determination of hardness and wear resistance of the NCs at different nanoclay contents in relation to the diameter of nanoclay clusters and their inter-particle distance is given.

© 2006 Elsevier B.V. All rights reserved.

Keywords: Hardness; Nanocomposites; Nanomaterials; Wear

1. Introduction

In everyday engineering applications, an excellent wear resistance of engineering materials is a critical requirement for surface coating applications in severe working environment. Furthermore, the maintenance cost can be kept as low as possible for an engineering component to possess a high wear resistance. In the past decade, many researches on the applications of various types of nanocomposite coatings for different engineering components have been conducted [1–3]. Recently, researchers have showed that polymer nanocomposites can provide high mechanical and tribological performance with wide applicability in both conducting and insulating surfaces of engineering products without adding much extra loading to the main engineering bodies. TiO₂ [4], SEBS [5] and carbon nanotubes [6] were being used as nanofillers in epoxy, polystyrene and other polymers for nanocomposite coatings.

Layered montmorillonite (MMT) or nanoclays (SiO₂) are newly invented nanofillers in polymers for extraordinary improvements in mechanical behaviors of polymer matrix. Fig. 1 shows three typical forms of MMT inside polymer matrix. MMT is composed by stacks of nanoclay platelets. They

can provide significant improvement to the mechanical properties of polymer matrix due to their high aspect ratio of the nanoclay platelets and thus provide large contacting interfaces for the interaction between the nanoclays and the matrix. Many researchers have begun to study the abrasive durability of nanoclay-based polymer composites in order to replace the traditional superhard nanoparticles-based surface coatings [7–9]. Nevertheless, fully exfoliated nanoclay/epoxy composites (NCs) can only exist in laboratory studies by absolute controlled experimental conditions. Lam et al. [10,11] have studied the effects of nanoclay clusters in NCs and the results showed that there was an optimum nanoclay wt.% inside NCs in order to possess the highest mechanical reinforcement. It was found that the maximum hardness can be achieved for the nanoclay content at 4 wt.%. Further increasing the amount of nanoclays resulted in decreasing the hardness of the NCs. The nanoclay clusters behaved like the novel superhard nanoparticles in conventional surface coatings. As a result, intercalated nanoclay clusters should be investigated for surface coatings that can cope with most engineering manufacturing processes instead of testing the applicability of fully exfoliated nanoclay platelets inside controlled laboratory conditions. To the best knowledge of the authors, the wear resistance of intercalated NCs has not yet been studied to date.

In this study, up to 4 wt.% of nanoclays mixed with an epoxy matrix to form NC samples were fabricated. Scanning Electron

* Corresponding author.

E-mail address: mmktilau@polyu.edu.hk (K.T. Lau).

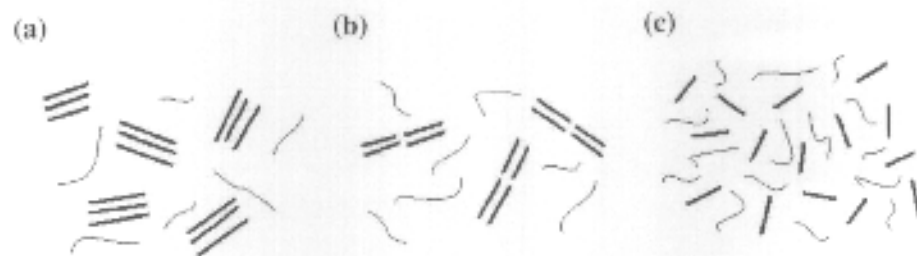


Fig. 1. Three existences of MMT inside polymer matrix. (a) Intercalated; (b) flocculated; and (c) exfoliated.

Microscopy (SEM) and X-ray spectroscopy (XRD) examination was used to verify the degree of intercalation of nanoclays inside the samples. Vickers micro-hardness test was conducted to test their hardness and twin SiC sliding wheels test was employed to visualize the wear resistance of the NC samples.

2. Experimental investigation

2.1. Materials

Nanoclay particles (SiO₂ Nanolin DK1 series from the Zhejiang Fenghong Nanoclay Chemical Technology Company) were used as nano-reinforcements for this study. The mean diameter, density and montmorillonite content of the nanoclays were 25 nm, 0.45 g/cm³ and 95%–98% of SiO₂, respectively. The epoxy resin and hardener selected for this study were Araldite[®] GY 251 bisphenol-A liquid epoxy resin and Hardener HY 956 aliphatic amine from Ciba Speciality Chemicals respectively. They were mixed in a ratio of 5 to 1 parts by weight.

2.2. Sample preparation

NC samples were fabricated by using mechanical mixing process with different amounts of nanoclay, 0 wt.% (NC-0), 1 wt.% (NC-1), 2 wt.% (NC-2) and 4 wt.% (NC-4). The predetermined amounts of nanoclays were dispersed in epoxy

resin. The mixtures were hand stirred for 10 min until the epoxy resin and the nanoclays were well mixed at room temperature. Ultrasound sonication was employed to further disperse the nanoclays in the resin. The sonication time was fixed at 20 min for all the samples in order to ensure their maximized mechanical performance [11]. Hardener was added into sonicated mixtures by hand stirring and followed by vacuuming for 24 h at room temperature for curing. The abrasive testing samples were prepared by curing them in same grade of surface-treated circular polypropylene discs with 4 in. in diameter.

2.3. Measurements

X-ray diffraction (XRD) of NC samples were conducted on a Philips PW 1830 X-ray Generator (Cu K_α, λ=0.154 nm) in order to visualize the degree of aggregation of the nanoclay clusters. Scanning Electron Microscopy (SEM) of the fractured surfaces of NC samples was conducted on a Leica Stereoscan 440 SEM.

Micro-hardness test of NC samples was conducted by using the micro-hardness tester (FM-7E) of the Future-Test Corporation from Tokyo, Japan. Each NC sample was indented ten times at different locations under the same indenting conditions and the average value was taken as a representing micro-hardness of the specified NC samples.

Wear resistance of the NC samples was obtained from an abrasive test performed on the circular NC samples with 4 in. in

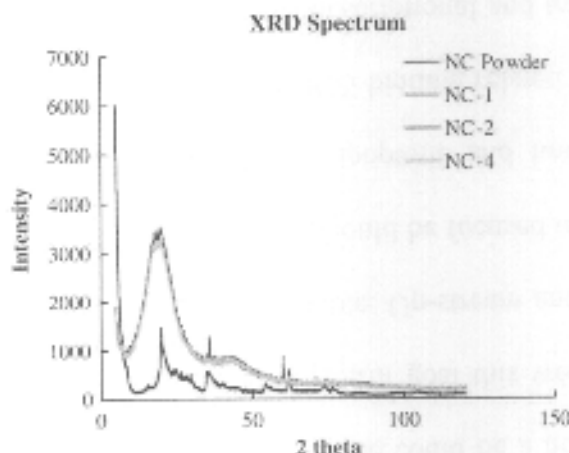


Fig. 2. XRD spectrum of different wt.% of NCs.

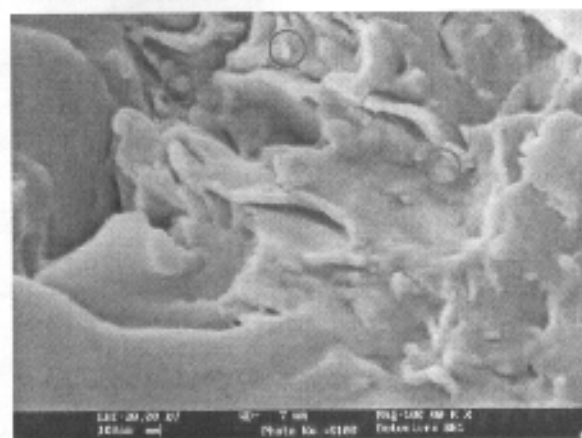


Fig. 3. SEM of the fractured surface of NCs with 4 wt.% of nanoclays.

diameter in a 5131 Abraser of Taber Industries, North Tonawanda, N.Y., USA. The sliders were two circular-disked like silicon carbide abrasive wheels manufactured by Taber Industries. The wear resistances of the NC samples were compared by the wear index (WI) calculated by,

$$WI = 1000(W_s - W_f)/R, \quad (1)$$

where W_s (measured in grams) is the initial weight of the NC sample before testing, W_f (measured in grams) is the final weight of the NC sample after testing and R is the number of testing cycles.

3. Results and discussions

3.1. X-ray spectroscopy

The XRD spectrums of the NC samples with different wt.% of nanoclays are shown in Fig. 2. Only one common peak at $2\theta = 18.8^\circ$ with maximum intensity exists in the NC samples when comparing with pure nanoclay powders. By using the Bragg's formula, $2d\sin\theta = n\lambda$, the interplanar distance between nanoclay platelets was 0.239 nm approximately. For a fully exfoliated NC sample, the angle 2θ in the XRD spectrum should be as small as possible in order to achieve the largest interplanar separation between the nanoclay platelets. Hence, there should be no obvious peaks in the XRD spectrums of totally exfoliated NC samples. Therefore, all of the nanoclay platelets of the NC samples in the experiments were intercalated.

3.2. Scanning Electron Microscopy

The SEM of the fractured surface of the NC sample with 4 wt.% of nanoclays is shown in Fig. 3. Nanoclay clusters were readily found and hence the nanoclays inside the NC samples existed in the form of intercalated nanoclay clusters.

3.3. Micro-hardness test

Fig. 4 shows the average hardness of different NC samples. By adding nanoclays into epoxy resin, the micro-hardness of the NCs increased proportionally with the nanoclay contents up to 4 wt.%. By Zhang et al. [8], the correlations between the inter-particle distances,

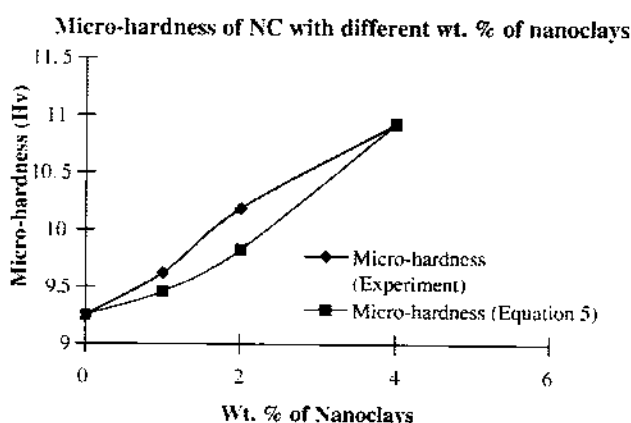


Fig. 4. Micro-hardness of different wt.% of NCs.

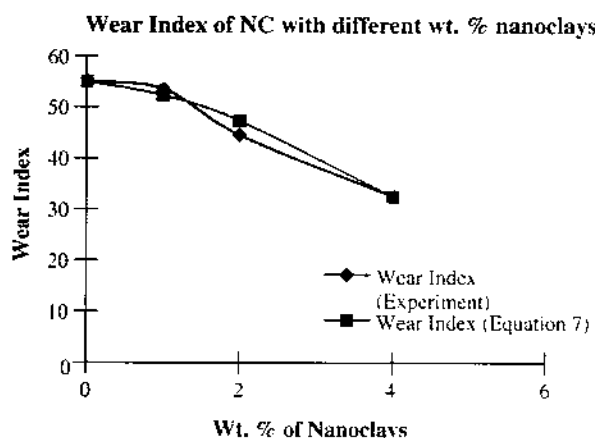


Fig. 5. Wear index of different wt.% of NCs.

diameters of the nanoparticles and wt.% of the nanoparticles in nanocomposites can be explained by

$$\tau = d[(\phi_p/6)^{1/3} - 1], \quad (2)$$

where τ is the inter-particle distance, d is the particle diameter and ϕ_p is the filler content.

As the micro-hardness of the NCs increases in proportion to the content of nanoclays, the diameter of the nanoclay clusters increases while the inter-particle distance between them decreases accordingly [10], the micro-hardness of the NCs can be modeled as,

$$H = H_i + k_{II}(\phi_p d/\tau), \quad (3)$$

where H is the micro-hardness of the NCs, k_{II} is the micro-hardness proportional constant and H_i is the micro-hardness of pure epoxy. Thus, Eq. (2) can then be rewritten as,

$$d/\tau = 1/[(\phi_p/6)^{1/3} - 1]. \quad (4)$$

Substituting Eq. (4) into Eq. (3), the micro-hardness of the NCs can be determined by,

$$H = H_i + k_{II}\phi_p/[(\phi_p/6)^{1/3} - 1] \text{ and} \\ H = H_i + k_{II}[1.817\phi_p^{4/3}/(\phi_p^{1/3} - 1.817\phi_p^{1/3})]. \quad (5)$$

3.4. Wear resistance

Fig. 5 shows the test results of the wear resistance of the NC samples. The higher the wear index, the lower the wear resistance and vice versa. Therefore, NC-4 has the highest wear resistance. As the wear resistance of the NCs increases in proportion to the nanoclay content, the wear resistance of the NCs can be co-related to the diameters of the nanoclay clusters and the inter-particle distance from the argument as stated in Eq. (3) by,

$$W = W_i - k_W(\phi_p d/\tau) \quad (6)$$

where W is the wear resistance of the NCs, k_W is the wear resistance proportional constant and W_i is the wear resistance of pure epoxy.

Substituting Eq. (4) into Eq. (6), the micro-hardness of the NCs can be determined by.

$$W = W_1 - k_W \phi_p / [(\pi/6\phi_p)^{1/3} - 1], \text{ and} \quad (7)$$

$$W = W_1 - k_W \{1.817\phi_p^{4/3} / (1.13 - 1.817\phi_p^{1/3})\}$$

The mathematical predictions of micro-hardness and wear resistance of the NCs were based on the empirical data with the nanoclay contents from 0–4 wt.% and the condition of fully intercalation of nanoclay platelets inside nanoclay clusters was assumed. In Figs. 4 and 5, the mathematical predictions of micro-hardness and wear index of the NCs are compared to the experimental results respectively. It shows that these mathematical models of the NCs are valid for the micro-hardness and wear index estimation once the nanoclay content is known.

4. Conclusion

In this paper, the micro-hardness and wear resistance of the NCs with the nanoclay content of up to 4 wt.% were investigated. Both properties increased with increasing content of nanoclays. The improvement in the wear resistance of the NCs compared to a pure epoxy can provide an adequate compatibility among novel nanocomposites for surface coatings. A mathematics correlation of micro-hardness and wear resistance of the NCs with the diameters of intercalated nanoclay clusters and inter-particle distance is proposed in this paper. This can aid the understanding of the infrastructure inside the NCs for everyday engineering applications. The intercalation of nanoclays in NC surface coatings on engineer-

ing products were accurately modeled instead of only considering ideally exfoliated NCs in many laboratory studies.

Acknowledgement

This project was supported by the Hong Kong Polytechnic University Grant (GT-861).

References

- [1] K. Miyoshi, B. Pohlchuck, K.W. Street, J.S. Zabinski, J.H. Sanders, A.A. Voevodin, R.L.C. Wu, *Wear* 225–229 (1999) 65–73.
- [2] L. Wang, Y. Gao, Q. Xue, H. Liu, T. Xu, *Mater. Sci. Eng., A Struct. Mater.: Prop. Microstruct. Process.* 390 (2005) 313–318.
- [3] L. Shi, C. Sun, P. Gao, F. Zhou, W. Liu, *Appl. Surf. Sci.* 252 (2006) 3591–3599.
- [4] B. Wetzel, F. Hauptert, K. Friedrich, M.Q. Zhang, M.Z. Rong, *Polym. Eng. Sci.* 42 (2002) 1919–1927.
- [5] H.S. Ahn, D. Julthongpiput, D.I. Kim, V.V. Tsukruk, *Wear* 255 (2003) 801–807.
- [6] Z. Yang, B. Dong, Y. Huang, L. Liu, F.Y. Yan, H.L. Li, *Mater. Chem. Phys.* 94 (2005) 109–113.
- [7] Q.M. Jia, M. Zheng, C.Z. Xu, H.X. Chen, *Polym. Adv. Technol.* 17 (2006) 168–173.
- [8] H. Zhang, Z. Zhang, K. Friedrich, C. Eger, *Acta Mater.* 54 (2006) 1833–1842.
- [9] A. Dasari, Z.Z. Yu, Y.W. Mai, G.H. Hu, J. Varlet, *Comput. Sci. Tech.* 65 (2005) 2314–2328.
- [10] C.K. Lam, H.Y. Cheung, K.T. Lau, L.M. Zhou, M.W. Ho, D. Hui, *Comput. Struct. Part B: Eng.* 36 (2005) 263–269.
- [11] C.K. Lam, K.T. Lau, H.Y. Cheung, H.Y. Ling, *Mater. Lett.* 59 (2005) 1369–1372.